University of Cincinnati

Date: 2/7/2013

I, Bolaji A Suberu , hereby submit this original work as part of the requirements for the degree of Master of Science in Mechanical Engineering.

It is entitled:

Multi-scale Composite Materials with Increased Design Limits

Student's name: **Bolaji A Suberu**

This work and its defense approved by:

Committee chair: Mark Schulz, Ph.D.

Committee member: Jude Iroh, Ph.D.

Committee member: Vesselin Shanov, Ph.D.

Committee member: David Thompson, Ph.D.

3403

Multi-Scale Composite Materials with Increased Design Limits

By

Bolaji Suberu

BSc, Obafemi Awolowo University, Ile-Ife, Nigeria: Metallurgical & Materials Engineering, 2004

A thesis submitted to the graduate faculty
in partial fulfillment of the requirements for the degree of

MASTER OF SCIENCE

Department: Mechanical Industrial and Nuclear Engineering
Major: Mechanical Engineering

Committee:
Dr. Mark J. Schulz, Chair, Mechanical Engineering
Dr. Vesselin Shanov, Member, Chemical and Materials Engineering
Dr. Jude Iroh, Member, School of Aerospace Systems
Dr. David Thompson, Member, Mechanical Engineering
University of Cincinnati

Abstract

Laminated composite materials have gained wide use in a vast range of high strength engineering applications due to the high specific strength and stiffness of composites. However, composites have a critical limitation which is their susceptibility to matrix micro cracking and delamination which can lead to premature failure at stress levels significantly below the tensile strength of the composite. Laminated composites also have low through-the-thickness strength and conduction properties which are important for aerospace vehicles and the military defense industry. These fundamental weaknesses in FRPC can be mitigated by the use of (CNTs) as a secondary reinforcement phase due to its excellent mechanical, electrical and thermal properties. In addition, the nano-reinforcement architecture will add significant multifunctionality to laminated composites. In this thesis, different reinforcement architecture are being investigated to improve the structural properties of laminated composite materials.

The first approach investigated to improve the interlaminar and flexural strength of composites was to reinforce the laminate interlayers using a short and dense CNT array. The CNT arrays toughen the matrix rich regions. A vertically aligned carbon nanotube (VACNT) laminated composite which consists of Multiwalled Carbon Nanotube (MWCNT) arrays are transferred unto IM7/977-3 carbon fiber prepreg and plies are stacked up to create a hybrid laminated composite material. A complete wetting of the short MWCNT array by the epoxy from the prepreg was sufficient to create a new interface which yielded higher interlaminar properties. Mechanical and SEM characterization of these composite materials was performed under different loading conditions which include interlaminar and in-plane shear, bending, and in-plane tension.

The second phase of reinforcement in this work was to improve the interlaminar shear properties of the laminated composite without reducing its in-plane tensile properties using a procedure that is minimally invasive to the carbon fiber prepreg. This process consists of using long CNT array posts to mechanically interlock all the plies together in order to impart a better load transfer mechanism than the previous approach. Micron-sized pin-holes are gently pressed into the prepreg layup and long CNT array posts are manually inserted into these pin holes prior to consolidation process. Also, mechanical and SEM characterization is performed on these composite samples under shear and in-plane tensile loading to determine the effect of pin-hole insertion density on the composite strength.

Lastly, fiber reinforced laminated composites exhibit high mechanical properties in-plane but micro-sized matrix pockets in these materials occur as a result of ineffective close packing of the carbon fibers due to their large diameters and one size of fiber. This section proposes future work where laminated composites are redesigned and manufactured to create a high volume fraction composite (HVFC) which consists of micron diameter CNT threads integrated in-plane with seven micron diameter carbon fibers. Through-the-thickness reinforcement with long CNT posts is proposed to be used with the longitudinal reinforcement. To further improve the load transfer mechanism between the CNT forms and resin matrix, CNTs will be functionalized using plasma annealing system. We believe nano scale reinforcement will be the future of composite materials.

Acknowledgements

First of all, my special thanks and sincere gratitude goes to my advisor Dr. Mark J. Schulz for his constant support and encouragement throughout my thesis. His inputs, advice and guidance throughout this work immensely provided the recipe for successful completion of my thesis. I would also like to thank him for giving me the opportunity to be a member of the Nanoworld research group.

Secondly, I would also like to acknowledge the support of Dr. Vesselin N. Shanov for also providing the necessary support and assistance when sought which also extends to the unflinching provision of CNT arrays, yarns, threads etc. when needed for without these materials, my thesis wouldn't have been possible.

Also, my gratitude goes to Dr. Yi Song, my research colleague who really helped me in getting up to speed with using the composite press machine, fabricating composite materials. He also assisted with data analysis and in characterizing the samples. I really appreciate his hard work and team-oriented effort in making this thesis possible.

My appreciation also goes to each and every member of the Nanoworld group for assisting me in one way or the other which ranged from growing CNT arrays, spinning of CNT threads which was critical in moving my thesis forward to preparing the samples for mechanical characterization prior to SEM imaging. These were made possible by Dr. Weifeng Li, Lucy Li, Arvind Krishnaswamy, Pravahan Salunke etc., and also General Nano and Boeing Seattle for providing materials used for this work. Appreciation also goes to Air Force Research Laboratory (AFRL) for carrying out SEM imaging on some batch of samples used for this work.

Finally, I would like to thank especially, my well-beloved mother Mrs. W.O Suberu for her selfless effort in showing both emotional and financial support and love during my trying times. My gratitude also goes to my brothers and sister who also kept me going by encouraging and showing me love and support which kept me motivated to achieve success.

Table of Contents

List of Figures

List of Tables

List of Symbols

τ_{13}	Interlaminar shear stress
P	Compressive load applied
w	Simple width
h	Tip-to-tip distance between the two v-notches
F^{sbs}	Short beam shear strength
P_m	Maximum load observed during the test
b	Sample Width
d	Sample thickness
σ_f	Flexural stress
P	Maximum load observed during the test
L	Span length
ε_f	Flexural Strain
D	Maximum deflection
σ_{11}	In-plane tensile strength
A_c	Reinforcement area
d_{cnt}	Diameter of the CNT
A_{cf}	Area of the carbon fiber
σ_c	Strengths of the composite
σ_e	Strength of 977 Epoxy
σ_{cf}	Strength of carbon fiber
σ_{cnt}	Strength of Carbon nanotube
v_e	Volume fraction of epoxy
v_{cf}	Volume fraction of carbon fiber
v_{cnt}	Volume fraction of carbon nanotubes
σ_{cwcnt}	Strength of composite with CNT
σ_{cwncnt}	Strength of composite without CNT
M_t	Total weight of prepreg after imprinting VACNT arrays
M_p	Initial weight of prepreg before imprinting VACNT arrays
M_{mwcnt}	Total weight of MWCNT arrays imprinted on prepreg
V_{mwcnt}	Volume fraction of MWCNT arrays
V	Volume of Composite
ρ_{mwnt}	Density of Multiwall carbon nanotube

Acronyms

CNT	Carbon nanotube
VACNT	Vertically Aligned carbon nanotube
MWCNT	Multi Wall Carbon nanotube
SEM	Scanning Electron Microscopy
CVD	Chemical Vapor Deposition
EPD	Electrophoretic Deposition
VARTM	Vacuum Assisted Resin Transfer Molding
RTM	Resin Transfer Molding
CNF	Carbon Nano Fiber
ASTM	American Society for Testing and Materials
SBS	Short Beam Shear
OHC	Open Hole Compression
HVFC	High Volume Fraction Composite

CHAPTER 1
Introduction

1.1 Motivation and Significance

A composite is a material system consisting of two or more phases on a macroscopic scale, whose mechanical performance and properties are designed to be superior to those of their individual material constituents acting independently. Composite materials are being used extensively in engineering applications due to their high specific strength and stifness and can also be tailored to specific applications since they are highly anisotropic materials.

Despite the excellent in-plane mechanical properties of laminated composite materials, they tend to show weak interlaminar and intralaminar shear properties both in-plane and through-the-thickness direction (z axis-direction) [1-6]. In order for laminated composite materials to be utilised for advanced military and aerospace applications, their through-the-thickness properties will have to be significantly improved to enable them compete with traditional metallic materials possessing no delamination and brittle failure problems. Since the discovery of carbon nanotube (CNT) [7], CNTs are known to be the stiffest material which possess an exceptional tensile strength of 50–100 GPa and a measured modulus of 1.4 TPa, and are by far the highest known. In addition, CNTs possess superior thermal [8] and electrically conductive properties [9] varying from metallic to semi-conductive behaviors depending on their chirality, size and purity.

Significant amount of work has been carried out by reserchers in using CNTs as a secondary reinforcing phase in laminated composites to the improve interlaminar shear properties in the z-direction. Results have shown that CNTs significantly improves the through-

the-thickness properties but often degrades the in-plane tensile properties along the fiber axis [10-17]. In order to utilize CNT reinforced laminated composite materials for advanced structural applications and exploit their properties to its full potential, these limitations must be overcome. We believe that this can only be done through improvement of its fabrication processes [18-19], surface modification of different CNT materials so as to create a functional interface which improves its load transfer efficiency [20], controlled orientation of CNTs in the polymer matrix to enhance the electrical and thermal properties of the polymeric composite while increasing its volume fraction and also design of an optimum reinforcement architecture in these weak failure modes etc.

There is also a great need for evaluating the properties of composite materials experimentally as opposed to designing computer based models to evaluate its mechanical properties. It is believed that experimental approach will incorporate various kinds of material and process conditions existing e.g. during fabrication process, prevailing environmental conditions and existence of microstructural flaws present to ascertain the structural integrity of the material. It is also a way of correlating the data and results achieved through modeling approach since modeling composite structure has limited predictive capability due in part to the lack of accurate data to describe local damage states and incorporating prevailing process condition into the model.

The main objective of this thesis is to improve the interlaminar and flexural properties of laminated composites without having degradation in its in-plane tensile properties by incorporating short transversely aligned CNT to mitigate these failure modes and reinforce the interlayers of laminated composite while improving its multifunctionality with respect electrical and thermal conductivities which is subject to future work in these areas.

We also believe better reinforcement architecture via novel fabrication process of reinforcing laminated composite with micro-sized long CNT post insertion will effectively improve the strength, strain to failure and interlaminar properties of laminated composite through effective load transfer mechanism between the matrix and the secondary reinforcing phase. Also, estimation of the amount of CNT loading in the bulk phase will be analyzed since research have shown that CNT loading effect improves the structural properties of CNT reinforced composite dramatically [21].

1.2 Background

Interlaminar shear stress (ILSS) is a limiting design problem which hinders laminated composite materials from reaching their design limits. This is partly attributed to conventional fiber manufacturing processes which do not produce vertically aligned fibers oriented in the thickness direction so as to sustain transverse load [12]. Laminated composites will often fail catastrophically if the issue of delamination is not mitigated or improved upon since it poses a safety concern for its primary use in the aerospace industry and for advanced engineering applications.

Delamination can be defined as a failure mode in which a composite material loses its structural integrity through the debonding of the ply interlayers [22-26]. Delamination in laminated Composite materials usually occur when the interlaminar shear stress applied reaches or exceeds the interlaminar shear strength of the composite interface according to the shear strength failure criterion. With respect to the fracture mechanics criterion, delamination occurs when the strain energy release rate reaches a critical value and as a result, leads to laminate debonding [22,27]. Delamination are susceptible at sites located within and around the composite

panel with poor load carrying capacity for e.g. free edges, bonded lap joints, moisture ingress [27, 28], bolted joints etc. The need to improve delamination resistance in laminated composite is very important since it reduces their predictability while in service. This will help facilitate their more efficient use in structural applications where complex failure modes and weight reductions are critical.

Researchers' have developed different techniques for possible solutions to this problem by improving the interlaminar shear and through-the-thickness properties of the laminated composite material. Common methods that are being used presently to reinforce composite materials involve lamination architecture at the nanoscale and microscale level. The microscale level reinforcement consists of integrating stitched fibers in the out-of-plane direction of the laminate [10-15], growing carbon nanotubes directly on carbon and glass fiber surfaces [3] etc. These methods can impart a significant improvement in mechanical properties like interlaminar shear modulus, shear strength, ultimate strains, and interlaminar fracture toughness by modifying 2D composite structures into 3D hierarchical hybrid laminate architecture.

The nanoscale level reinforcement consists of dispersing nanoscale particles that are integrated into the polymer matrix to reduce the effect of matrix micro cracking in composite. The nanoscale reinforcements include nanoscale particles such as clay [29-31], layered materials (graphite) and fibrous materials like CNTs [32-35], dispersed nanofibers [6,18-19] which have been extensively investigated in literature. These methods impart considerable amount of improvement in mechanical properties but still have some short comings with respect to load transfer efficiency since the particles are not long enough to create a continuous load transfer path and low volume fraction of particles due to increased viscosity of the resin matrix and uneven dispersion.

However, despite the improved higher interlaminar shear properties achieved with CNT fiber stitching method, there is often a degradation of the in-plane properties of the laminated composites due to high stitching densities. The shortcomings of these methods limit their extensive application in terms of industrial scale up of its fabrication processes. This led to the development of our novel approach of integrating nanoscale phase into laminated composite materials. A high strength carbon nanotube-reinforced laminated composite material with improved mechanical properties will be fabricated and characterized in this research.

The main idea behind some existing methods is to increase the interlaminar properties of laminated composites while modifying the reinforcement architecture at the ply interfaces. This modification is achieved by reinforcing the laminates with tows composed of thousands of nanoscale filaments in the through-the-thickness direction (z- direction) to carry higher tensile load in that direction and higher shear stresses in the interlaminar planes [36,37].

Microscale reinforcement architecture:

i. Three-dimensional reinforcement architecture (3D) woven fabrics that include through-the thickness tows with components in the z-direction besides those in the in-plane and transverse directions [2-3, 15].
ii. Stitched woven fabric or stitched unidirectional reinforcements [11-14].
iii. Surface functionalization of fibers to improve their load transfer properties between the matrix and fibers.

Since the discovery of carbon nanotubes, significant amounts of new reinforcement approach have been developed to reinforce conventional composite materials due to their excellent electrical and mechanical properties. Among the nanofillers that could be used to improve the

interlaminar shear properties of the resin matrix phase are multi-walled-walled carbon nanotube (MWCNT), single-walled carbon nanotubes (SWCNT) and carbon nanofibers (CNF). A host of researchers have focused on improving the properties of conventional composite materials with nanotechnology approach and these include.

i. Improving the mechanical properties of composite by dispersing CNT particles in polymer solutions have been a subject of continuous research [38–41] due to the fact that aggregation of nanotubes occur which result to viscosity build-up during dispersion, agglomeration due to Van Dar Waals forces and entanglement of the tubes limits this approach. Different mechanisms and approaches have been modified to enhance the mechanical properties of CNT particle reinforced composite.

ii. Growing carbon nanotubes on the surface of the fabric tows [3].

iii. A modified technique by Fan Z. et al [42] was developed to improve the Interlaminar shear strength of traditional glass fiber reinforced epoxy composite by strategically injecting multi-walled carbon nanotube (MWNT)–epoxy suspensions into stationary wooven glass fiber. This suspension was prepared by combining techniques such as high-speed mechanical stirring, ultrasonic agitation and acid oxidation. Two interlaminar shear test methods showed about 33% increase in ILSS when compared to the traditional glass fiber reinforced composite.

Although different studies using carbon nanotubes reinforcements in polymer composites have been done in recent years, more work still have to be done in improving and optimizing the fabrication processes of nanocomposite since a near-flawless manufacturing process will ultimately yield a composite material with increased design limits.

In this work, we developed a method to use long and strong micron bundles of radially/vertically aligned multiwalled CNTs (MWCNTs) and a short CNT array forest to reinforce carbon fiber laminated composite in the through-the-thickness direction. Here the CNT posts penetrates directly from the top to bottom of the stacked-up laminated composite panel by manually inserting CNT post into micron size pin-holes which eventually creates a hybrid composite panel with higher mechanical properties. Also, Micron-high vertically aligned CNT arrays were also transfer printed unto IM7-977/3 carbon fiber prepreg. These CNTs are grown using chemical vapor deposition (CVD) process which is an economical way of producing aligned CNTs [43]. The CNTs grow perpendicular to the surface of a substrate that is placed inside the quartz tube in an optimum location. Once CNT arrays and posts are transferred to the prepreg surface, the same procedures for matrix impregnations, lay-up laminations, and curing process that is employed in a traditional wet lay-up technique for composites manufacturing [44] is then used to develop a 3D- hybrid nanocomposites panel with superior through-the-thickness properties and multifunctionality [45-49].

Another novel process we developed in this work is the use of strong 2μm size diameter CNT threads to reinforce the matrix micro cracking sites which lies in between a woven fabric cloths or unidirectional aligned carbon fiber tows. Here, the CNT threads are laid up unidirectionally with the carbon fibers and fiber sizing process is done in order to fill up the micro spaces in between the larger diameter carbon fibers. This process is designed to improve the in-plane tensile properties and also act as a strain sensor [50-53] due to piezoresistive property of CNTs.

Also, a new process proposed in this thesis is the combined reinforcement of carbon fiber laminated composite using both longitudinally and transversely aligned CNT forms to reinforce

the weak failure modes in laminated composite materials and also improve on its multifunctionality in terms of increased electrical, thermal, mechanical and strain sensing properties of traditional carbon fiber composite.

1.3 Potential Applications of CNT Reinforced Nanocomposite

Structural materials are of critical importance in the field of aerospace, military, automotive, medical and general/industrial applications. Due to the excellent mechanical and electrical properties of CNTs [8,9], researchers have suggested that they have the potential to be used as reinforcing fibers in high-toughness nanocomposites, where stiffness, strength and low weight are to be considered for composite application.

There are numerous possible applications for CNT reinforced laminated composite but significant progress can be made if these challenging tasks of improving the structural properties are effectively tackled. Some application include aerospace structural panels, sporting goods, food packaging, bio medical, and ultra-lightweight thin-walled space structures for use in space. Highlighted below are some possible industrial applications of CNT nanocomposite in the near future.

1.3.1 Renewable Energy

Inexpensive, renewable energy sources are the driving force for research efforts on photovoltaic device technologies [54], so organic solar cells are an important application. Additional applications involving the optical and electronic properties are electron emitting flat-panel displays, electromechanical actuators, light-emitting diodes; super-capacitors, field-effect transistors, sub-picosecond optical switches and optical limiters [54].

1.3.2 Industrial Structural Application

The production of longer CNTs that can be formed into ropes would create obvious possibilities for applications such as suspension bridges [55], where CNT strengths and moduli of elasticity would allow for the design of significantly longer spans than existing technology makes possible. Similarly, the use of CNT ropes can be envisioned in improved pre-cast concrete beams. Carbon nanotubes have also been discussed as materials for the construction of very large, space based structures [56]; including space elevators [55].

These cable systems have the theoretical capability of reaching from the earth's surface to far beyond geosynchronous orbit. Elevator cars running simultaneously up and down the cable would allow cargo and goods to be transferred from space to the earth and vice-versa with minimal energy requirements.

1.3.3 Automobile Industry

Another application for these types of nanocomposites is for fabrication of automobile bumpers. It is envisaged that bumpers will have good mechanical properties and lower weight than the standard fiberglass bumpers that are being used, since only 1- 5 wt. % CNT will be needed as compared to 30 wt. % or more of fiberglass. The need for using CNT nanocomposites for automobile bumpers is based on their multi functionality, enabling good mechanical properties, low weight and electrical conductivity [56].

Direct application of electrostatic spray of base and clear coat will be easier due to the electrically conductive nature of the bumper, thereby eliminating the need for an additional primer coat prior to painting. Additionally, coast can be saved based on paint consumption and reductions in volatile emissions from paint lines.

1.3.4 Additives and reinforcement

CNT composite can also be used for reinforcement and additives in polymer due to their electrical properties, large aspect ratio and their tendency to be fabricated into a three dimensional, interconnecting network in the molten plastic [12]. Nanotube-filled polymers could potentially be used for electrostatic dissipation (ESD), electrostatic painting and EMI-shielding applications [57]. Their greater flexibility, space and weight savings, mechanical strength, better durability, and capability to tailor thermal and electrical conductivity gives them more advantage over other conductive fillers.

These properties enable production of advanced on-board shielding of electronic components and flexible electronics, and electromagnetic shields for mobile phone handsets [54]. There may be numerous other applications where the nanocomposites could be of significant use. At present, many research and commercial organizations are undertaking active research in discovering the potential applications of nanotube/fiber reinforced polymer composites that would use their unique mechanical, electrical conductivity, electromagnetic, and optoelectronic properties.

The core and most sought after application will be the effective utilization of these new classes of nanocomposites in technology transfer devices. All these predictions of potential applications of nanocomposites can pose a challenging task for researchers working in the field of nanotechnology.

1.4 Thesis Structure

To achieve the objective of improving the interlaminar shear properties both in-plane and through-the-thickness direction, different failure modes in laminated composite are

evaluated by subjecting them to different test as recommended by ASTM. To highlight a brief overview of how this thesis is organized, the component of the thesis is listed below.

Chapter 1 discusses the motivation and objective for improving the mechanical properties of fiber reinforced composite materials for advanced engineering applications. It also gives a background work in order to understand what the objectives of this reserch will be centered on. The potential advantages of reinforcing composite materials using carbon nanotube for multifunctional engineering application is also highlighted.

Chapter 2 gives an introduction to composites, CNTs, CNT-based composites, fabrication processes involved in production of high strength CNT composite, factors affecting the mechanical properties of CNT forms and its composites followed by the prediction for potential applications. Literature study on the past research and the results published related to this topic using various approaches to improve the interlaminar and overall structural properties of composites.

Chapter 3 discusses the phase I process of fabrication, testing and characterization of both non reinforced and reinforced short CNT array laminated composite which are used to reinforce in between each ply interface so as to improve interlaminar and flexural properties of composite while in service. Also SEM studies were carried out to understand the failure mechanism of both composite and how best to further reinforce the interface.

Chapter 4 talks about the discussion of a phase II process of fabrication, testing and characterization of both non reinforced and reinforced long vertically aligned CNT post (VACNT) laminated composite to mechanically interlock all plies and its results are obtained in

order to understand its reinforcement mechanisms. Also SEM images of the failure are captured to further understand the reinforcement pattern and failure modes.

Chapter 5 talks about theoretical analyses proposed for fabricating and characterizing super high strength, high volume fraction composite (HVFC) for extreme application. Theoretical analyses of both tensile and interlaminar shear property improvement with respect to in-plane and interlaminar shear is also discussed to back this claim.

Chapter 6 sumarrizes and conclude results achieved in this work and also talks about future work proposed in this research.

Finally, references and appendix are compiled at the end of this thesis to highlight work that has been done in this regard and SEM images showing composite failure mechanism.

CHAPTER 2

Overview of Laminated Composite Materials Reinforced with Carbon Nanotube Forms

2.1 Basics of Composite Materials

Composite is a combination of two or more constituents/additives (or fillers), designed to improve the overall structural properties of advanced engineering materials. In general all composites have two or more phases, in which the phase that is continuous in the composite is known as the matrix. The fundamental principle of the composite is to optimize material properties of the composite, which are usually very brittle and are more susceptible to failure damages while in service i.e., the properties of the matrix are to be improved by incorporating the reinforcement phase or additives such as fibers, sheets etc.

In general, reinforcing phase provides the desired stiffness for polymer matrix with weaker strength and low stiffness. Fibers possess the principal load-carrying constituents while the surrounding matrix helps bond them in desired location, preference and orientation coupled with the interface which also acts as a load transfer medium between them. Composites also include additives like coupling agents and coatings. They are applied on the fibers which improves wetting with the matrix thereby enhancing a better load transfer between the fibers and the matrix and creating an interface which has a different morphological and microstructure different from the matrix and fillers. Figure 2.1, shows the three broad classifications of composite structures depending on the type, geometry, orientation and reinforcing phase.

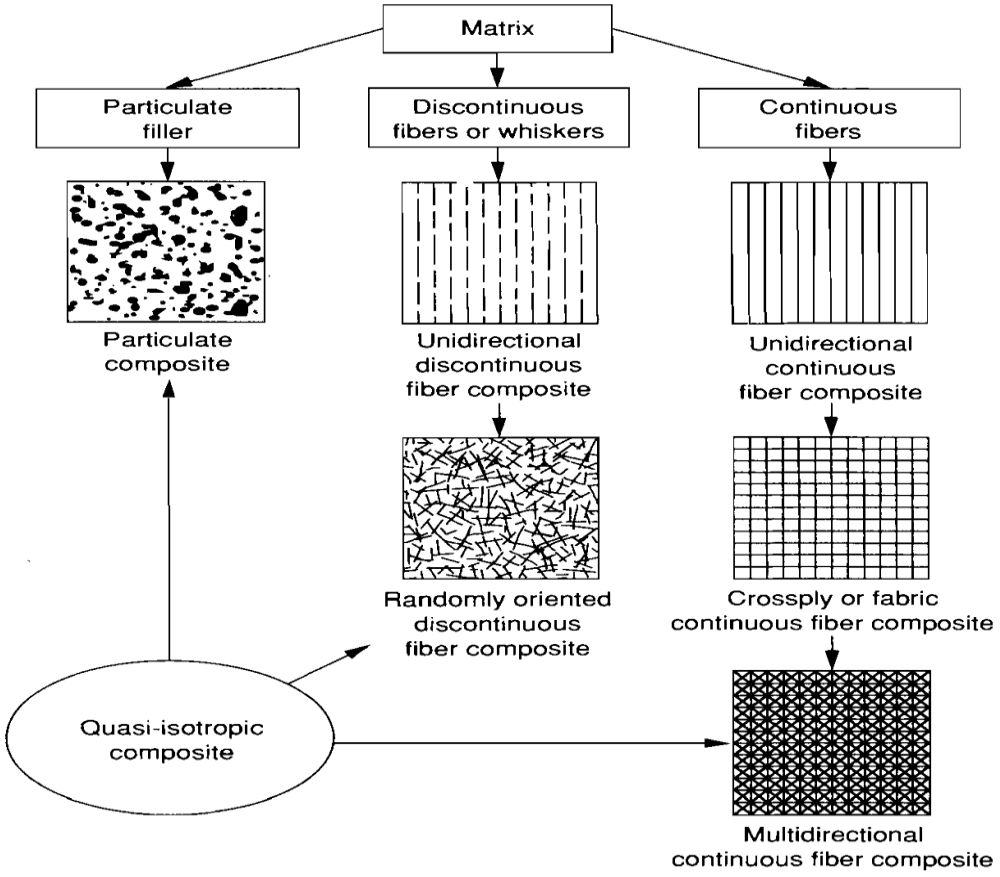

Figure 2.1 Classification of Composite material System [Daniel, I.M, 2006 [22].

The main reason behind using fillers in polymeric matrices is a function of the intended properties these filler materials are proposed to contribute. However fillers may also be specifically introduced to improve toughness, stiffness, hardness and impact strengths providing dimensional stability. Fiber-reinforced polymeric composites are being predominantly used in many structural components in the aircraft, automotive, marine and other industries because of their low density, high stiffness to weight ratio and high strength. Ideally, structural materials are isotropic in nature in that, they exhibit equal properties in any orientation irrespective of the direction of measurement. However, the structural properties of fiber reinforced composites strongly depend on the direction of reinforcement.

Results have shown that the strength and modulus of fiber-reinforced composites attain a maximum when they are measured in the direction parallel to the fiber axis i.e. in the longitudinal direction. Results being observed at other orientations of fiber, shows a lower value which is at a minimum when the fibers are at 90^{o} to the longitudinal direction of fibers (transverse/out-of-plane direction) or in the thickness direction (Z axis-direction).

Another unique characteristic of the fiber-reinforced composites is their high internal damping, enhanced electrical conductivity, good thermal properties and absorption of vibrational energy within the material resulting in reduced transmission of noise and vibration to neighboring structures. This characteristic is very beneficial in many automotive and aerospace applications in which this positive effect would create a greater comfort for passengers. Good corrosion behavior is another added advantage of the fiber-reinforced polymers.

2.2 Laminated Composite Materials

A form of composite structures employed in engineering applications is composite laminates [58-60] which are basically assemblies of layers of fibrous composite materials which can be laid up to provide required engineering properties, including bending stiffness, coefficient of thermal expansion, in-plane stiffness and strength,. The individual laminas consist of high-strength, high-modulus fibers in a polymeric, ceramic matrix and metallic matrix material. Typical fibers used for laminated composites include carbon, glass, silicon carbide, graphite, boron, and other matrix materials are epoxies, alumina, aluminum and polyimides.

Materials of different layers can be fabricated, resulting in a hybrid laminate [61]. The respective individual layers are generally orthotropic (that is, with principal properties in

orthogonal directions) or transversely isotropic (with isotropic properties in the transverse plane) with the laminate exhibiting anisotropic (with variable direction of principal properties), orthotropic, or quasi-isotropic properties. As shown in figure 2.2, quasi-isotropic laminates exhibit isotropic (that is, independent of direction) in-plane response but are not restricted to isotropic out-of-plane (bending) response. Due to fiber orientation of the individual layers, the laminate may exhibit coupling between in-plane and out-of-plane response. An example of bending-stretching coupling is the presence of curvature developing as a result of loading laminate composite in the in-plane direction.

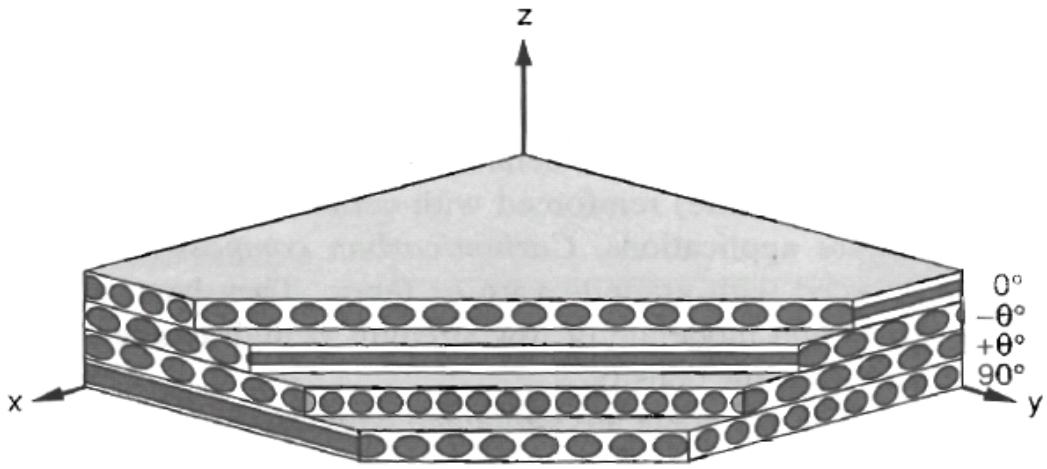

Figure 2.2 Cross-section of a typical multidirectional laminated composite [Daniel, I.M, 2006 [22].

2.2.1 Failure Modes of Laminated Composite Materials

Failure in laminated composite materials can occur in different modes such as matrix micro cracking, fiber matrix de-bonding, and separation of individual laminae from each other (delamination) [27-28,62]. Amongst these failure modes, delamination is the most fundamental mode of failure due to the existence of interlayer created by laminated composite. Delamination

is a matrix dominated failure which is susceptible to crack initiation and growth along the interface between two adjacent laminae.

This effect is severe in laminated composite since there are usually no reinforcement in the through-the- thickness direction that would carry the load in the out-of–plane direction (z-direction) so as to resist or mitigate crack propagation at the ply interface. When composites are subjected to complex or combination of simple loadings, delamination can cause the materials to fail at strengths well below their maximum load carrying capacity which eventually leads to catastrophic failure of the material in service. Previous results have also shown that external loading of laminated composite material may also induce delamination, whether under dynamic or static loadings for e.g. in-plane, bending or fatigue loading and also poor fabrication process can also induce this effect. Impact loading is also a damage contributing factor since these damages are usually not visible to visual inspection and they occur within the material interface which is known to be stress raisers.

Delamination are susceptible at sites located within and around the composite panel with poor load carrying capacity for e.g. free edges, bonded lap joints, moisture ingress [63-66], bolted joints etc. The mismatch of coefficient of thermal expansion between adjacent plies and the Poisson's ratio effect are primarily responsible for giving rise to interlaminar shear stresses. Since delamination usually occurs at interlaminar region between plies, there exist both interlaminar shear and tensile stresses at the interface which leaves laminated composite to susceptible to a mixed mode failure process rather than a pure shear failure effect.

Various techniques have been developed to measure the interlaminar shear strength of laminated composites under different loading. Therefore, creating a 3D hierarchical structure of

fiber reinforcement which creates a new interfacial property that is different from that of the bulk phase will help inhibit the effects of delamination in laminated composite materials. Research has also shown that CNTs are well placed to utilize there multifunctional and exceptional properties to improve the interlaminar properties of composites [1-4, 61]

2.2.2 Matrix-Dominated Composite Properties

To improve the usage of composite in structural application, composite materials have to be designed to withstand impact damage [67] and its consequences which also include delamination. In order to tackle this problem, it means that interlaminar shear properties in traditional laminated composite as shown in figure 2.3 will have to be reinforced in the transvers direction (2- direction) and the through-the-thickness direction (3-direction). The interlaminar properties in these directions are usually controlled by the mechanical properties of the matrix material which are very weak in these failure modes.

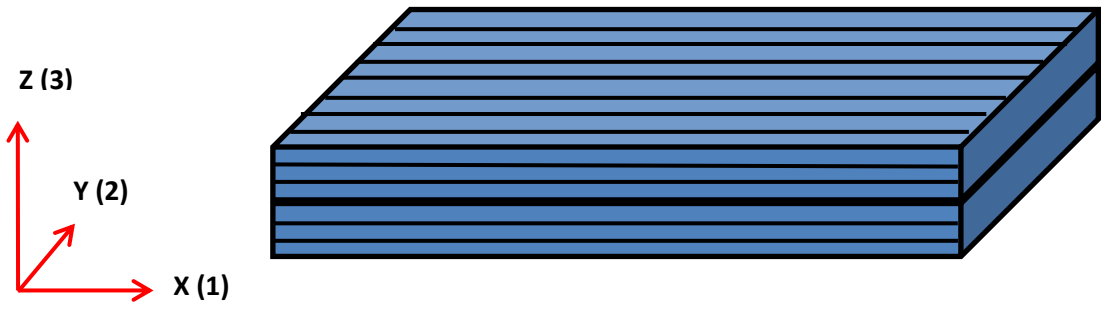

Figure 2.3 Schematic of unidirectional composite lamina and coordinate system.

The matrix constitutes the weaker phase in composite materials and a variety of efforts have been made to modify the matrix by either with the use of toughened epoxy matrix or dispersion of nano particles in the matrix in order to improve their fracture toughness (particles include carbon nano fibers, CNT particles, silica, clay and expanded graphite). Progress has been

made with the use of this technique with the addition of 1-5% volume fraction of the nano particles.

An inherent problem with this technique has to do with particle dispersion which creates an increase in viscosity build-up in polymer matrix due to increased inter-particle interaction. To overcome this problem, a technique of creating a 3D composite structure with CNT arrays and bundles placed in the through-the-thickness (3-direction) with possibility of a higher volume fraction is being done in this work.

2.3 Carbon Nanotubes (CNTs)

Like diamond, graphite and fullerenes (C60), carbon nanotube (CNT) is another form of carbon with a cylindrical nanostructure reported first by Iijima in 1991 [7]. CNT consists entirely of the sp^2 carbon, which bonds to three neighbor carbon atoms. The carbon bonds in a CNT are similar as those in graphite, but stronger than the sp^3 carbon bonds found in diamond. Depending on the diameter and the arrangement of C-C and C=C bonds along the nanotube length, CNTs could exhibit extreme diversity and richness in structure-related properties [23]. Table 2.1 shows the exceptional properties of CNTs.

Table 2.1. Showing the exceptional properties of Carbon nanotubes for High-end Engineering application.

Properties of carbon nanotubes (CNTs).	Mechanical properties of carbon nanotubes (CNTs)
Stiffness	Elastic modulus: as high as 1 TPa (Dependent on their structure and diameter)
Strength	Tensile strength: as high as 50 GPa. Failure strain: around ~8%
Current density	4×10^9 A/cm^2
Thermal conductivity	MWNT : (600 W/m-K)
Thermal stability	2800°C in vacuum (450°C in atmosphere)
Aspect ratio	~1000 (length/diameter ratio)

CNTs can consist of only one single layer of the graphitic sidewall to form single-wall CNTs (SWNTs). There may be additional graphitic sidewalls around the SWNT core to form multi-wall CNTs (MWNTs). The nanotube lengths for both SWNTs and MWNTs can be up to hundreds of microns or even centimeters while their diameters are normally less than 100 nm. Compared with MWNTs, SWNTs often show less defects with a shell of sp^2 hybridized carbon atoms forming a graphitic hexagonal network. CNTs have attracted considerable interest for a wide range of potential applications [68-70].

2.3.1Carbon Nanotube Synthesis by CVD Method

The process of producing carbon nanotubes using CVD method dates back to 1993 [71]. This process has been the most widely used over other carbon nanotube synthesis process since large

scale production with well aligned nanotubes can be achieved through this process. The CVD process for growing carbon nanotube growth is shown in Figure 2.4.

The system for CVD method is simpler than those of laser and arc method. A substrate (usually of silicon wafer, stainless steel plate or quartz plate) is heated up to about 1000-1200 ºC in a furnace controlled atmosphere. Carbon based precursors, such as methane, ethylene, acetylene, or mixed gas, is injected into glass chamber and decomposed right at the surface of metal catalyst particle [72] (e.g. iron, cobalt or nickel etc.) which is pre-coated on the substrates to provide the necessary recipe for CNT growth.

The size of these metal particles catalyst will affect the diameters of the resultant nanotubes. By extending growth processes used in semiconductor industry, CVD can be used in conjunction with E-beam lithography to produce patterned CNT array which are beginning to have diverse application in nano composites and electronics industry.

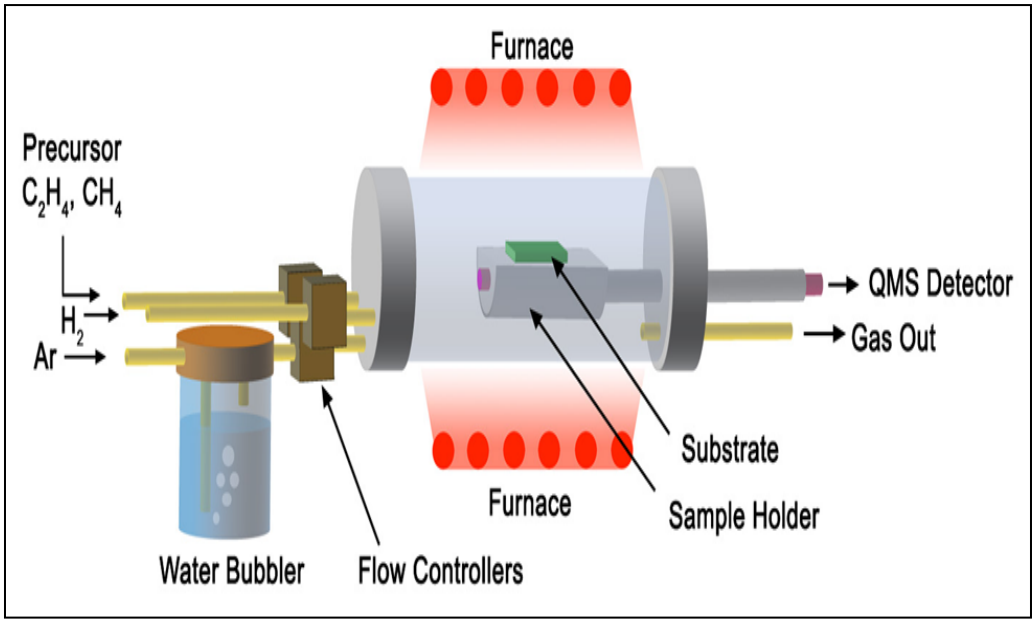

Figure 2.4 Schematic illustration of Chemical Vapor Deposition (CVD) synthesis [Figure by Dr. Sergey Yarmolenko, North Carolina A&T State University with permission].

2.4 Polymeric Composites Reinforced with Dispersed Carbon Nanotubes.

Due to the exceptional properties of CNTs i.e. (mechanical, electrical, and thermal) [8, 9], a great amount of research of CNTs have been explored and more work is being done to tailor the properties of polymeric materials to yield multifunctional nanocomposite. Recent work in this field shows that researchers are adopting a variety of methods to develop these multi-functional composites with varying levels of success [73-78].

Basically, in order to achieve a reasonable level of success, it is paramount to into consideration these steps in fabricating CNT polymer composites which include CNT synthesis and purification process, their alignment in the matrix, reinforcement architecture, geometrical and structural properties of the CNTs, and the fabrication process. In the following sections, different fabrication processes of CNT composite will be highlighted and emphasis will be placed on key processes which in turn leads to a more structurally stable nano engineered material. The multi-functional properties of CNT polymer nanocomposite and the factors that influence these properties can then be explored both from theoretical and experimental standpoints.

2.5 Critical Issues in Polymer Nanocomposite

Just as in traditional fiber composites, the major challenges in the research of nanocomposite can be categorized in terms of the structures from nano, micro to macro levels. There is still considerable uncertainty in theoretical modeling and experimental characterization of the nano-scale reinforcement materials, particularly nanotubes. Then, there is a lack of

understanding of the interfacial bonding between the reinforcements and the matrix material from both analytical and experimental viewpoints. Lastly, the challenges at the level of nanocomposites have mainly to do with the following issues related to composites processing:

2.5.1 Functional Interface (Fiber and Matrix)

In the processing of nanocomposites, carbon nanotubes need to be separated from bundles and dispersed uniformly or used as a bundle in a polymer matrix for maximizing their contact surface area with the matrix. Modification of nanotube surfaces, for example, the creation of covalent chemical bonds between nanotubes and the polymer matrix, enhances their interactions and gives rise to higher interfacial shear strength than van der Waals bonds [79-83]. The two major approaches to functionalization are chemical methods and irradiation with electrons or ions. The chemical methods involve the attachment of chemical bonds to either the nanotube ends or sidewalls.

First, nanotube caps, which are more reactive because of their high degree of curvature, can react with a strong acid. The open ends can be stabilized by carboxylic acid and hydroxide groups. Chemical functionalization of nanotubes can also be accomplished through irradiation with electrons or ions. Electron irradiation of carbon nanotubes causes their collapse in an anisotropic manner due to the knockout of atoms in the nanotube walls [29]. Ion deposition can induce cross-links between nanotubes in the bundle and between shells in MWNTs, which could lead to efficient load transfer among the tube layers.

In their tailoring the interface of MWCNT/polymer composites, nanotube chemical modification, Bao J.W. and co-workers [84] first attached carboxylic acid to the tube surface as seen in figure 2.5. This was followed by further reactions to attach di-glycidyl ether of

bisphenol-A-based epoxide resin. It is then possible to further react with the epoxide functional group to enable better interaction between the polymer matrix chains of the composite and the surface of the nanotube.

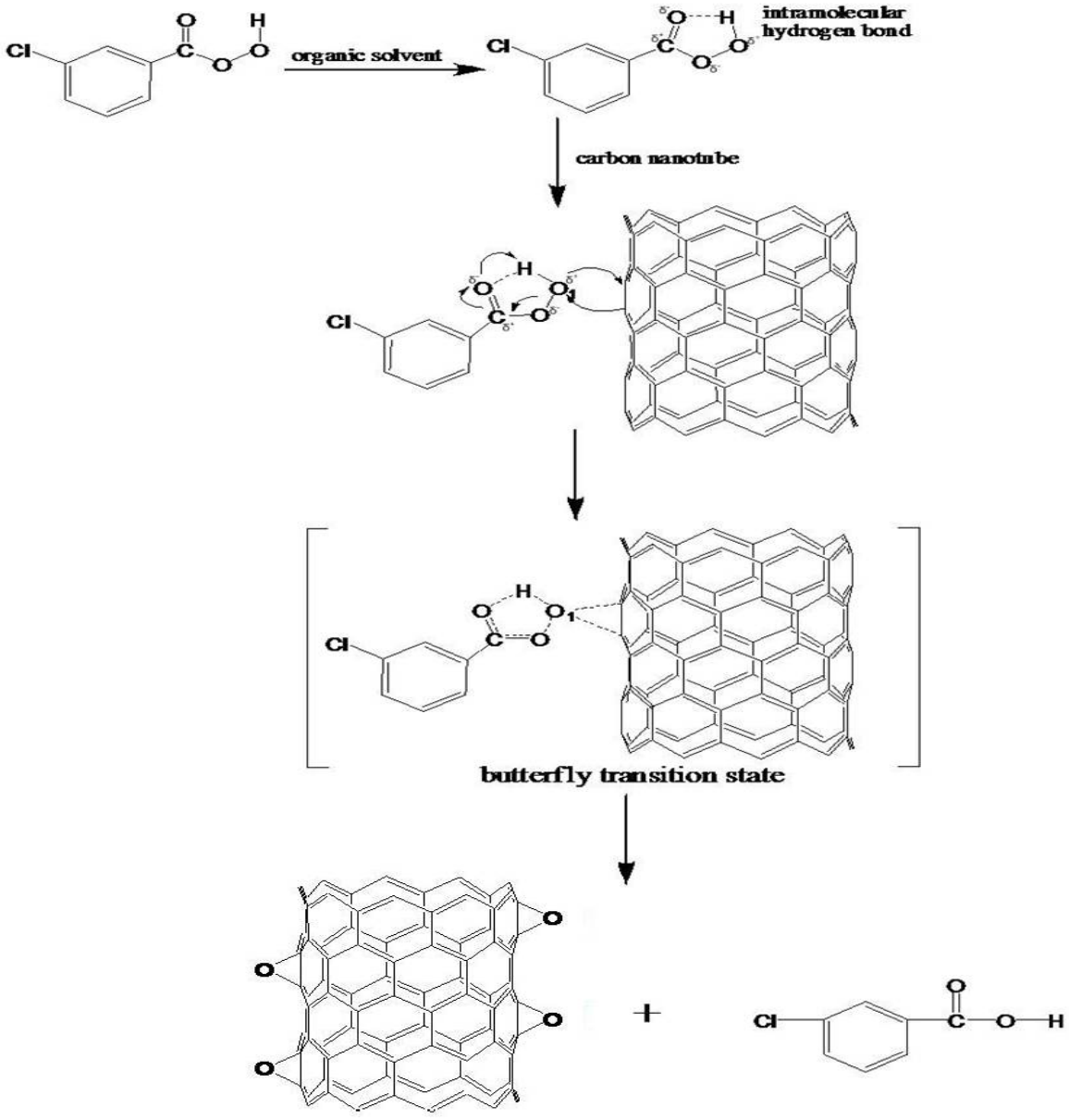

Figure 2.5 Mechanism of functionalizing nanotube using m-CPBA [Bao, J. W., et al. [84].

2.5.2 Dispersion of CNT

Uniform dispersion of nanoparticles and nanotubes against their agglomeration due to van der Waals bonding is the first step in the processing of nanocomposites. Beside the problems of agglomeration of nanoparticles, exfoliation of clays and graphitic layers are essential. SWCNTs tend to cluster into ropes and MWCNTs produced by chemical vapor deposition are often tangled together like spaghettis. The separation of nanotubes in a solvent or a matrix material is a prerequisite for aligning them.

2.5.3 CNT Alignment

Because of their small sizes, it is exceedingly difficult to align the nanotubes in a polymeric matrix [85] material in a manner accomplished in traditional short fiber composites. The lack of control of their orientation (e.g. CNT dispersion or through-the-thickness orientation) diminishes the effectiveness of nanotube reinforcement in composites whether for structural or functional performance.

2.5.4 Volume fraction and rate of Fabrication

High volume and high rate fabrication is fundamental to manufacturing of nanocomposites as a commercially viable product. Results have shown that increasing the volume fraction of reinforcement phase in composite material usually increase the strength of the material [86].

However, an optimum amount needed for better mechanical and electrical properties etc. should be well defined since excess amount of reinforcement sometimes result to incomplete wetting of fibers, CNT agglomeration, uneven dispersion etc. The lessons learned in the fabrication of traditional fiber composites have clearly demonstrated that the development of a

science base for manufacturing is indispensable. Efficiency in manufacturing is pivotal to the future development of nanocomposites.

2.5.5 Cost of CNT

Besides high volume and high rate production, the cost of nanocomposites also hinges on that of the nano reinforcement material, particularly, carbon nanotubes. It is anticipated that as applications for nanotubes and their composites increase, the cost will be dramatically reduced. This also points to the fact why presently, lower volume fractions of CNTs are being used for structural composite reinforcement so as to keep the cost of these products affordable.

2.6 Processing Methods for CNT Reinforced Composite

A number of fabrication methods are available for producing CNT/polymer composites based on the properties of the matrix which can be either thermoplastics or thermosets. Although the processing techniques are inherently different, they all try to address issues that primarily affect the composite overall properties, such as CNT dispersion, interfacial bonding, alignment, transfer printing and CNT growth on fibers [36, 37].

The effective utilization of carbon nanotubes in composite applications depends strongly on their ability to withstand high strain to failure, uniformly align them throughout the matrix without destroying their integrity or reducing their aspect ratio [85]. Below, are a few processing methods used for fabrication of CNT reinforced polymer nanocomposite.

2.6.1 Resin Transfer Molding (RTM)

Resin transfer molding is a composite fabrication process which is usually carried out in a closed mold [86]. The critical issues involved in this process are fiber infiltration or wet-out and

resin flow. Fiber wet-out is a function of fiber architecture, orientation and permeability of the preform while resin flow takes into account fiber infiltration through the planes and also in the transverse direction. Researchers in both fiber design and resin manufacturing technology have made these critical issues a lot easier to handle and a high volume fraction of fiber in composites is now achievable. Figure 2.6 shows the steps required to fabricate composite through this process.

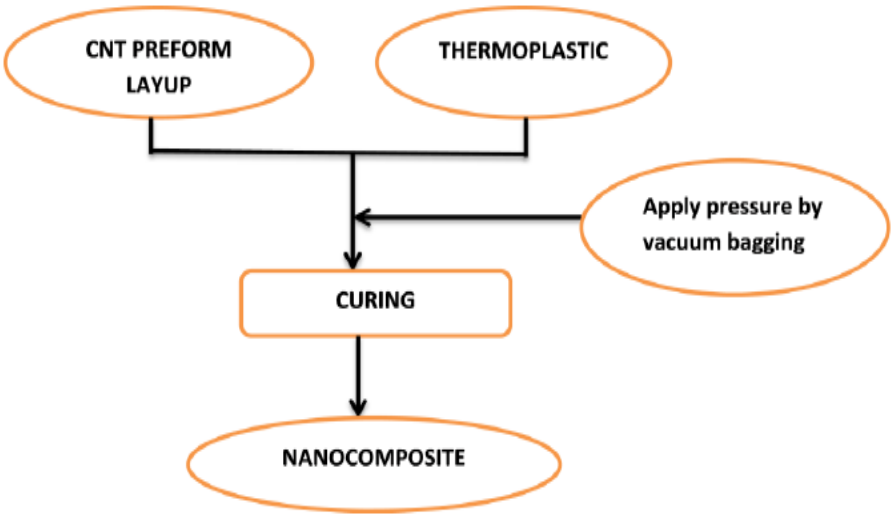

Figure 2.6 Flowchart presenting the different steps of Resin Transfer Molding process.

2.6.2 Vacuum Assisted Resin Transfer Molding (VARTM)

This process is an advanced modification of RTM since resin flow and infiltration of the fiber preform is carried out in a vacuum medium with the simultaneous application of vacuum pump for taking air out of the vacuum bagging area while taking in resin from the opposite end for easy wetting of fiber preform. VARTM [87] is more advantageous than the RTM since a more uniform resin distribution is achieved, more complex parts, low cost of production at higher production rates, higher volume fraction of reinforcement can be achieved. The viscosity

of the resin is quite critical in this process since wetting is carried out by a vacuum process. The addition of nano constituents to the resin matrix prior to fiber wetting is not an option for this process since it further increases the viscosity of the resin.

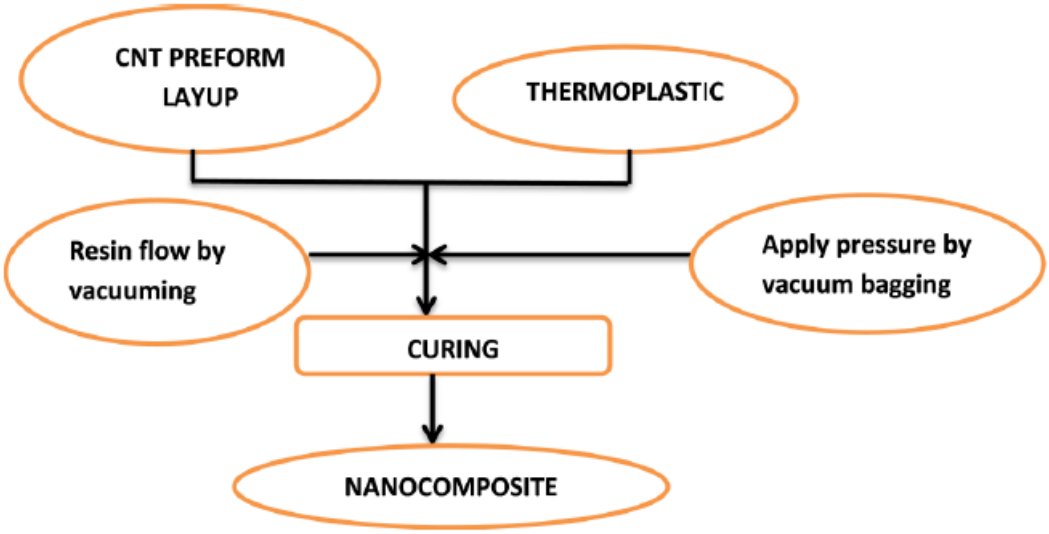

Figure 2.7. Flowchart presenting the different steps of Vacuum Assisted Resin Transfer.

2.6.3 Solution Processing of Composites

Perhaps the most widely used method for processing polymer nanotube composites has been to mix the nanotubes and polymer in a suitable solvent before subsequently evaporating the solvent to form a well dispersed composite film. The choice of solvent is generally made based on the solubility of the polymer.

The advantages of solution-based method provide a reasonable advantage through low viscosities, which facilitate mixing and dispersion of the CNTs [88]. Many researchers have used these methods for fabrication of both thermoset and thermoplastic polymers [88]. Agitation of the nanotubes in a solvent is one of the advantages that facilitate nanotube de-agglomeration and

dispersion. Majority of all solution processing technique follows a general theme with a little variation here and there which can be summarized as

1. Dispersion of nanotubes in either a solvent or polymer solution by energetic agitation.

2. Mixing of nanotubes and polymer in solution by energetic agitation.

3. Controlled evaporation of solvent leaving a composite film.

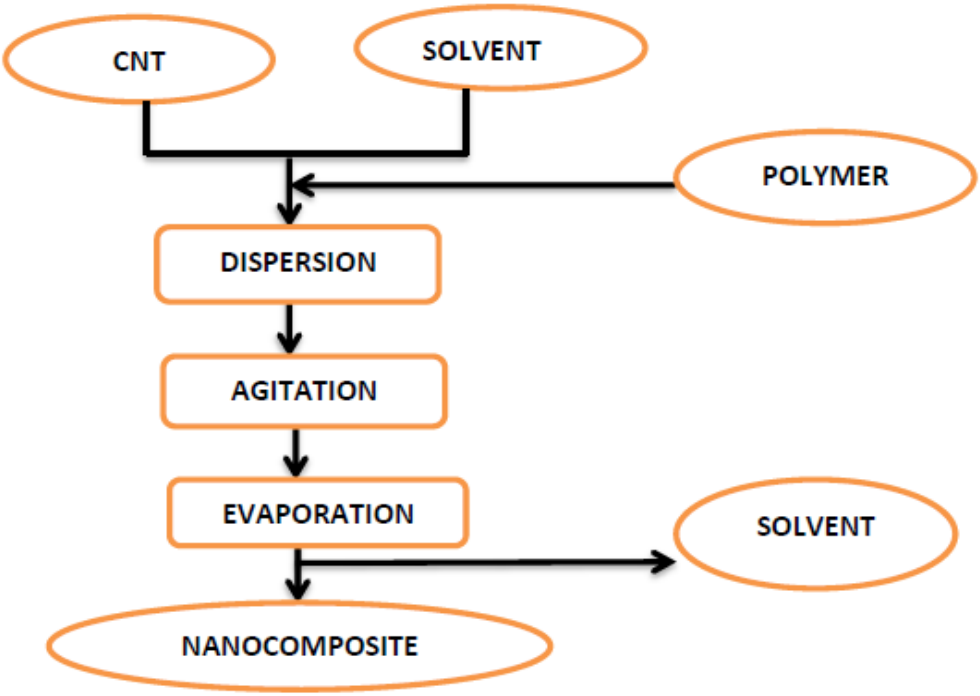

Figure 2.8 Flowchart presenting the different steps of the solution processing.

2.6.4 In-situ Polymerization

This fabrication method [89] involves the dispersion of nanotubes in monomer followed by polymerizing the monomers. As with other processing methods, functionalized nanotubes help improve the initial dispersion of the nanotubes in the liquid (monomer, solvent) and consequently in the composites using different condensation reaction. This process has been

extensively explored for the preparation of polymer nanotube composites, its main advantage being the creation of a covalent bond between the tube and the matrix.

The presence of polymeric chain onto the tubes surface facilitates their dispersion providing a strong interface at the same time. This technique allows the preparation of composites with high CNT loading, which has been shown by researchers [89] to improve the strength and stiffness of CNT composite. Figure 2.9 shows the flowchart for in-situ polymerization processing. The process can be summarized by the underlining sequence;

1) The nanotubes are dispersed in the monomer and the reaction is initiated.
2) For the thermosets such as epoxies or unsaturated polyesters, a curing agent is added to initiate the polymerization. For thermoplastics, the polymerization can be initiated either by the addition of an initiator or by an increase of temperature.
3) Production of a CNT polymer composite film after polymerization.

In studies involving epoxy, Vigolo et al [90] developed a coagulation spinning method to fabricate a nanotube/polymer composite with very high CNT loadings which predominantly comprise nanotubes.

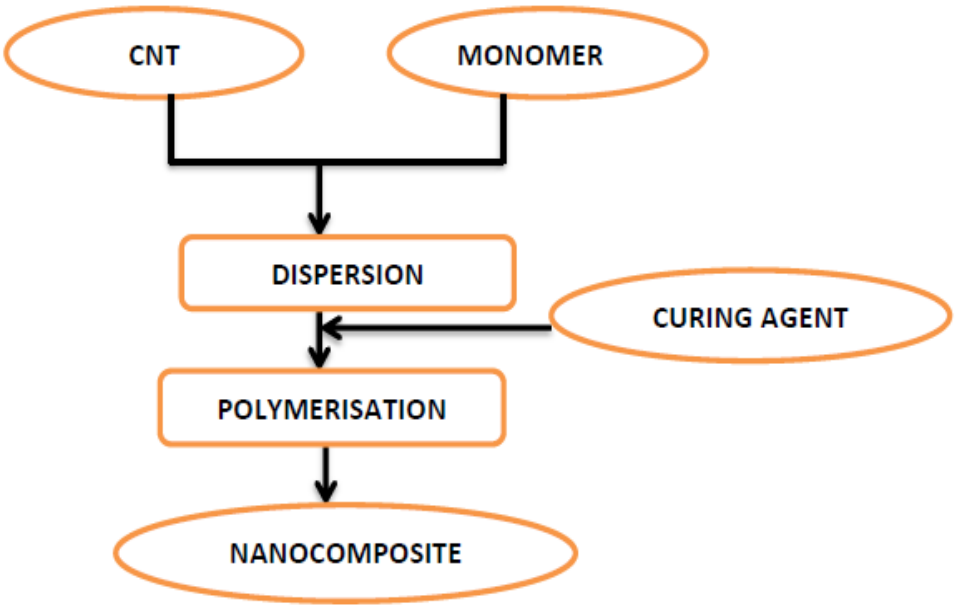

Figure 2.9 Flowchart presenting the different steps of the in-situ polymerization processing.

2.6.5 Melt Blending

In this process, the procedure entails blending a molten thermoplastic with the nanotubes in order to create an optimum blend between the polymer-nanotubes interactions and form a nanocomposite. Melt blending incorporates high temperature and high shear forces to disperse nanotubes in a polymer matrix and is most compatible with current industrial practices. These methods are also beneficial because they are free of solvents and contaminants, which are present in solution processing methods and *in-situ* polymerization [88].

However, relative to solution blending methods, melt blending is generally less effective at dispersing nanotubes in polymers and is limited to lower concentrations due to the high viscosities of the composites at higher nanotube loadings.

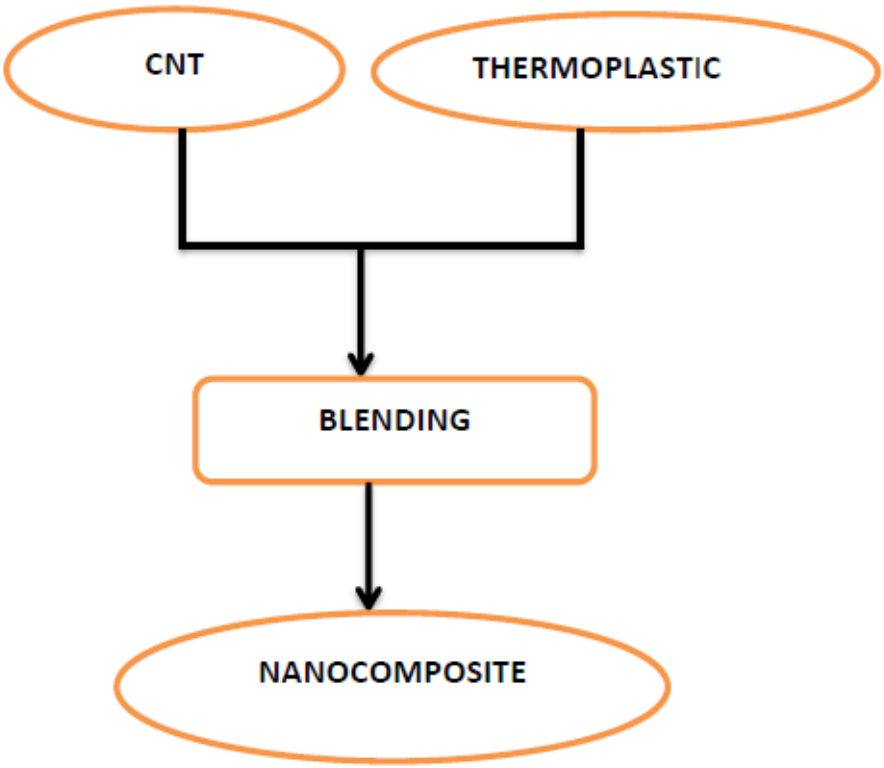

Figure 2.10 Flowchart presenting the different steps of the melt blending processing.

2.6.6 Other Processing Methods

A variety of novel composite fabrication methods have also been adopted by researchers which have shown little or significant improvement in strength and toughness of CNT composite materials. They are generally, optimization of existing fabrication processes in order to produce a much better structural properties of CNT reinforced composites.

2.6.6.1 Bucky Paper Composite Film

One these novel methods that have gained significant contribution in the fabrication of nanocomposites are the Buckner filtration method otherwise known as Bucky paper composite. This method involves the infiltration of polymer from solution into pre-existing nanotube networks of CNT sheets. In 2003, Coleman et al. [91] first used this fabrication process. First, thin sheets of SWNT were made by Buchner filtration (Bucky paper).

The structure of the sheet is very much porous and contains up to 70% free volume. These as produced sheets were then soaked in polymer solutions for various times before rinsing. SEM images of fracture surfaces showed that the polymer had infiltrated throughout the paper. In addition, the advantage of this process is that it allows for high loading of CNT in the composite in excess of >40%.

2.6.6.2 Layer by Layer Assembly Method

This method was first described by Mamedov [92] and has been subsequently refined by other researchers [93, 94]. This procedure involves building thin film composite layers by alternate dipping of substrate into a dispersion of CNT and polyelectrolyte solution. Using this process, large amount of layers can be built up depending on the point of interest.

Cross-linking can be induced into the process in order to further enhance the structural integrity of the film. After numbers of the desired deposition cycle, a layer of CNT could be replaced with a layer of the polymer resin of interest to introduce carboxyl functionalities for amide cross-linking between polyelectrolytes.

2.7 Review of Related Work

The unique structure and remarkable properties of carbon nanotubes have led to a new dimension of research efforts worldwide. Most of the studies have majorly been centered on the characterization of mechanical, electrical and thermal properties of both SWNTs and MWNTs [57, 95]. Carbon nanotubes have a reported Young's modulus and tensile strength of up to 1 TPa and 60 GPa, respectively, while their densities have been estimated to be as low as 1.3 g cm^{-3} [96,97].

As a result, much work has been put in to incorporate nanotubes into conventional materials (such as polymers) in order to improve both in-plane and interlaminar shear strength and electrical conductivity [61, 74-77]. Moreover, many potential engineering applications have been envisioned for carbon nanotubes, including conductive and high-strength composites; sensors; field emission displays and radiation sources; hydrogen storage media and nanometer-sized semiconductor devices; devices for power storage and conversion probes and interconnects [98].

Composite materials consisting of a polymer and CNT reinforcements with very little addition often exhibit improved mechanical, electrical and thermal properties when compared to those of unreinforced polymers. Improved properties include increased strength, high modulus, and high electrical, thermal and thermo-mechanical stability. However, the degree of improvement of thermal and mechanical properties of epoxy-based nanocomposites materials actually depends on the inherent properties of MWCNTs and matrix, reinforcement orientation and also on the fabrication process used for the nanocomposites.

A study [99] has shown that tube diameter, wall thickness, tube length, high CNT loading and level of defects has been found to play a major role in the mechanical properties of CNT fibers and bulk arrays than did tube waviness and initial tube alignment.

The use of CNTs as a primary and secondary reinforcement phase for the improvement of in-plane and out-of-plan interlaminar shear strength, electrical conductivity and fracture toughness have been achieved by reinforcing the polymer in through-the-thickness direction [100-103] and has also been a subject of further research in improving its multifunctionality. Carbon fiber as primary reinforcement has been the most reliable reinforcement for polymer

matrix for high strength and advanced composite due to its very high strength, elastic modulus and stiffness.

Due to the critical drawback encountered in textile structural composites which is mostly the presence of micro sized gaps that is filled by the matrix rich region between the interwoven fiber bundles and the matrix dominated regions which lie in between the individually stacked laminate. These regions are usually points of crack nucleation, growth and failure and are difficult to reinforce with traditional microscale fiber reinforcement. Limited success has been achieved with the use of various nanoscale materials for selective reinforcement of matrix-rich region [102].

Due to their nanoscale diameter and other properties embedded in CNTs, it has been suggested that carbon nanotubes (CNTs) are the ideal candidate for reinforcement of micro size gaps in the matrix-rich interlaminar regions [1-4]. In a recent study, Fu-Huang Zhang [104] studied the interfacial strength of epoxy based composite of T300 carbon fiber/ CNT interface. His result showed that the interfacial strength of the hybrid composite was 150% higher than that of the as-received T300 fiber composite. The mechanism for this improvement was interpreted as chemical bonding, Van der Waals binding, mechanical interlocking, and surface wetting. Also, a similar result was achieved by Enrique J. Garcia [105] where he directly grew CNT arrays on woven alumina fabric cloth through a CVD process and demonstrated an improvement of 69% in interlaminar shear strength and an improvement in electrical conductivity both (in-plane) 10^6 and (through-the-thickness) 10^8 direction.

A novel approach which involved fabrication process of hybrid composite which was also conducted by Enrique J. Garcia [106] is the transfer printing process where Aligned CNTs were grown at high temperature and then transfer printed to a unidirectional carbon fabric

prepreg at room temperature, maintaining CNT alignment in the through-thickness direction. Results showed that CNT-modified interface increased the fracture toughness about 1.5–2.5 X in Mode I, and 3X in Mode II failure. The mechanism for toughening process was due to CNT bridging and interlayer process.

Another approach which also showed a promising improvement in properties of hybrid composite was investigated by Bekyarova et al [45]. This process involved electrophoretic deposition (EPD) of multi and single walled carbon nanotubes (CNTs) on woven carbon fabric. The CNT-coated carbon fabric panels were subsequently infiltrated with epoxy resin by vacuum transfer to fabricate a multifunctional composite. The result obtained also showed that there was an improvement of about 30% in the interlaminar shear strength as compared to the as-received carbon fiber composite and there was also a significant improvement in the electrical conductivity both in-plane and out of plane.

This shows that improvement and optimization of fabrication processes of composite material will go a long way in improving and imparting exceptional properties to advanced structural materials. A variety of other techniques to reinforce the laminate ply interface have also been adopted by other researchers. This is adopted towards improving the volume fraction of the CNTs phase in the composite since higher CNT loading will positively improve the interlaminar shear and in-plane properties of composites.

Another technique used for improving the mechanical properties composite is the "powder method" which was carried out by Li et al. [46]. The process adopted involve manually transferring vapor grown carbon nano-fibers onto the surface of CFRP laminates at the mid-plane by manually sifting the VGCF powders with a 70μm mesh directly and finally forming a VGCF interlayer in the mid-plane by consolidation using autoclave process. Arai et al. [47] also

adopted a CNT-solvent paste approach, e.g. CNF-ethanol paste, where the paste was applied manually on a CFRP prepreg using a metal roller. After evaporating the solvent on the prepreg sheets, the two parts of prepregs were bonded together and cured. A CNF interlayer of 50-200 μm in thickness at the interface was manually formed by evaporating the solvent in the paste and leaving behind a layer of CNF unto the surface of two parts of the prepreg before final consolidation.

Also, a spray gun deposition method [48] has also been used. This process involves coating the surface of CFRP by spraying a pre-dispersed CNT-solvent solution using a spray gun, and deposition of CNTs at the prescribed volume fraction on the fabric after evaporation of the solvent. This technique is limited to low CNT volume fraction because the thin films are obtained by either dispersing CNTs in solvents or dispersing CNTs in a resin using conventional processing methods which results in increased viscosity and agglomeration of the CNT particulates. However, the CNT contents in the laminate interlayers can be drastically increased if processes that can produce high volume fractions are adopted. CNT thin films known as Bucky-paper have recently been used to produce laminate reinforcement with high volume fraction using partially cured epoxy-CNF/CNT Bucky papers of high CNF/CNT contents in the ply interfaces of CFRPs. Khan and Kim [49] recently used this approach where the CNF Bucky paper was first impregnated with an epoxy resin by vacuum infiltration and then partially cured in between CFRP prepregs where the tacky surface of the prepreg was taken advantage of before curing to improve the interlaminar fracture resistance of the bulk composites.

Mechanical characterizations of the laminate composite interlayers have also been critically examined by various researchers using different interlaminar and intralaminar test methods and approach to estimate the effect of CNTs at the ply interface. These approach are

often known to have their advantages and disadvantages with respect to their abilities of creating pure shear failure at ply mid-plane rather than creating a mixed failure mode effect at the interlayers.

The interlaminar shear properties of laminated composites have been investigated [107] using the single lap shear adhesion test method. The adhesives used for reinforcement was infiltrated with evenly dispersed MWCNTs which were used to bond the carbon fiber/epoxy composites adherends together. Results showed that 46% increase in average shear strength due to the addition of 5 wt. % MWCNT into the epoxy adhesive. Also, Fan et al. [50] characterized the interlaminar shear strength of the composites using the short beam shear and compression shear tests methods. Results show that up to 33% increase in ILSS due to 2 wt. % MWCNTs. The preferential orientation of the MWCNTs in the thickness direction was found to contribute to the increase in the interlaminar shear properties.

CHAPTER 3

Mechanical Characterization of Laminated Composite Materials Reinforced With Carbon Nanotube Arrays

3.1 Materials for Fabrication of CNT Array Reinforced Laminated Composite

The constituent materials used in the fabrication of CNT array reinforced composite are an aerospace-grade unidirectional IM7/977-3 carbon fiber prepreg material and a 20µm high CNT array grown on a stainless steel substrate. To fabricate the composite panel, prepregs are removed from the refrigerator and brought slowly to room temperature. This is done so as to keep the resin on the prepreg intact and less tacky. Once the prepreg is brought to room temperature, they are placed on a cutting table and cut into respective orientation, length and width with respect to desired dimension based on prior calculation.

Here, a multi directional laminate is stacked and laid up to produce a balanced and symmetric quasi-isotropic laminated composite of $[0^o, 90^o, +45^o, -45^o, 0^o, 90^o, +45^o, -45^o, 0^o, 90^o]_s$ ply orientation. The prepreg is then cut with respect to the above named ply orientation followed by the layup of individual plies to produce a quasi-isotropic laminate.

3.2 Transfer Printing of VACNT Array on IM7/977-3 Carbon Fiber Prepreg

Transfer of vertically aligned CNT arrays on the prepreg is a critical part of the process since the feasibility and scale up of this process is highly dependent on the height of the VACNT array. Too high an array could result to incomplete resin wetting of the array hence, a reduction

in the overall performance of the hybrid composite. Based on previous research work done in this field [108], a 20µm high VACNT array was determined as the optimum height of array that would enable an optimum resin infiltration.

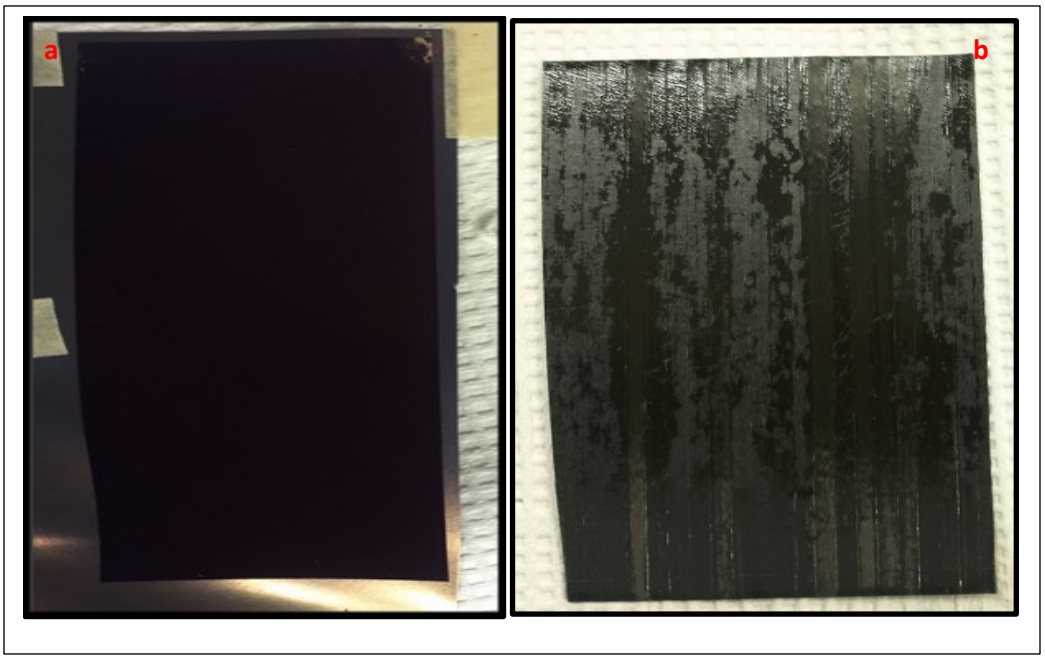

Figure 3.1. a) IM7/977-3 carbon fiber prepreg; b) 20 micron high VACNT array grown on stainless steel substrate [Materials provided by General Nano and Boeing Seattle].

The process of transferring the vertically aligned CNT array onto 19 plies of carbon fiber prepreg was done with the use of a moderately hot pressing iron and dry ice. Here, VACNT array grown on a stainless steel substrate as seen in figure 3.1a was inverted on the prepreg surface shown in figure 3.1b in such a way that a moderately hot pressing iron is placed on the stainless steel-back and slight pressure is applied while moving the hot pressing iron in a forward and backward stroke until the vertically aligned CNT arrays are fully transferred to the prepreg surface as seen in figure 3.2.

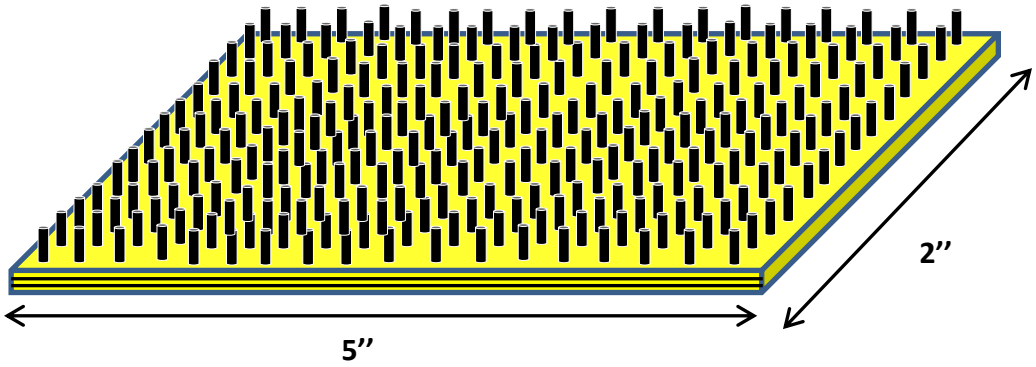

Figure 3.2. Drawing showing a fully transplanted 20µm high VACNT array on IM7/977-3 carbon fiber prepreg.

While the hot pressing iron is applied, a dry ice is also applied on the back of the steel substrate so as to create a cooling effect during the transfer process which enables the resin to cool very fast and in turn keeps the 977-3 epoxy in a B-stage cure regime where the epoxy remains tacky. The advantage of tacky surface of the prepreg is being utilized for effective transfer printing. The VACNT arrays are subsequently transferred on each of the 19 ply prepreg and the individual plies are stacked up based on the ply stacking sequence and ready for vacuum bagging process.

3.3 Mold Preparation

Mold preparation is an important step in composite processing since it helps improves the reliability and surface finish of the fabricated composite. It generally reduces the effect of inclusions, weak material properties, poor surface finish etc. The presence of any kind of dust or impurities on the mold before fabrication will ultimately effect the properties of final fabricated

sample. Here are some steps taken while preparing the mold for vacuum bagging and final curing:

1. Sanding the mold surface: Prior to vacuum bagging process and final layup of the prepreg, cleaning the surface of the mold is an important step which involves sanding the bottom surface of the mold with a sand paper (emery 400) in order to remove irregularities and contours on the surface of the mold. After sanding of the mold, a paper towel is dipped into acetone solution which is being used to wipe the surface so as to create a smooth and dry surface in no time due to fast evaporation of acetone. The mold is finally allowed to dry up for a while under room temperature.
2. Applying cleaner: After the first step, the mold is subsequently cleaned with XTEND CX-500 Cleaner (AXEL PRODUCTS, Cleaner). XTEND CX-500 Cleaner is a cleaner designed to create an effective surface adhesion of the release agent which is usually applied after this procedure. XTEND semi-permanent cleaner is designed to also remove styrene build-up. The cleaner was carefully applied on the surface of the bottom of the compression mold and applied by using a natural soft bristle brush. Also health and safety procedures were adhered to while applying the cleaner on the surface of the mold in order to mitigate any lab accidents like spills and skin burns etc. Personal protective equipment like Butyl Rubber Gloves, Goggles with side shields were worn while applying the cleaner on the mold to eliminate these effects. The mold was allowed to dry after the application of the cleaner. The cleaner is supposed to chemically prepare the surface of the mold for release agent.
3. Applying the release agent: After the cleaning and drying process is done based on the above steps, release agent is then applied on the surface of the mold. The release agent

when applied on the mold helps in easy removal of the composite sample, stainless steel block and bagging tape from the mold. Also, the release agent was thoroughly allowed to dry up after its application so it does not create spots on the surface of the sample during curing, hence; the release agent has to be carefully chosen. The release agent used is XTEND 19 SAM Release agent (AXEL PRODUCTS, Release) as seen in figure 3.3. It's an external mold release agent which can be used for all types of molds. A very thin layer of release agent was applied uniformly on the mold surface and stainless steel block. Two coats had to be applied with an interval of 10 minutes as directed by the manufacturer.

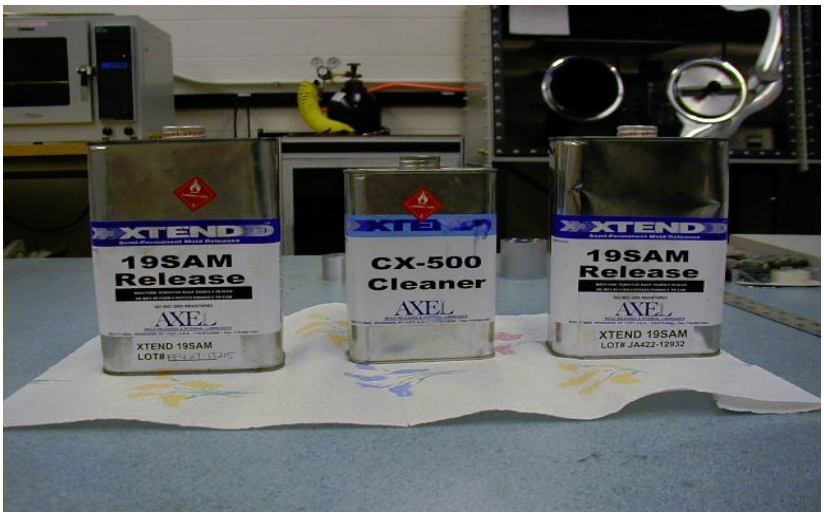

Figure 3.3. Image of XTEND release agent and cleaner used for mold preparation.

3.3 Vacuum Bagging Process

Once all the prepregs are laid in the desired sequence and fiber orientation, vacuum bagging preparations are made as shown in Figure 3.4 for curing and consolidation of the part. The steps required for vacuum bagging are:

1. A bleeder, a cloth with tiny pores, is placed directly on top and below the separator layer. The bleeder serves to absorb moisture and excess resin coming from the stack of prepreg composite sample.
2. Apply separator film directly on top and bottom of all the stacked up prepreg composite sample. The film is porous which allows entrapped gases and excess resins to escape. Peel ply fabrics are applied on the top and bottom of prepreg layers if consolidated parts are to be adhesively bonded at a later stage. The peel ply creates a good bondable surface finish on the fabricated part.

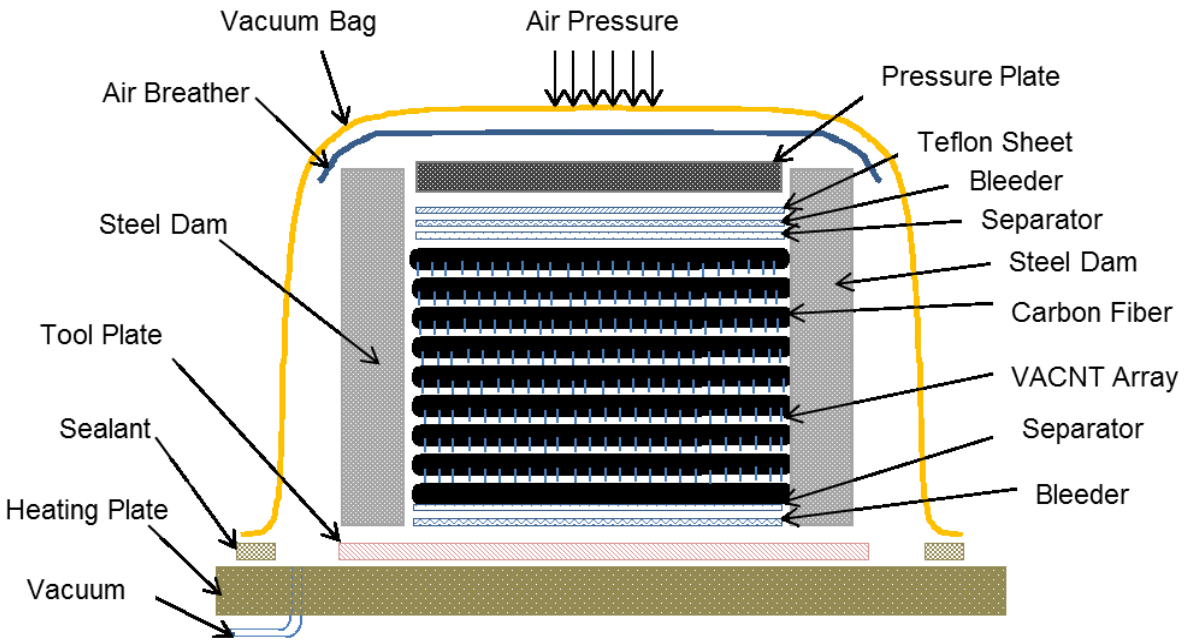

Figure 3.4. Short CNT array reinforced laminated composite fabrication process.

3. Apply a breather layer, which is a porous fabric that is quite similar to the bleeder. The breather helps create a uniform pressure around during the curing process while allowing air and volatiles to escape.

4. Apply a pressure plate, a stainless steel block of the same cross section with composite sample of interest. Its function is to create direct pressure on the sample when the vacuum bag is compressed. This creates a better interlocking between the transferred VACNT arrays and the carbon fiber prepreg during compression process.
5. Apply the air breather layer, a porous fabric which is similar to the bleeder. This shares same function with respect to creating uniform around the consolidated part.
6. Vacuum bag, the topmost layer, is a reusable elastomeric film. This film is sealed on all sides of the stacked prepreg using bagging tape. Once the vacuum bag is sealed up, the top mold is placed on the bottom mold and then ready for curing process. The bagging tape is a sticky elastomeric tape that adheres to both the vacuum bag and bottom mold.

After lamination and bagging, the mold is placed in between the top and bottom of a composite press machine for curing and consolidation. The composite press can equally maintain the desired pressure and temperature inside the chamber when the top and bottom of the press is fully closed due to application of load at the top and bottom. A typical cure cycle is shown in Figure 3.5 where the assembly is introduced into a composite press in which a vacuum (15 psig) is applied, and the specimens are cured following the manufacturer recommendations (100 psig) of total pressure, heat at 5^{o}F/min to 355^{o}F, hold for 6 h, cool at 5^{o}F/min to 140^{o}F and vent pressure and the let it cool to room temperature). The cure cycle depends on the type of resin material and the geometry of the part involved. The pressure required for composite consolidation is created in two ways: Using the steel block to apply direct pressure on the sample via compression of the vacuum bag as well as the external pressure inside the enclosed mold

via a high pressure line. The vacuum bag creates a vacuum inside the bagging material and thus helps in proper consolidation.

Care is taken to ensure that the vacuum is maintaned inside the bag by adequately sealing the bagging area and then connected to the vacuum pump using a hose. The vacuum pump squeezes air out of the bag and in turn compresses the stainless steel block directly on the sample for efficient consolidation. External pressure inside the closed press is created by injecting pressurized air through a high pressure line connected to the mold.

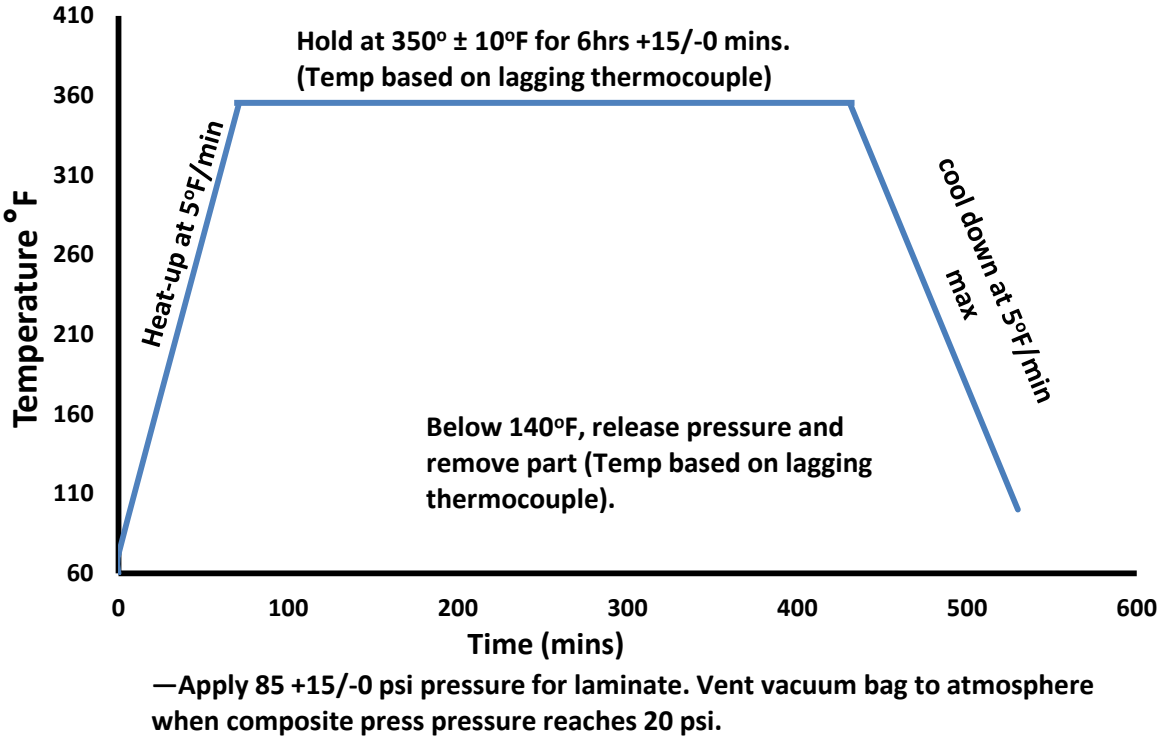

Figure 3.5. Recommended cure cycle for CYCOM 977-3 Epoxy.

Thus, the external pressure outside the bagging area and the vacuum inside the bag creates sufficient pressure to compact the laminate against the mold and create intimate contact between each layer. The heat for curing comes from heated air since the pressurized gas supplied

to the chamber comes heated to increase the temperature inside the composite press as seen in figure 3.6. The laminated composite panels for carbon fiber composite baseline sample and that of VACNT array reinforced laminated composite are then brought out of the mold after the consolidation process as shown in figure 3.7.

Figure 3.6. Automated composite press machine for composite fabrication process.

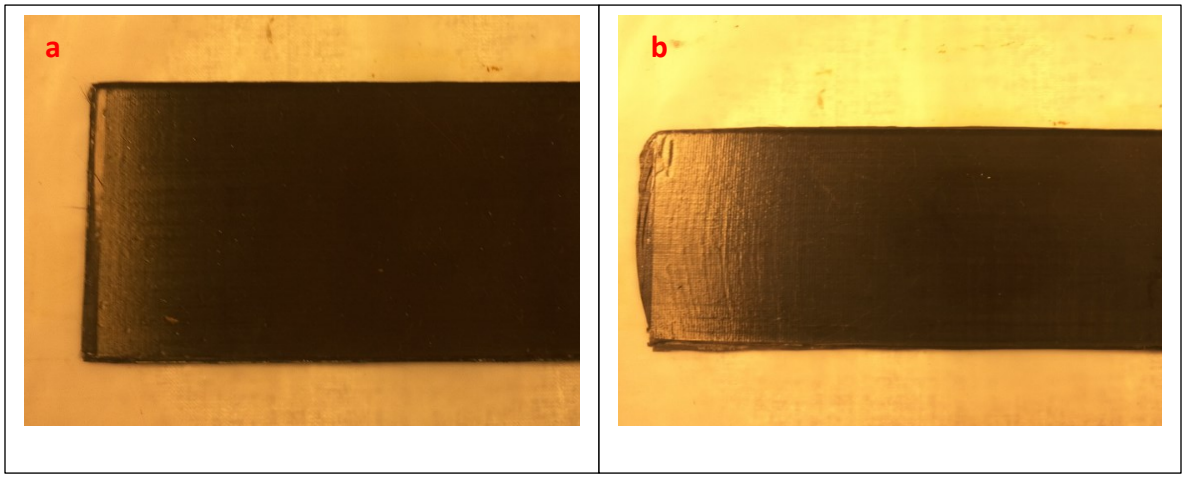

Figure 3.7. Image showing a) 20ply-CNT array reinforced composite; b) 20-ply carbon fiber baseline composite.

3.4 Composite Volume Fraction

Volume fraction of reinforcing phase in composite material is very important since it is known that these phases provide the mechanical properties needed for composite application [109]. With a multi walled carbon nanotube (MWCNT) used as a secondary reinforcement for improving the interfacial and interlaminar properties of state-of-the-art aerospace-grade carbon fiber composite prepreg for structural applications [106], it is important to quantify the volume of MWCNT that imparts such increase in properties in the high composite.

Typical IM7 977-3 carbon fiber prepreg with 62% of carbon fibers and 38% of epoxy matrix was used for this fabrication process. It is envisaged that the volume fraction of epoxy matrix would reduce due to the imprinting of VACNT array on the prepreg surface since the VACNT array will eventually occupy the spaces filled by the epoxy matrix by absorbing the epoxy. The parameters needed for calculating the volume fraction of MWCNT arrays are; the initial weight of prepreg before imprinting VACNT arrays(M_p), final total weight of prepreg after imprinting VACNT arrays (M_t), total weight of MWCNT arrays imprinted on prepreg(M_{mwcnt}), calculated volume fraction of MWCNT arrays (V_{mwcnt}) total volume of the composite (V)

The MWCNT wt. % can be converted to vol. % using the ASTM D3171-99 method. Therefore the weight of VACNT arrays will be;

$$M_{mwcnt} = M_t - M_p \tag{3.1}$$

Therefore, the VACNT volume fraction will be;

$$V_{mwcnt} = \frac{M_{mwcnt}/\rho_{mwcnt}}{V} \tag{3.2}$$

Where ρ_{mwcnt}, the density of the MWCNT arrays.

The volume fraction of the VACNT reinforced composite is estimated theoretically with parameters derived above. Here, the volume fraction of VACNT estimated is about 2.8% and the value is small since due to the height of the array which is in line with previous work [106, 108]. The volume fraction can be increased with denser CNT arrays with tight spacing in between the individual arrays but longer arrays will be detrimental to the mechanical properties based on previous work [108]. The nano reinforced laminated composite shows a high increase in interlaminar shear properties with shorter array height since it interlocks the plies much effectively than the longer arrays.

3.5 Sample Preparation for Mechanical Testing

After curing of the composite samples, both the baseline and the VACNT array reinforced composite plates were brought out of the mold. The edges of the 5" x 2" composite plates were first sectioned in order to create a well-shaped rectangular pattern so that the plates can be cut into the desired dimensions prior to testing. Three sets of test are to be performed on these samples namely;

1. Short Beam Shear Test
2. 3-Ponit Bend Flexural Test
3. Iosipescu Interlaminar Shear Test

For the short beam shear samples, five samples each from both 20-ply baseline laminated composite specimen and 20-ply vertically aligned CNT array reinforced laminated composite specimen were cleanly cut from the bulk composite panel using Beuhler ISOMET 1000 diamond abrasive cutting machine. In order not to create notches and delamination on the samples during

preparation, the rotation of the circular diamond saw blade was kept at a low speed and dimensions were marked on the panel in order to achieve a better dimensional tolerance of all samples. Based on ASTM specification for short beam shear test, the span-to-thickness ratio is 4 as recommended [110] and Figure 3.8 shows the nominal dimension sample.

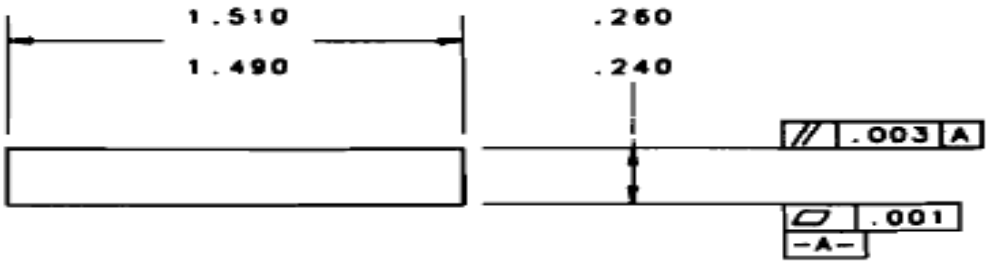

Figure 3.8. Nominal dimension for Short Beam Shear Sample [ASTM D2344/D2344M [110].

For the 3-point bend test samples, three samples each from both 20-ply baseline laminated composite specimen and 20-ply vertically aligned CNT array reinforced laminated composite specimen are cleanly cut from the bulk composite panel using Beuhler ISOMET 1000 diamond abrasive cutting machine. In order avoid creating notches and delamination on the samples during preparation, the rotation of the circular diamond saw blade was kept at a low speed and dimensions were marked on the panel in order to achieve a better dimensional tolerance of all samples.

Based on ASTM specification and nominal sample dimension [111] , the basic difference difference between the short beamshear test and 3-point bend test is the span-to-thickness ratio. ASTM D790 specification with a span-to-thickness ratio of 10:1 was used for cutting the samples into the desired dimension. With respect to the Iosipescu interlaminar shear test samples, three samples each from 20-ply baseline laminated composite specimen and 20-ply

vertically aligned CNT array reinforced laminated composite specimen were cleanly cut from the bulk composite panel using Beuhler ISOMET 1000 diamond abrasive cutting machine.

Then the notches were machined to size from the cured composite panel per ASTM D5379 [112]. The notches are created at both sides of the specimen blanks using a diamond coated cutting tool. The specimen were clamped while creating the notches so as to avoid stress concentration effect, matrix cracking and delamination. A typical sample dimension can be seen in figure 3.9 below.

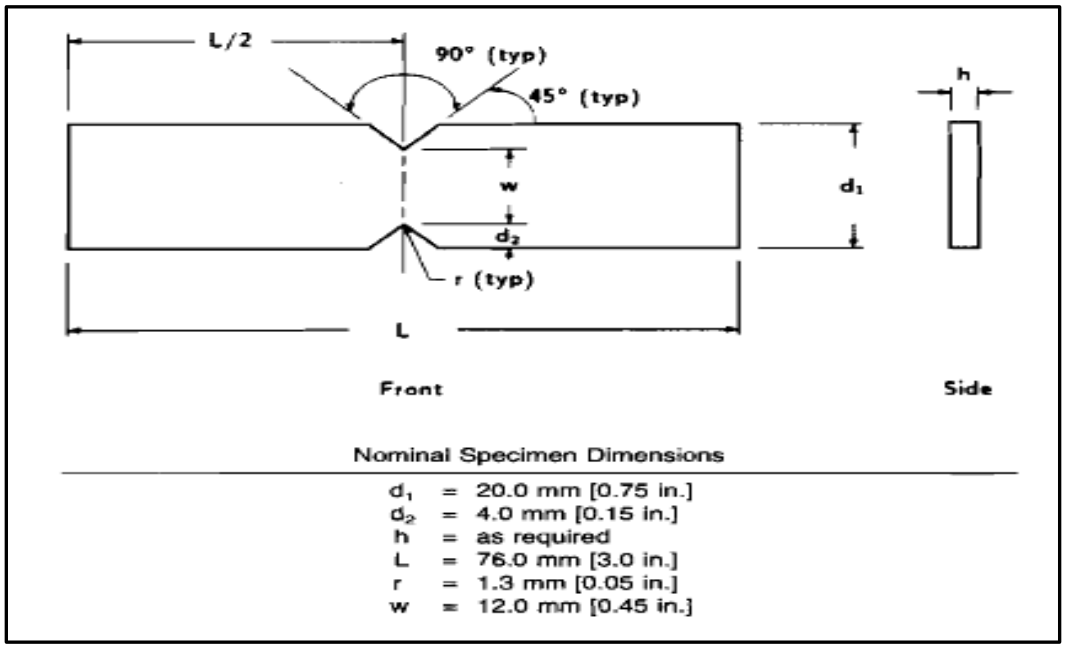

Figure 3.9. Nominal dimension for Iosipescu Interlaminar Sear Sample [ASTM D5379/D5379M-05 [112].

All fabricated samples are labeled to create uniqueness from one another so that they can be traceable back to the bulk composite panel from which they were prepared and also back to the sample after mechanical testing and failure characterization has been performed. Dimensions

of the samples are checked and the following are recorded prior to testing; length, width, thickness, span-to-thickness ratio, notch-to-notch distance and span length.

3.6 Mechanical Characterization

3.6.1 Interlaminar Shear Test

Interlaminar shear strength (ILSS) of a composite laminate is often a critical design characteristic; hence the evaluation of this parameter is best done by a number of ILSS shear test methods [50] to comparatively evaluate the effect in the essential design of composite laminates. Delamination, which is a major mode of failure for composite laminate occurs when there is a low bond strength between the ply interfaces and a failure usually occurs when an external shear load is applied on the composite laminated which exceeds the interlaminar shear strength of the composite. A state of pure shear should be generated between the laminae which is a function of the span-to-depth ratio [110, 111] of the composite laminate in order to introduce a shear failure.

Sample dimension and careful loading of the composite laminate on the test fixture is very critical in order to avoid inducing normal stresses transverse to the fiber layers which can alter the failure modes thereby making it difficult to accurately measure the value of ILSS. Different test methods [113] have been developed to characterize the interlaminar shear strength of a composite laminate as shown in figure 3.10. These experiments are designed to load the specimen to failure in a pure shear mode and the average shear stress across the failure surface is then taken as the ILSS.

In this study, the Iosipescu Interlaminar shear test and short beam shear test (SBS) are used to quantify the interlaminar shear strength (ILSS) and also measure the effect of VACNT array reinforcements between the laminae as against that without CNT reinforcements [114]. The

shear strain for both tests could not be obtained during the test due to the absence of a data acquisition module that would have been used to extract data from the strain gages mounted on the sample in real time. As a result, the shear modulus could not be calculated rather a plot of interlaminar shear strength against the displacement is calculated.

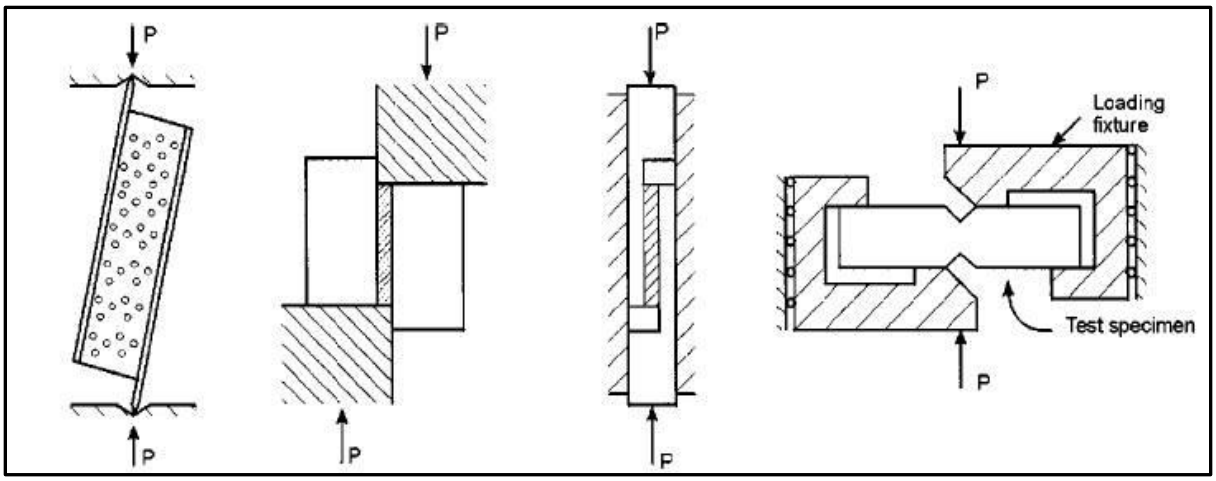

Figure 3.10. Different compression shear tests (from left: shear test between metal plates, block shear method, single lap compression shear test, IOSIPESCU shear test) [K. Schneider et al., 2001 [113].

3.6.1.1 Iosipescu Interlaminar shear Test

Once the Iosipescu test samples are been cut and machined from the bulk composite laminate as highlighted above, the dimensions of the samples are accurately measured and inserted into the setup fixture as shown figure 3.11, which is designed to produce a state of pure shear. This fixture is simple to operate and inexpensive to design. The sample was loaded using thick stainless steel block test fixtures clamped onto the sample and loaded through two 6mm dowel pins mounted at the top and bottom of the opposite halves of the fixture.

To eliminate slipping between the sample and the gripping surface, small grooves of depth (0.86 mm) were machined into the inner faces of the top and bottom halves of the fixture.

The two halves of the fixture are screwed together, clamping the sample in between. In order to eliminate the effect of samples being crushed during testing which is quite observed during shear test [115], the screws on the fixture were tightened with a torque wrench so that equal amount of torque was applied on each screw which eliminated excessive application of compressive force on the samples.

No crushing was observed in any of the testing done. Using this test setup, to obtain pure shear in the reduced section between the notch roots, the sample was aligned such that the notch roots were perfectly aligned with the top and bottom lines drawn on the stainless steel block. This serves to align the top and bottom fixture in order to create a pure shear. The sample is then placed into the bottom halves of the fixture and aligned so as to form a straight line with the top half. The sample position is adjusted until the pins match up to the notch roots aligning the sample so that it is perfectly centered with respect to the loading fixture.

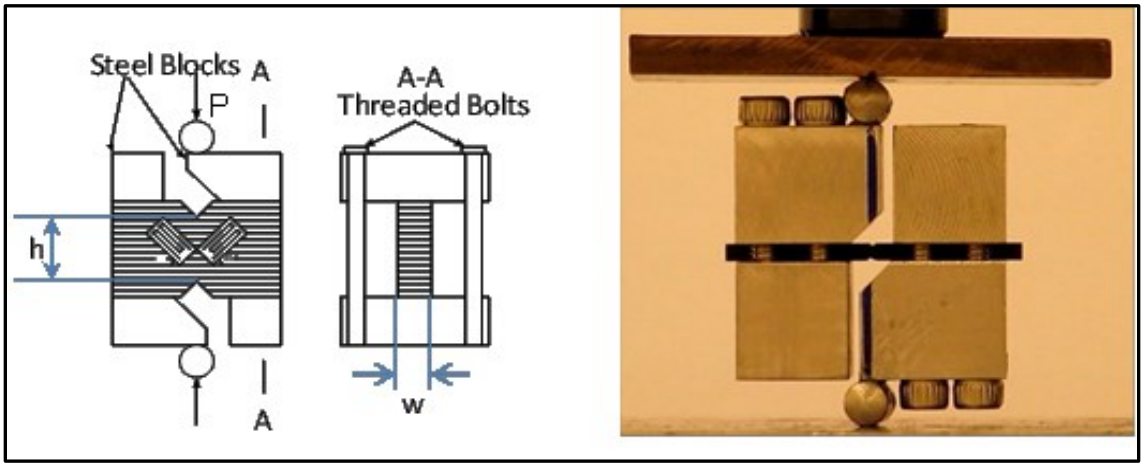

Figure 3.11. Schematic of Iosipescu interlaminar shear fixture and an interlaminar shear test setup in an instron 4465 test machine [Figure by Dr. Song Yi with permission].

Next, both halves are each clamped together with four screws used to tighten the left part of the top half to the bottom half while the other four screws is used to tighten the right part

bottom half to the top half. The fixture was the mounted on a universal tensile test machine. An Instron 4465 machine with a standard load cell of 2KN was used to perform the interlaminar shear test. The machine can measure static loads ranging from 5N- 2KN and has a resolution of 1mN for loads and 1micron for displacements. The specimen is placed in the fixture such that the 0^0 direction of the fibers is in the laminated composite axial direction which has more than 10% of the overall fiber reinforcement as recommended [112] and then subjected to compressive load at a constant crosshead speed of 0.05 in. /min.

The load is then applied on the left side of the movable fixture while the right side of the fixture is fixed. A point is reached when failure occurs and the maximum load needed to create a shear stress in the laminate is used in the calculation of the apparent shear strength of the laminate ply interface. Three specimens for each sample type (with and without VACNT array reinforcement) were further tested using the same procedure and condition so as to determine the mean interlaminar shear stress and displacement and analyze the effect of CNT array reinforcement.

3.6.1.2 Short Beam Shear Test (SBS)

After sample preparation and machining of the sample from the laminate as highlighted above, the samples were ready to be tested using a short beam shear test which is a standard 3-point bending test [111] as shown in figure 3.12a and b. The thickness of the sample used in this test is very critical since it dictates the span-to-thickness ratio of the sample and also the mode of failure of the sample as recommended by ASTM D2344/D2344M. For a state of pure shear to exist between the laminate in a standard Short Beam Shear test, the span-to-thickness ratio should be at least 4. Hence, the thickness of the laminate was accurately measured in order to achieve the nominal span-to-thickness ratio required for this test.

The experiments conducted measure the effectiveness of the CNTs to reinforce the interface of a laminated composite. An Instron 4465 universal test machine with a 2-KN load cell is calibrated to measure quasi static load ranging from 5 N to 2 KN. The resolution is 1 mN for load and 1 μm for displacement and a data sampling point of 800 points/sec. The specimen dimensions were measured and recorded following the standard [110] with length (.582 in.) equal to 6 times the thickness (0.097 in., 20 plies thick) and width (0.265in.) equal to twice the thickness of the sample.

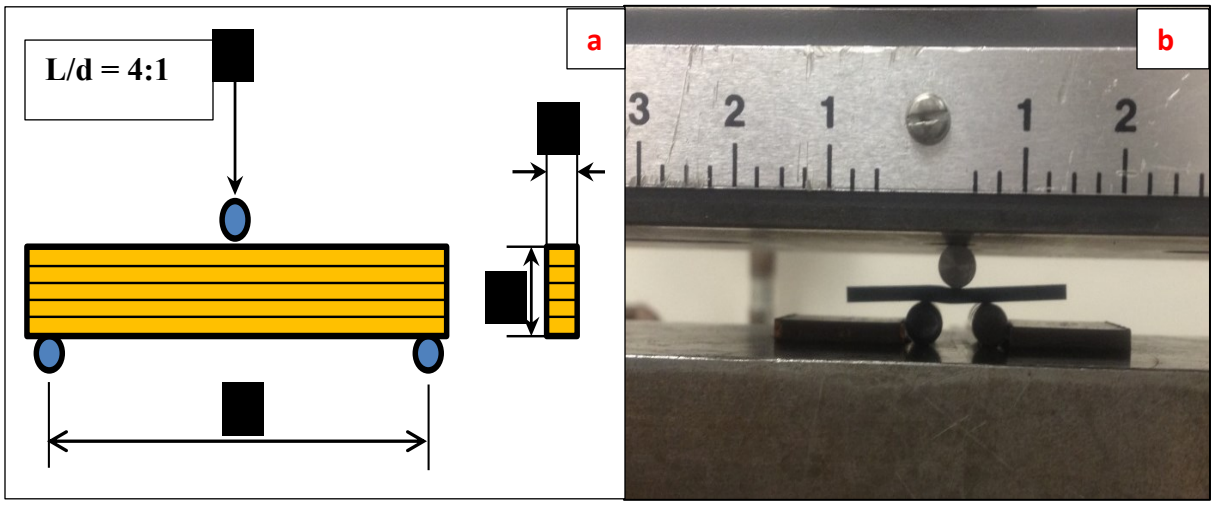

Figure 3.12. Short Beam Shear test: a) front view; b) Sample under shear loading.

The span length for the short beam shear test is equal to 4 times the thickness. The sample fiber direction has more than 10% of 0^0 reinforced in the laminate/test axis of the specimen. The laminate is subjected to a 3-point bending test at a constant crosshead speed of 0.05 in/min. Each sample was placed on two support pins and the load was applied via a 6mm loading nose. The compressive load is applied until fracture occurs and maximum failure load is used in the calculation to determine the apparent short beam shear strength of the laminate ply interface.

Based on visual inspection of the failed sample, it is seen that the sample failed by delamination which occurred at the mid-plane of the laminate as seen in figure 3.13, following guidance in the standard. The test was automatically stopped when the applied load dropped by 30% or crosshead travel exceeded the specimen nominal thickness. Five specimens were tested for each specimen type (baseline without VACNTs and hybrid composite with VACNTs).

The equation is based on classical beam theory by Euler which assumes shear stresses vary parabolically through the thickness [116] which is only approximately correct for a short beam and for the experimental three point bending loading conditions. The quasi-isotropic laminate configurations of fibers make the interlaminar shear stress state complex, however, the short beam shear test allows for a quantitative and relative comparison of the SBS of composites with and without CNTs, and has similarly been used by others for precisely this purpose, e.g., [117].

Figure 3.13. Short beam shear (SBS) test showing shear failure mode at the mid plan where the maximum shear stress occurs.

3.7 Flexural Test

3.7.1 3-Point Bending Test

After sample preparation and machining of the sample from the laminate as highlighted above, the samples flexural strength, strain and modulus were obtained using a standard 3-point bending test [111] as shown in figure 3.14. At lower span-to-depth ratio, a rectangular beam under load is expected to fail by shear at the mid-plane. At higher span-to-depth ratio, the mode of failure becomes flexural. Under these conditions, the outer section of the beam is expected to fail in tension while the inner section fails in compression.

There is an intermediate range of L/t ratios in which the behavior of failure is transitional, i.e there exists a combined effect of both flexural and interlaminar shear failure which is believed to be at a critical span-to-depth ratio of 9. For a fully flexural failure to occur, ASTM recommends that the span-to-depth ratio should be at least 16:1 and generally recommended to be at a 32:1 span-to-depth ratio as recommended by ASTM D790.

All the test conditions are the same as that for short beam shear test except for the span length. A span length of 1" was selected for the 3-point bending test. From the 3-point bend test carried out in this work, a 10:1 span to depth ratio is selected due to the limitations of CNT reinforcements and the insufficient length of sample dimension fabricated. For a flexural failure to exist in a standard three point bend test, the span-to-thickness ratio should be large enough so as to develop a high bending moment at the central loading nose. The experiments measure the effectiveness of the CNTs to improve the flexural strength and stiffness of the laminated composite. An Instron 4465 universal testing machine with a 2-KN load cell was calibrated to measure quasi static load ranging from 5 N to 2 KN.

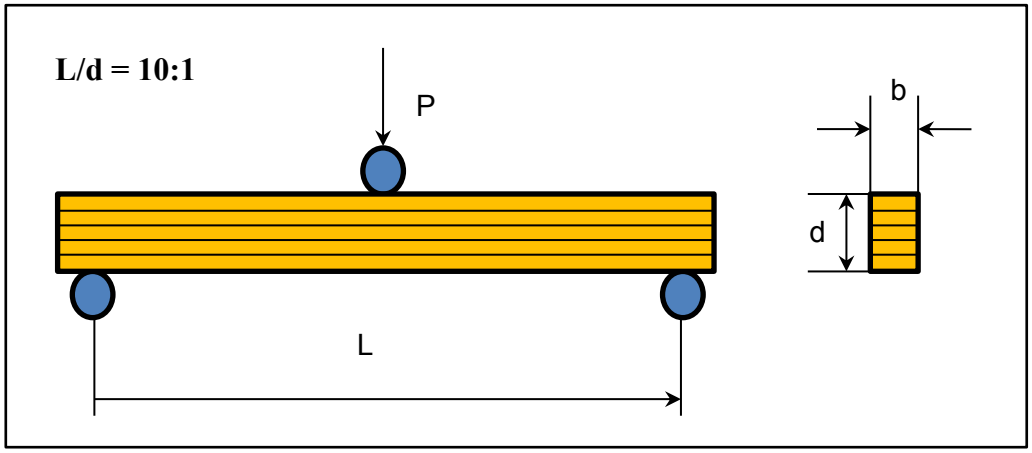

Figure 3.14. 3-Point Bend Test showing the front view and Sample cross section.

The resolution is 1 mN for load and 1 μm for displacement and a data sampling point of 800 points/sec. The specimen dimensions were measured and recorded following the standard [111]. The span length for the short beam shear test is equal to 10 times the thickness. The sample fiber direction has more than 10% of 0^0 reinforced in the laminate axis of the specimen. The laminate is subjected to a 3-point bending test at a constant crosshead speed of 0.05 in/min.

Each sample was placed on two support pins and the load was applied via a 6mm loading nose. The compressive load is applied until fracture occurs and maximum bending load is used in the calculation to determine the flexural strength while sample deflection off the mid plane was recorded in order to determine the flexural strain and modulus of the laminate ply interface. Care was taken to ensure that maximum normal stresses occurred at the top and bottom surfaces of the laminate which can be seen in figure 3.15 following guidance in the standard.

The test was automatically stopped when the applied load dropped by 30% or crosshead travel exceeded the specimen nominal thickness. Three specimens were tested for each specimen type (baseline without VACNTs and hybrid composite with VACNTs). The equation is based on classical beam theory by Euler which assumes bending moment increases from zero at supports

to a maximum at the central loading point [111] which is only approximately correct for the experimental three point bending loading conditions.

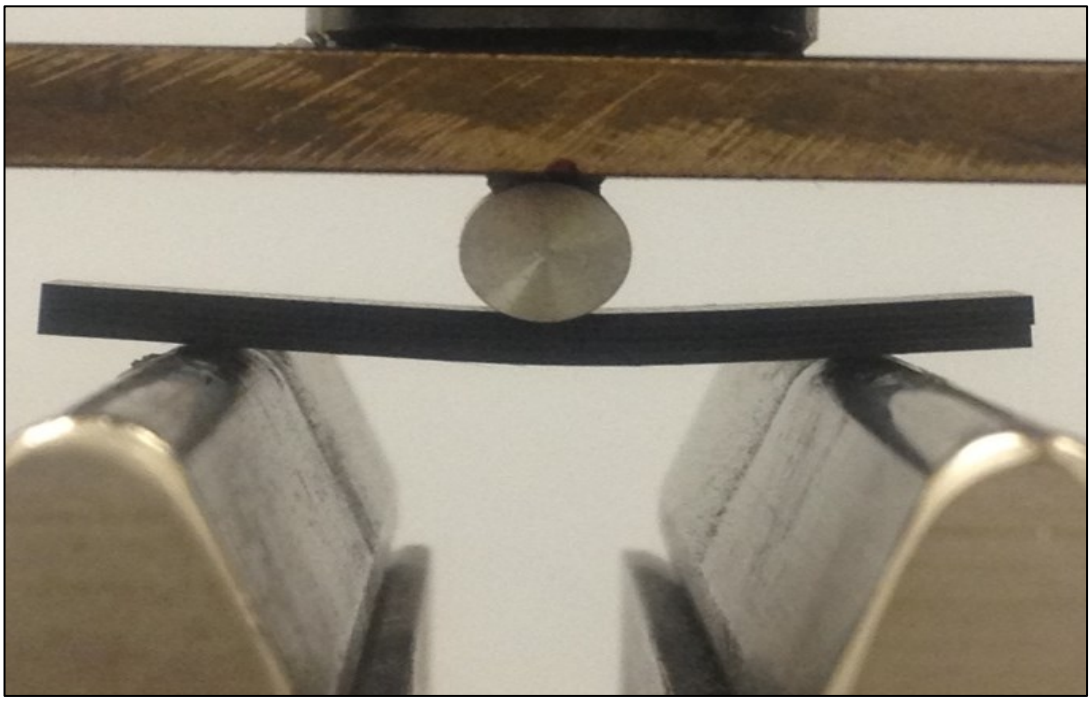

Figure 3.15. Sample undergoing compressive loading using 3-point bend test.

The quasi-isotropic laminate configurations of fibers make flexural stress state quite robust to analyze but the essence of 3-point bending test allows for a quantitative and relative comparison of the laminated composites with and without CNTs.

3.8 Analysis of Test Data

3.8.1 Analysis of Iosipescu Interlaminar Shear Test Data

Since the shear stress is relatively uniform between the notches of the sample specimen, interlaminar shear stress is calculated by equation (3.3) as recommended by ASTM D5379, where the maximum load prior to failure is divided by the cross section of the specimen.

$$\tau_{13} = P/wh \tag{3.3}$$

Where P, the compressive load applied by the material test machine, w is the sample width and h is the tip-to-tip distance between the two v-notches.

Three samples from both 20-ply baseline laminated composite specimen and 20-ply vertically aligned CNT array reinforced laminated composite specimen were tested with an Iosipescu interlaminar shear test fixture in which all test are carried out in the same conditions under room temperature. The load-displacement results acquired from the Instron software is used to estimate the shear strength–displacement data and plot acquired for this test. Plots from each test are averaged to determine the shear strength of both samples for comparison.

Figure 3.16 and 3.17 shows the shear strength- deflection plots obtained during the test and the results obtained for each of the tested specimens demonstrate good repeatability and strength values between each test. It can also be seen from Table 3.1, that the standard deviation of sample dimensions as regards the width and tip-to-tip distance from the mean value is very much within close interval.

The average interlaminar shear strength is 33 MPa with a standard deviation of 3.5 MPa while the vertically aligned reinforced CNT array nano composite shows an interlaminar shear

strength value of 48 MPa with standard deviation of 5.05 MPa. This represents acceptable data correlation within the test carried out as seen in figure 3.18.

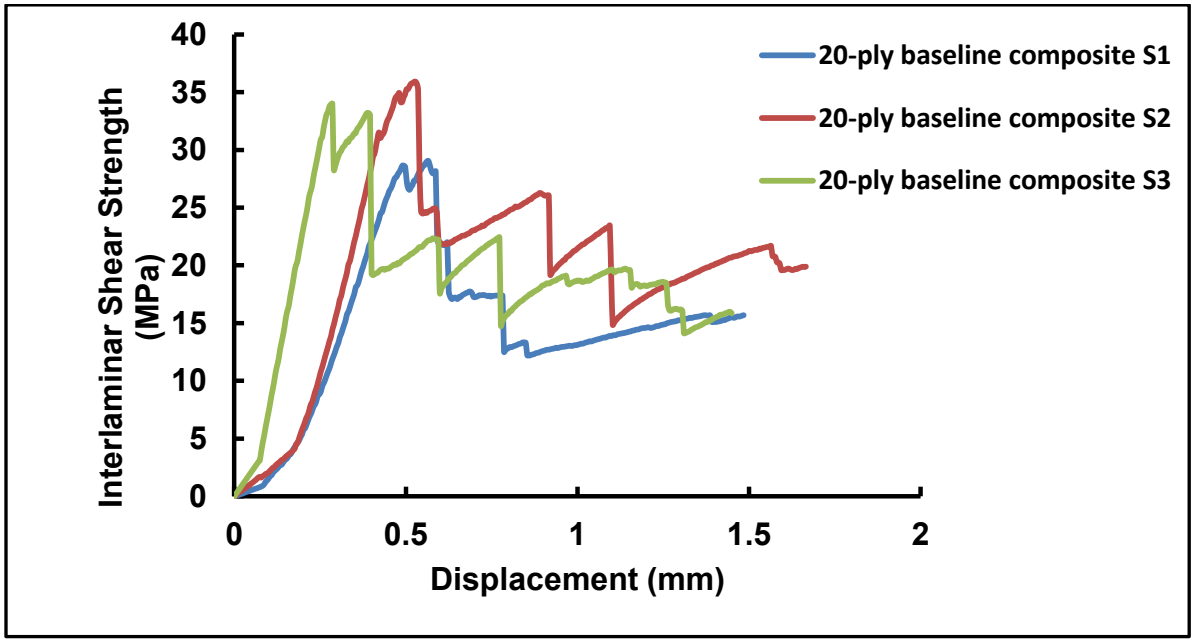

Figure 3.16. Interlaminar shear test curves for 20-ply baseline laminated composites samples.

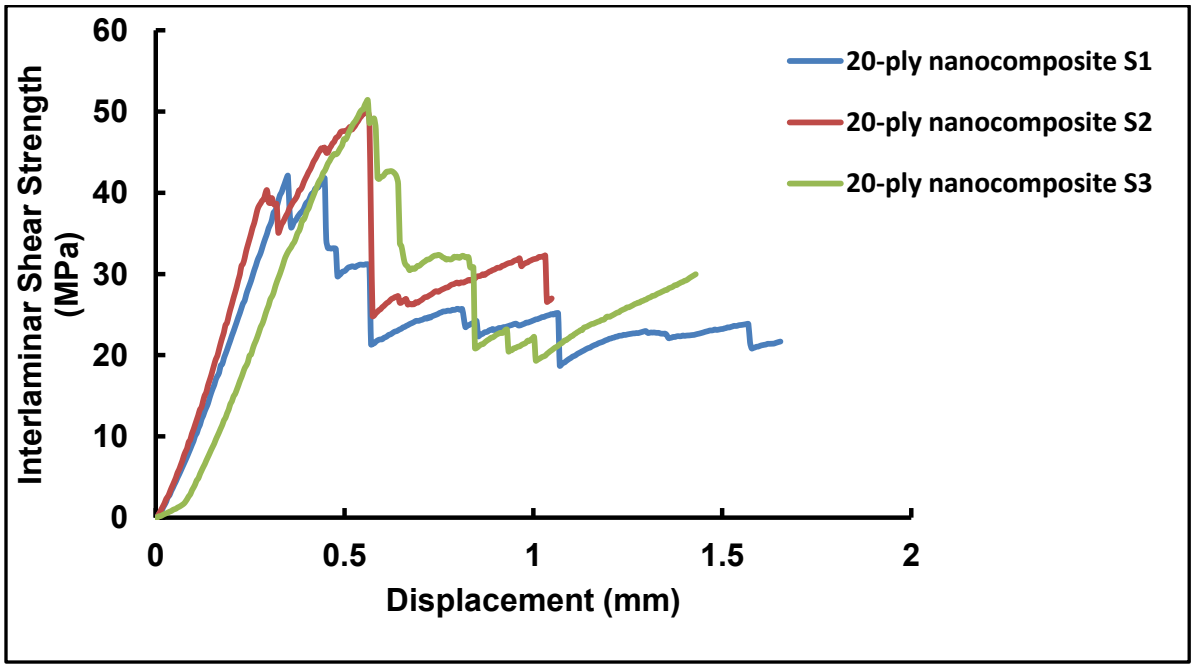

Figure 3.17. Interlaminar shear test curves for 20-ply 20µm CNT array reinforced composite samples.

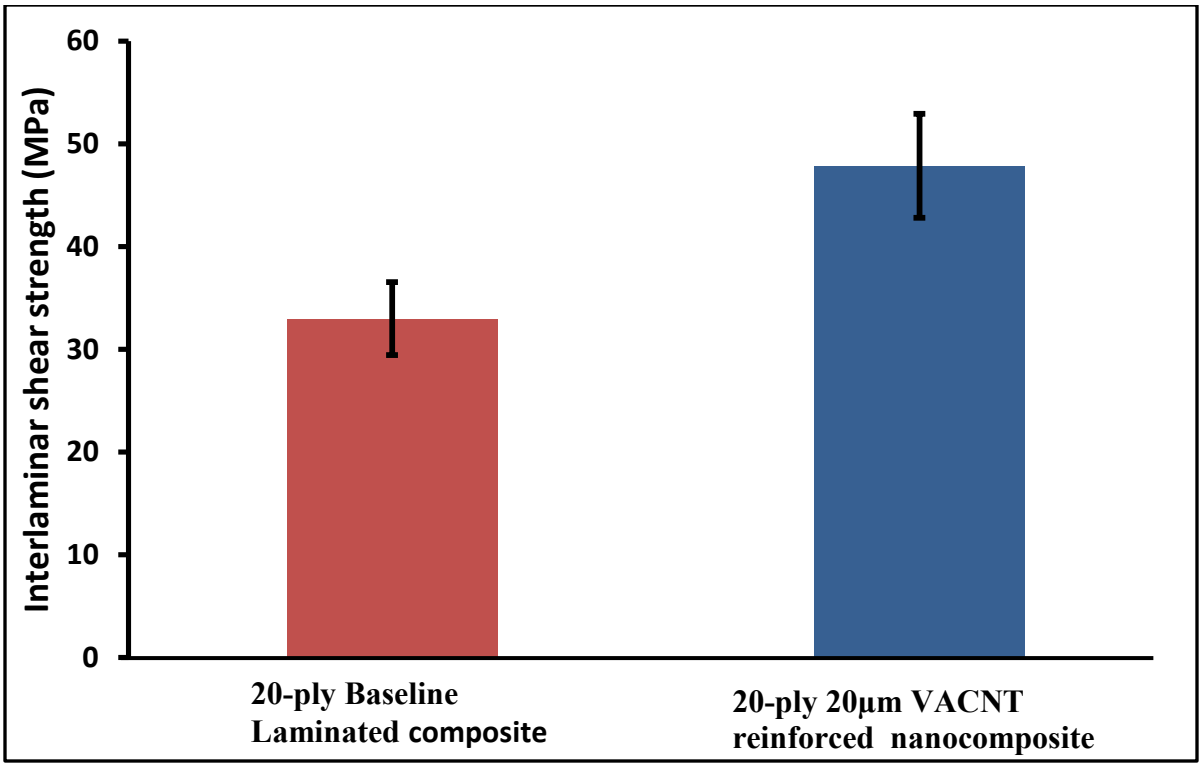

Figure 3.18. Shows the error bar of the data scatter of two different specimen types subjected to interlaminar shear test and its respective mean interlaminar shear strength.

Table 3.1 Interlaminar Shear Test results.

		Width (mm)	Tip-Tip Thickness (mm)	Max Load (N)	Interlaminar Shear Strength (MPa)
20-ply baseline laminated composite	S1	6.76	1.68	329	29
	S2	7.47	1.52	409	36
	S3	6.58	1.42	318	34
	Mean	**6.93**	**1.55**	**352**	**33**
	STDEV	0.48	0.13	49.5	3.6
20-ply 20mm CNT array reinforced composite	S1	6.53	1.78	488	42
	S2	6.93	1.65	574	50
	S3	7.87	1.75	709	51
	Mean	**7.11**	**1.73**	**590**	**48**
	STDEV	0.69	0.07	111.5	5.1

It can be seen that about 45% increase with respect to CNT reinforcement on the hybrid composite laminate was observed. From figure 3.16 and figure 3.17, the shear strength-displacement test plots for both types of samples follow the same shear failure process which shows a steep increase in the shear strength value with corresponding increase in displacement until a point is reached where the failure precipitates a slight drop in shear strength.

This drop is believed to be either as a result of the onset of unstable shearing in the ply interlayers, failure of the fiber-matrix bond and matrix micro-cracking or a combination of these failure modes. The shear strength subsequently increased rapidly to a maximum value before a significant drop in the load carried by the fibers in 0^0-direction parallel to the loading axis. This point denotes the ultimate shear failure of the specimen after which an alternate drop and increase in load far below the peak value of the shear strength is observed. Based on specimen observations, both notch roots in the samples were devoid of fiber crushing which is sometimes observed in Iosipescu test samples [106] due to stress concentration at the tips and also failure initiation points.

The influence of vertically aligned CNT arrays showed a significant influence on the shear strength of the hybrid samples since these arrays help in reinforcing the matrix-rich region since shear failure is mostly matrix dominated and combination of other failure modes. The CNT reinforcement also improved the shear properties since the load needed to create shear is further raised to a much higher value which is directly proportional to the interlaminar shear strength of a material. The mechanism observed for interlaminar shear strength increase as a result of CNT reinforcement is based on; energy dissipation mechanism [118, 119] in which a huge amount of energy is absorbed when the horizontal shear failure at the fiber/matrix interface tries to propagate through the transversely aligned CNT array. This in turn, increase the amount of load

that is needed to propagate the crack through the strong and stiff VACNT arrays there by increasing the interfacial shear strength of the hybrid composite. From figure 3.16 and 3.17, there exists a zigzag saw-tooth failure mode of the baseline and CNT array reinforced composite. This is believed to be as a result of the complex failure mode associated with quasi isotropic laminate configuration due to different ply orientation.

Here, from the layup configuration used in the test, the $+45^0$ and -45^0 off-axis plies situated at the mid-plane failed first which resulted in slight drop in load applied. Subsequently, the load applied were transferred unto the 90^0 plies directly following the off-axis plies which resulted in a slight increase in load applied since it is believed to withstand more shear load than the off-axis plies. This alternate increase and decrease in shear strength is also as a result of delamination at multiple ply resin rich interfaces where failure at these regions reduces the shear strength and subsequently increases when the load is then transferred unto the fibers.

Research has also shown that that the fracture toughness mechanism for nanocomposite materials both in mode I, II show a different crack deflection and arrest mechanism which is significantly different from that without nano phase materials because the nano phase materials helps in toughening the matrix due to their high specific surface area and molecular interaction at nano level with the resin matrix in order to create a functional interface which impedes crack initiation and subsequent crack growth under a steady load application.

Another toughness mechanism involves the mechanical interlocking [120,121] of transversely aligned CNT arrays in between the fibers/matrix interface of the composite thereby making it difficult to easily create a shear affect at low load application thus enhancing the fracture toughness and interlaminar shear strength. Thus the presence of CNTs aligned

perpendicular to the surface of quasi-isotropic laminate considerably contributes to a more efficient shear stress load transfer and enhances the interface properties of the laminated composites.

3.8.2 Analysis of Short Beam Shear Test data

In the SBS test, the determination of ILSS is based on classical (Bernoulli–Euler) beam theory. For a beam of rectangular cross-section loaded in three-point bending, the maximum interlaminar shear stress occurs at the mid plane of the beam and is calculated to be;

$$\mathbf{F^{sbs} = 0.75 \cdot \frac{P_m}{bd}} \tag{3.4}$$

Where F^{sbs} , the short beam shear strength, P_m is the maximum load observed during the test, b is the sample width and d is sample thickness.

Five samples from both 20-ply baseline laminated composite specimen and 20-ply vertically aligned CNT array reinforced laminated composite specimen were tested using a 3-point bend test fixture with a span-to-depth ratio of 4 in which all test are carried out in the same conditions under room temperature. The load-displacement results acquired from the Instron software is used to estimate the shear strength–displacement data and plot acquired for this test shown in figure 3.19. Plots from each test are averaged to determine the shear strength of both samples for comparison.

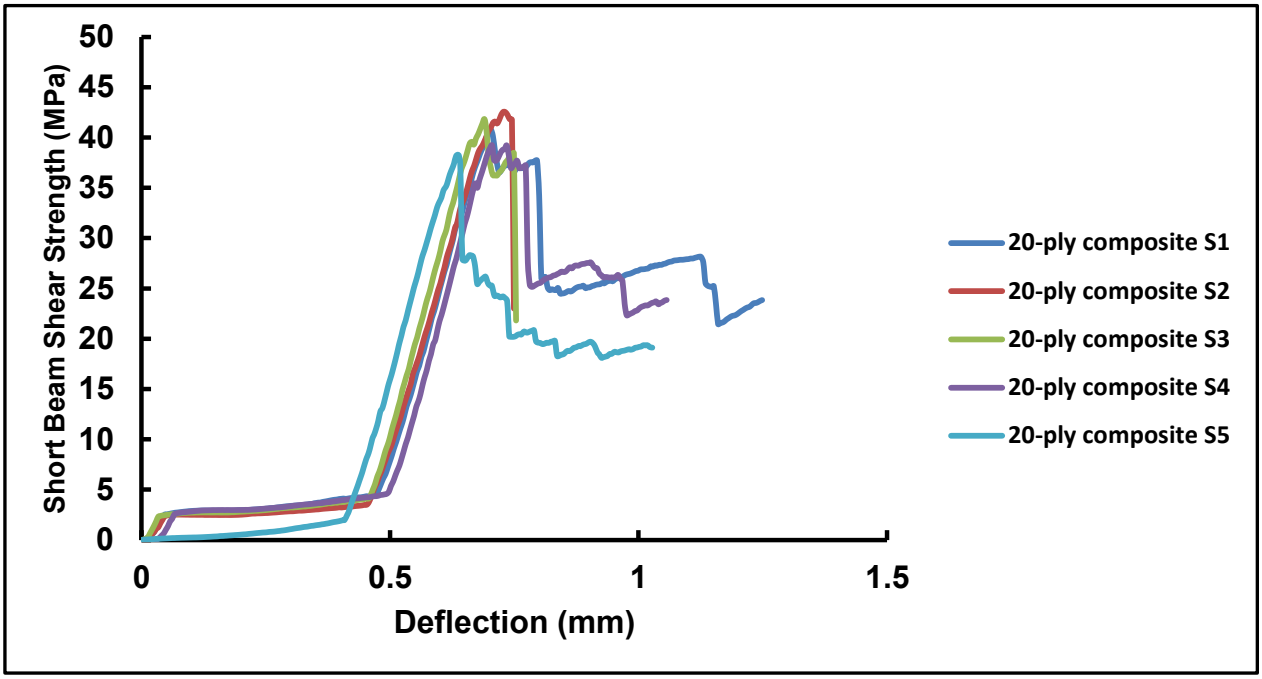

Figure 3.19. Short beam shear test curves for 20-ply baseline laminated composites samples.

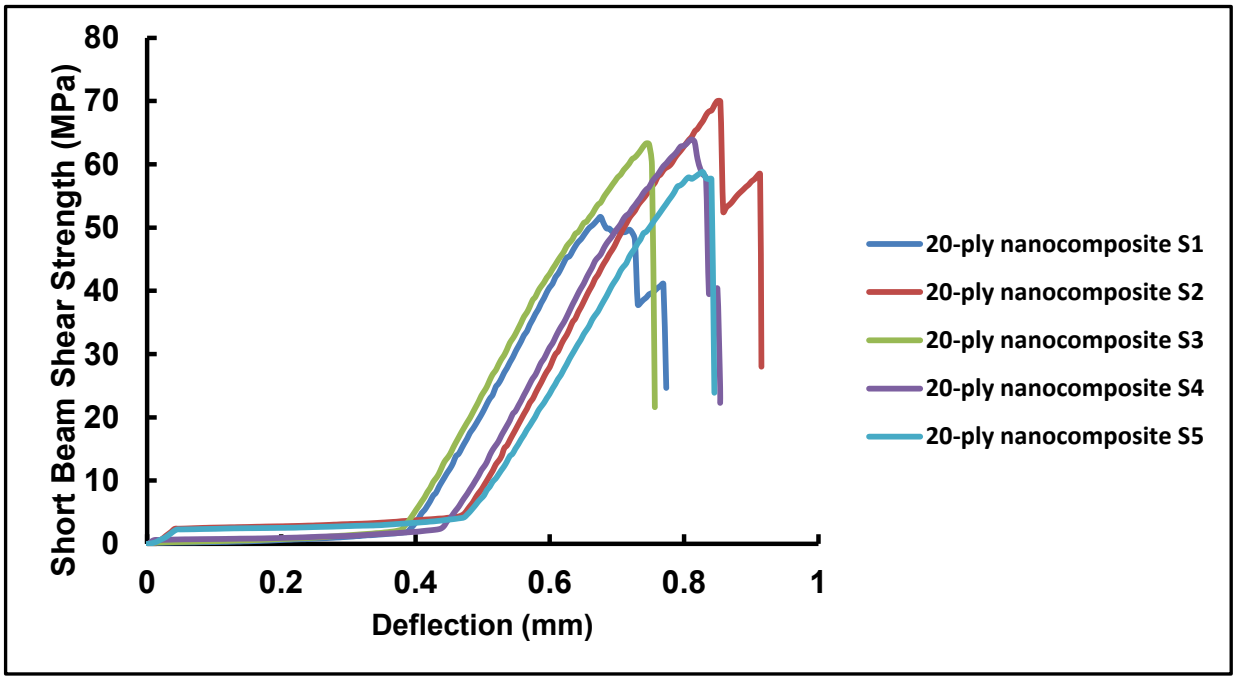

Figure 3.20. Short beam shear test curves for 20-ply 20µm CNT array reinforced composite samples.

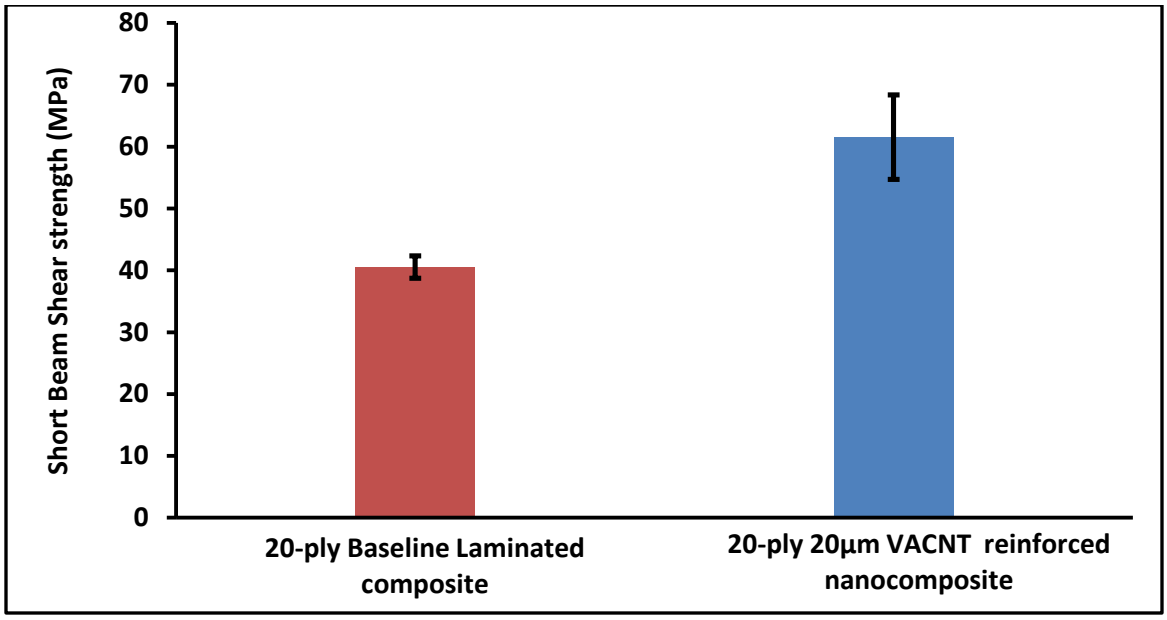

Figure 3.21. Bar chart showing a comparison between the shear strength of 20-Ply baseline composite and 20µm high CNT reinforced laminated composite.

Table 3.2 Short Beam Shear test results

		Width (mm)	Thickness (mm)	Max Load (N)	Short Beam Shear Strength (MPa)	Thickness/Ply (mm)
20-ply Baseline laminated Composite	S1	7.04	2.24	855.5	40.8	0.11
	S2	7.06	2.31	926.1	42.6	0.12
	S3	7.16	2.31	923.3	41.8	0.12
	S4	6.63	2.26	783.6	39.2	0.11
	S5	6.15	2.24	700.5	38.2	0.11
	Mean	**6.81**	**2.26**	**837.8**	**40.5**	**0.11**
	STDEV	0.43	0.05	96.5	1.8	
20-ply 20mm CNT array reinforced composite	S1	6.76	2.51	1170.7	51.7	0.13
	S2	6.60	2.46	1518.9	70.0	0.12
	S3	6.73	2.46	1400.0	63.3	0.12
	S4	6.81	2.49	1444.4	63.9	0.12
	S5	6.78	2.41	1282.5	58.8	0.12
	Mean	**6.73**	**2.46**	**1363.3**	**61.5**	**0.12**
	STDEV	0.08	0.03	137.6	6.8	

Figure 3.19 and Figure 3.20 shows the shear strength-deflection plots obtained during the test and results obtained for each of the tested specimens demonstrate good repeatability and strength values between each test. Table 3.2 shows the overall data for both test, and it can also be seen from figure 3.21 that the mean short beam shear strength of the 20-ply baseline laminated composite is 40.52MPa with a standard deviation of about 1.8MPa while that of the 20-ply 20μm CNT array reinforced composite is 61.54MPa with a standard deviation of 6.81MPa which is an acceptable data correlation within the test carried out.

The introduction of 20μm CNT array between each plies leads to a 52% increase of the short beam shear strength while slightly increasing the sample thickness from a mean value of 0.11mm - 0.12mm. From visual inspection of the failed sample it was observed that the samples failed in pure shear at the mid-plane which showed a matrix dominated failure. This failure is believed to have occurred in the samples when the shear stress applied exceeded the maximum shear strength of the fiber matrix interface of the composite as seen in both figures 3.19 and 3.20.

From the test carried out for both baseline and CNT reinforced composite samples, it can be seen from figure 3.19 and 3.20 that there is a delay in the increase of interlaminar shear strength with corresponding displacement from the neutral axis. At displacement value of about 0.4mm, the sample then experienced a sharp and steady increase in shear strength with corresponding increase in deflection. This anomaly that occurred between 0-0.4mm for both baseline and CNT array reinforced composite is believed to be as a result of test setup while compressive load was applied on the samples. At this point on the graph, the 6mm loading nose was not directly touching on the sample surface in order to create a pre-loading effect on the sample prior to start up of the test so this resulted in increased displacement of the top fixture with no relative application of load on the sample which resulted in the lag in curve.

At the maximum shear stress applied, there is a fiber/matrix debonding at the interface which might have been as a result of interface slipping or matrix micro cracking at a much lower shear strength for the baseline laminated composite as compared to the CNT reinforced laminated composite which failed at a much higher shear strength which is believed to be due to efficient load transfer between the matrix and the transversely aligned CNT arrays, little or no mechanical interlocking of adjacent carbon fiber lamina with vertically aligned CNT arrays which creates a "z pinning" effect through-the-thickness direction to resist sliding of the laminas or a combination of both reinforcing effect in order for the Nano-engineered laminated composite to sustain a higher shear stress effect.

Also, from figure 3.12b showing the short beam test setup, it could be seen that the sample has a slightly longer overhang at both ends of the span support. As recommended by ASTM, the overhang should be about the thickness of the laminated composite sample so as to create room for near pure shear effect. Slight overhang also imparts stability on the samples during shear and maximum bending so that they do not fall off the loading supports. It can be seen from the shear strength plotthat the short beam shear failure of the sample occurred due to shear effect as a result of in-plane sliding at the laminate interface and also higher bending stresses which could have resulted due to a longer overhang of sample at both ends of the supports.

This reinforcement mechanism can be better understood from figure 3.22 below which depicts the effect of short vertically aligned CNT array reinforcement at the interface in the mid-plane. It is seen that the CNTs create a crack bridging effect to delay crack propagation and it is also assumed that the CNTs are also pulled in tension while undergoing in-plane shear effect at

the mid-plane interface. A combination of the effects would have improved both in-plane and interlaminar shear properties of the nano reinforced laminated composite.

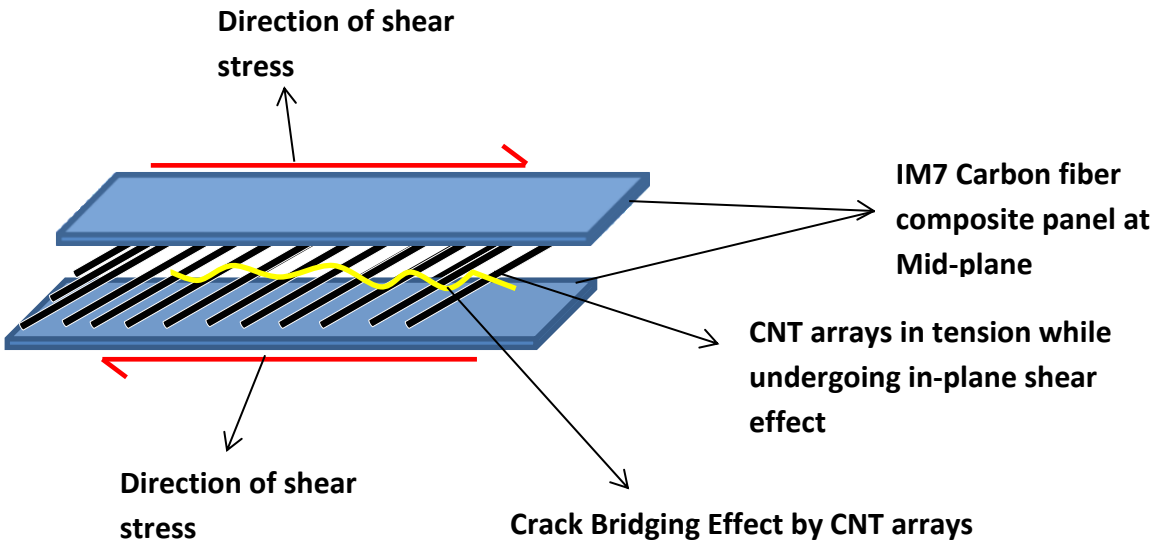

Figure 3.22. Image showing the failure mechanism of CNT reinforced laminated composite at the mid-plane interface.

3.8.3 Flexural Test Data (3-point bending)

As earlier mentioned, in a 3-point bending test, the beam's flexural strength is based on the classical beam theory. For a rectangular beam of cross section subjected to bending, the maximum flexural strength of the sample usually occurs at the bottom of the beam which is subjected to tensile stresses and is calculated by using the formula below as recommended by ASTM D790.

$$\sigma_f = 3PL/2bd^2 \tag{3.5}$$

Where P, the maximum load is observed during the test, L is the span length between the two supports, b is the width of sample and d is the sample thickness.

Also the flexural strain is calculated by using the formula below as recommended. This is based on the fractional change in length of an element at the outer surface of the specimen where the maximum strain occurs.

$$\varepsilon_f = 6Dd/L^2 \tag{3.6}$$

Where D is the maximum deflection of the center of the beam and d is the thickness of the sample while L is the support span length of the sample.

Three samples each were tested from both 20-ply baseline laminated composite specimen and 20-ply vertically aligned CNT array reinforced laminated composite specimen were tested using a 3-point bend test fixture with a span-to-depth ratio of 1in. which all test are carried out in the same conditions under room temperature.

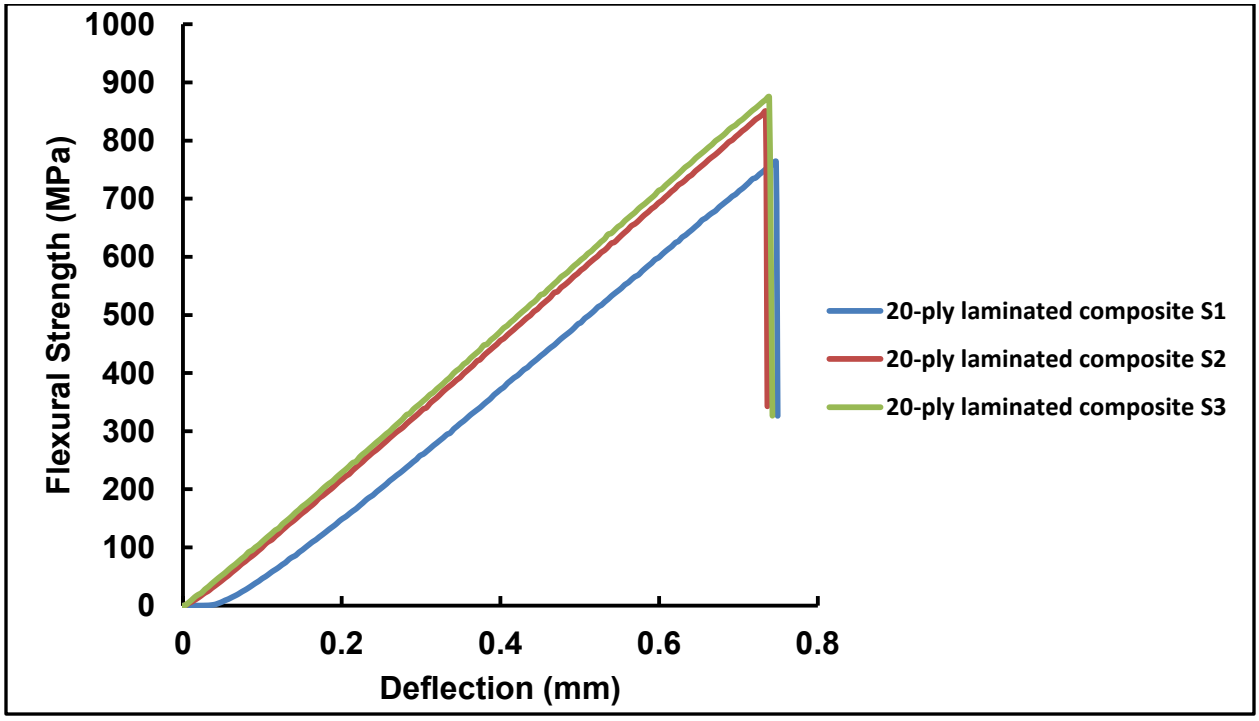

Figure 3.23. 3-point bend test curves for 20-ply baseline laminated composites samples.

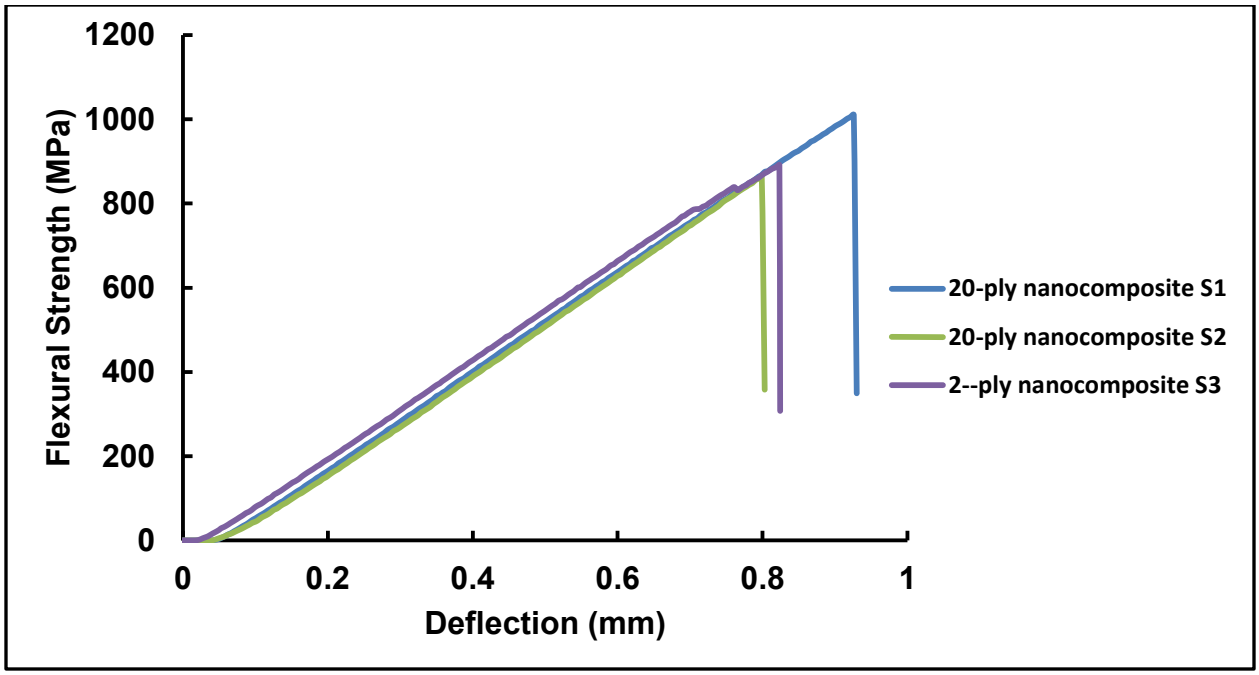

Figure 3.24. 3-Point bend test curves for 20-ply 20µm CNT array reinforced composite samples.

The load-displacement results acquired from the Instron software is used to estimate the flexural strength–displacement data and plot acquired for this test as shown in figure. Plots from each test are averaged to determine the flexural strength and strain of both samples for comparison. Figure 3.23 and Figure 3.24 show the flexural strength-deflection plots obtained during the test and results obtained for each of the tested specimens demonstrate good repeatability and strength values between each test.

From Table 3.3 below, it can be seen that the mean flexural strength of the 20-ply baseline laminated composite is 829.48MPa with a standard deviation of about 58.39MPa while that of the 20-ply 20µm CNT array reinforced composite is 921.55MPa with a standard deviation of 78.33MPa which is an acceptable data correlation within the test carried out. Figure 3.23 and 3.24 also show that both baseline and CNT reinforced composite failed by brittle failure which is

usually the case for brittle materials. Here, there was a sharp drop in strength when the samples were subjected to plastic failure.

Figure 3.25 shows a bar chart of both samples (baseline and VACNT reinforced laminated composite) with their respective mean flexural strength showing error bars. Also, it is believed that the reinforcement pattern of CNT array played a less significant effect on the flexural strength of the hybrid composite since the arrays are transversely aligned in between the laminae. From the results and image of the test conducted for both baseline and nano reinforced laminated composite samples as shown in figure 3.15, it could be seen that the failure mode showed a combination of flexural and shear failure. This is believed to be as a result of shorter span-to-depth ratio used for this test.

Therefore the slight increase in flexural strength might have been as a result of the orientation of the CNT reinforcement when compared to significant increase in interlaminar shear strength as seen from the Iosipescu and short beam shear test results respectively. Table 3.3 also shows the flexural strain dadta for for both baseline and CNT array reinforced composite. It shows an increase in strain value from 1.5% to 1.8%. This shows that the mean CNT array reinforced composite increased its strain to failure value by 25% when compared to the baseline samples which we believe will also improve the fracture toughness of the CNT array reinforced laminated composite.

This shows that the VACNT array reinforcement imparted a reasonable amount of stiffness to the hybrid composite which allowed the nanocomposite to withstand higher bending stresses and prolonged the crack initiation and propagation process prior to failure. The nano modified interface could have also reduced the effect of matrix micro cracking which have also

bridged cracks during propagation process thereby improving the fracture toughness of the nanocomposite when compared to the baseline sample.

Table 3.3 3-Point Bend Test results.

		Width (mm)	Thickness (mm)	Max Load (N)	Flexural strength (MPa)	Flexural strain (%)	Thickness/Ply (mm)
20-ply baseline laminated composite	S1	7.21	2.29	726.5	763.6	1.47	0.11
	S2	7.04	2.29	788.9	850.0	1.45	0.11
	S3	6.83	2.24	753.8	874.8	1.43	0.11
	Mean	**7.04**	**2.26**	**756.4**	**829.3**	**1.45**	**0.11**
	STDEV	0.20	0.03	31.2	58.4	0.020	
20-ply 20μm CNT array reinforced composite	S1	6.35	2.44	962.9	1010.5	1.72	0.12
	S2	6.81	2.49	918.5	862.8	1.80	0.12
	S3	6.86	2.54	995.4	891.4	1.95	0.13
	Mean	**6.68**	**2.49**	**958.9**	**921.6**	**1.82**	**0.12**
	STDEV	0.28	0.05	38.6	78.3	0.117	

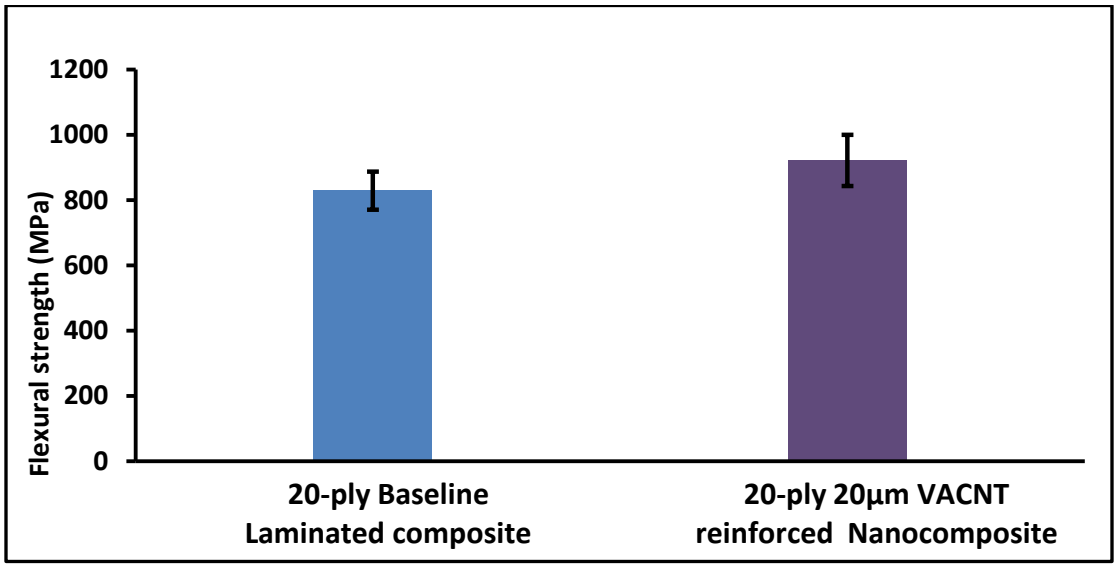

Figure 3.25. Bar chart showing a comparison between the flexural strength of 20-Ply baseline composite and 20μm high CNT reinforced laminated composite.

3.9 Characterization of Failure Surface

3.9.1. Fracture Surface of Interlaminar Shear Samples

Scanning Electron Microscope (SEM) is utilized to characterize the failure surface of both the baseline and nano reinforced laminated composite samples. It provides high resolution at relatively high magnification and also helps to relate the failure response observed during the mechanical test and crack propagation observed by SEM imaging.

The microscopic examination of the failed specimen was carried out at the Air Force Research Lab (AFRL) in collaboration with General Nano. The SEM images show the crack propagating from one edge of the specimen to the other end. The crack initiation occurred as a result of shear failure at the matrix/ fiber interface which is maximum at the mid-plane of the laminate (see Figure 3.13). This is also in line with work done by researchers in this field. It can also be seen that the failure occurred at the off-axis ply interface ($+45^0$ or -45^0). This can also be as a result of tensile or compressive failure from the principal stresses associated with near-pure shear situation.

When there is an existence of combination of stresses which are usually predominant in a quasi-isotropic composite configuration, principal stresses will exist at a given angle according to the following formulas;

$$\tan 2\theta_p = \frac{2\tau_{xy}}{\sigma_x - \sigma_y} \tag{3.7}$$

$$\sigma_{1,2} = \frac{\sigma_x + \sigma_y}{2} \pm \sqrt{\left(\frac{\sigma_x - \sigma_y}{2}\right)^2 + \tau_{xy}{}^2} \tag{3.8}$$

$$\tau_{\max} = \sqrt{\left(\frac{\sigma_x - \sigma_y}{2}\right)^2 + \tau_{xy}^{\ 2}} = \sigma_1 - \sigma_2 \tag{3.9}$$

$$\tan 2\theta_s = -\frac{\sigma_x - \sigma_y}{2\tau_{xy}} \tag{3.10}$$

$$\theta_s = \theta_p = \pm 45^{\circ} \tag{3.11}$$

SEM images seen in figure 3.26 and figure 3.27 show that of the failed sample for composite specimen. Images for that of VACNT array reinforced composite is also analyzed in order to understand the reinforcement effect of the CNT arrays on the interlaminar shear properties of the nano composite. However, it is seen that the failure propagation of the nano reinforced composite share similar property as that seen in Figure 3.22 in which the VACNT arrays delay crack initiation and deflects crack to a more tortuous path during propagation which eventually improve the interlaminar shear resistance of the composite.

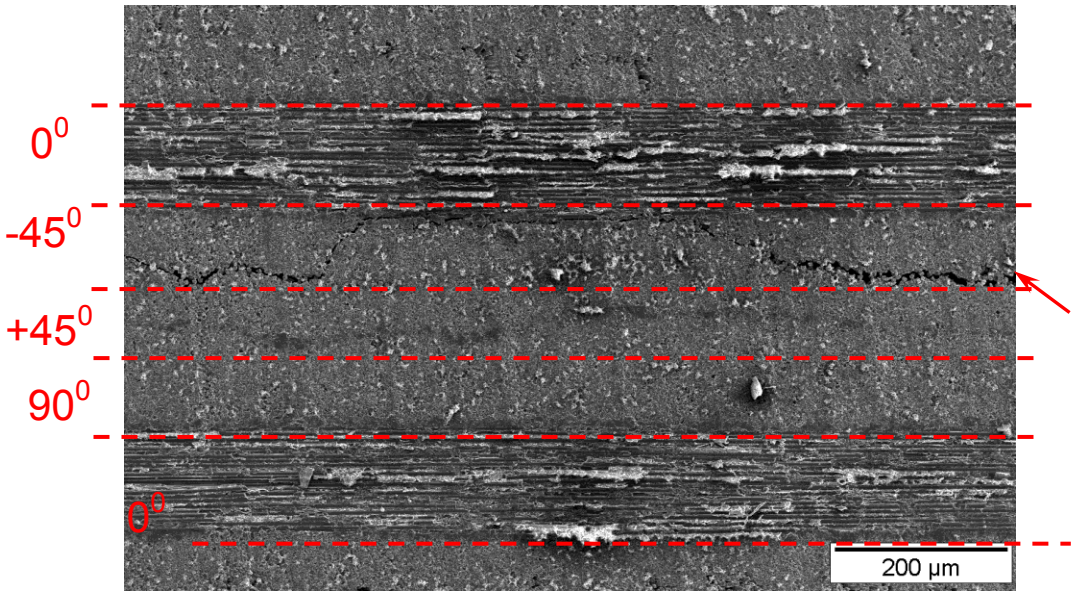

Figure 3.26. SEM image showing crack propagation in the off-axis plies where there exists a weak failure mode [Figure by Air Force Research Lab with permission].

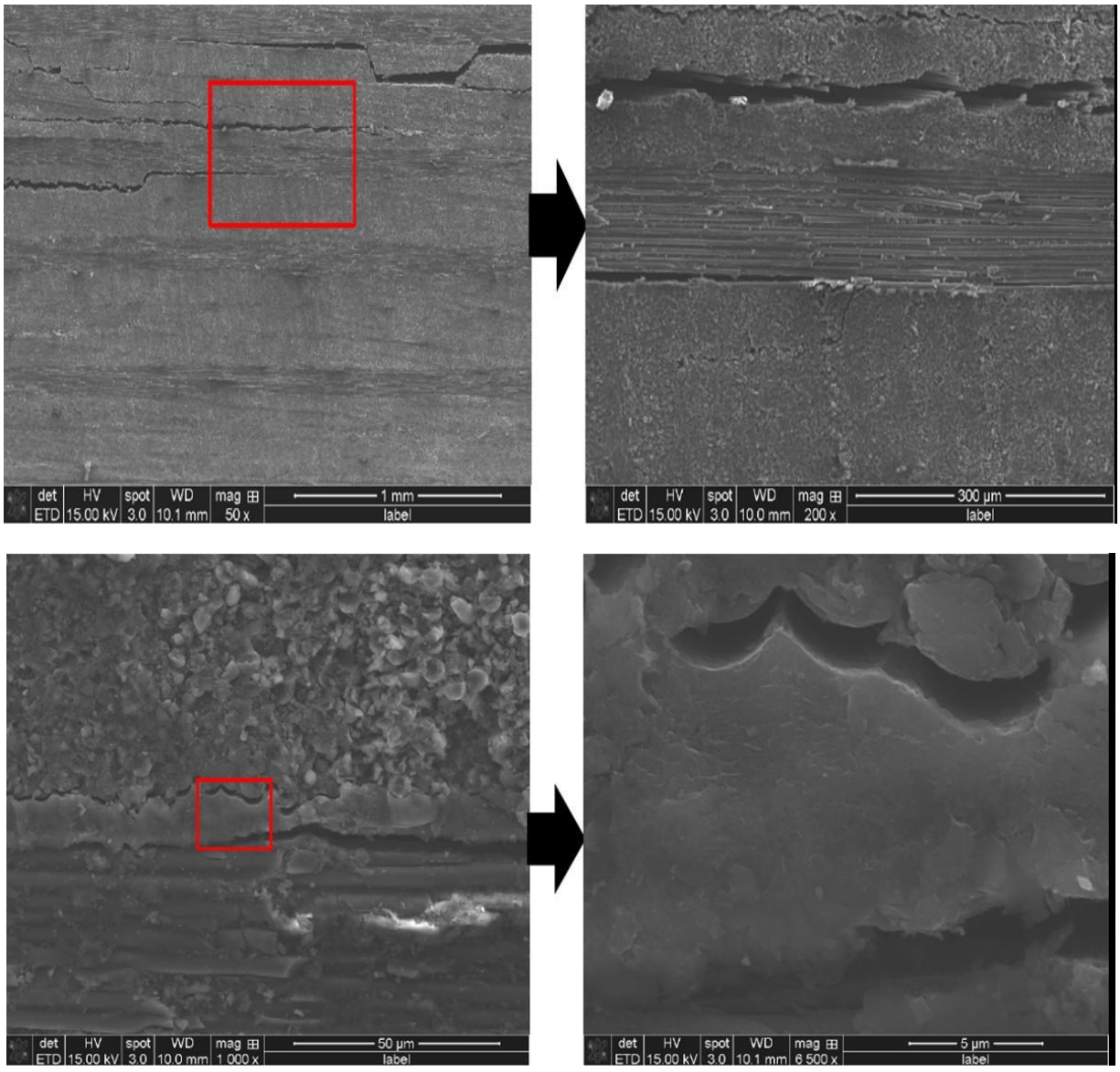

Figure 3.27. SEM image of carbon fiber composite baseline sample showing severe delamination at the interlayer of the composite laminate at both low and relatively high magnification [Figure by Air force Research Lab; Lucy Li with permission].

CHAPTER 4

Fabrication and Characterization of Carbon Nanotube Post Reinforced Laminated Composite

4.1 Introduction

As earlier highlighted in previous chapters, several approaches have been utilized to improve the interlaminar shear strength of laminated composite [117-121]. An optimized reinforcement pattern used in chapter 3 also showed that transfer printing of CNT arrays composed of thousands of Nano scale filaments on each ply laminae in the composite structure is seen to have imparted a significant increase in the mechanical and interfacial properties of nano reinforced composite. Based on SEM examination of the failure surface of the nanocomposite, it was observed that the VACNT arrays resisted crack growth and also a "z-pinning" effect along the fiber matrix interface which drove the cracks along the tortuous path.

However, despite the improved properties from the reinforcement morphology above, the load transfer mechanism between the polymer matrix interface and the CNT arrays was not as effective as would have been expected if the VACNT arrays were to be reinforced with a long and continuous VACNT post which would run from the top to bottom of the entire thickness of the sample. This assumption is based on the fact that the testing described in chapter 3 showed that short CNT arrays placed in between each plies in composites increased the mechanical properties, but still shear failure occured at moderate load application because the carbon fibers are not tied up together from ply to ply. This indicates that the CNT reinforcement if spanned through-the-thickness of the composite, will interlock all the carbon fiber plies together to form a continuous load path for effective stress transfer which is analyzed in this chapter.

4.2 Materials for CNT Post Reinforced Laminated Composite Fabrication

Hybrid laminated composite panels were fabricated with the use of high-grade unidirectional IM7/977-3 carbon fiber prepreg with an approximate volume fraction of 62% carbon fiber and 38% 977-3 epoxy like that used in the previous chapter. This is an aerospace grade material used for making high strength engineering composites for aerospace application which was made available by Boeing Seattle and General Nano.

A stainless steel pressure plate of the same dimension with that of the prepreg cross-section is placed on the reinforced and stacked sample in order to create application of direct pressure on the prepreg layup during consolidation. Transversely aligned CNT array tiles processed through CVD method is used as reinforcing phase for a continuous through-the-thickness interlaminar reinforcement. A long CNT array is grown on silicon substrate with rectangular dimension. The high purity carbon nanotube array was made available by Chaminda Jayasinghe in collaboration with UC Nano world lab and General Nano.

A long, CNT array tile is then sectioned into micro-sized VACNT posts which are then slotted into micron-sized pin holes created on the surface of the stacked up laminated composite prior to consolidation. A 12-ply laminated composite panel is made with and without VACNT array reinforcement in order to understand the effect of nano reinforced interface and the effect of its reinforcement mechanism.

4.3 Fabrication Process of Transversely Aligned CNT Post Laminated Composite

4.3.1 Pin-hole Creation and Stacking Process of Hybrid CNT Post Laminated Composite

The process for fabricating multi- scale composite material with increased designed limits involves some critical steps that will improve the scalability and repeatability of the hybrid composite material. The first step in this process involves the cutting and laying-up of 10 plies of IM7/977-3 carbon fiber unidirectional prepreg which is cut into a 5’’x 2’’ cross section based on the analysis of the required number of pin-hole patterns that will be subsequently inserted into the prepreg layup for optimum reinforcement through the thickness direction. This process can also be used for other types of ply stacking sequence (cross ply, off axis ply, quasi-isotropic stacking etc.) and also irrespective of the thickness of the composite.

The stacked up unidirectional 10 ply prepreg layup is reinforced by manually placing millimeter length of manually chopped VACNT post with micron-sized diameter into the pin holes created by slightly pushing the carbon fibers apart as seen in figure 4.1 while figure 4.2 shows an improved procedure for CNT post insertion. The pin hole created is just about the diameter of the micro-sized pin. These impressions created did not affect the integrity of the carbon fiber since the pin holes were created at the interface between carbon fibers and 977-3 epoxy holding the unidirectional fibers together. The manual reinforcement pattern can be modeled and designed to produce an easy prototype on the laminate layup for repeatability and scale-up purpose. Dense Multi-wall vertically aligned carbon nanotube (VACNT) arrays which is produced through CVD method, is subsequently sectioned into about 300µm in diameter to

perfectly fit into the drilled cylindrical pin-hole pattern created on the prepreg layup with the use of the die tool.

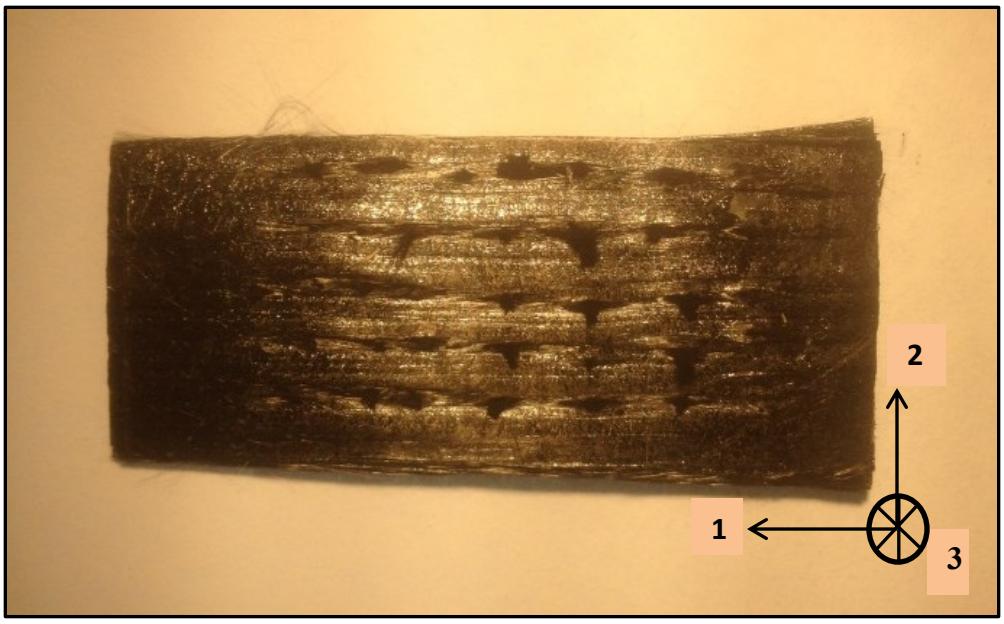

Figure 4.1 Image showing CNT post insertion through a 10-ply carbon fiber prepreg.

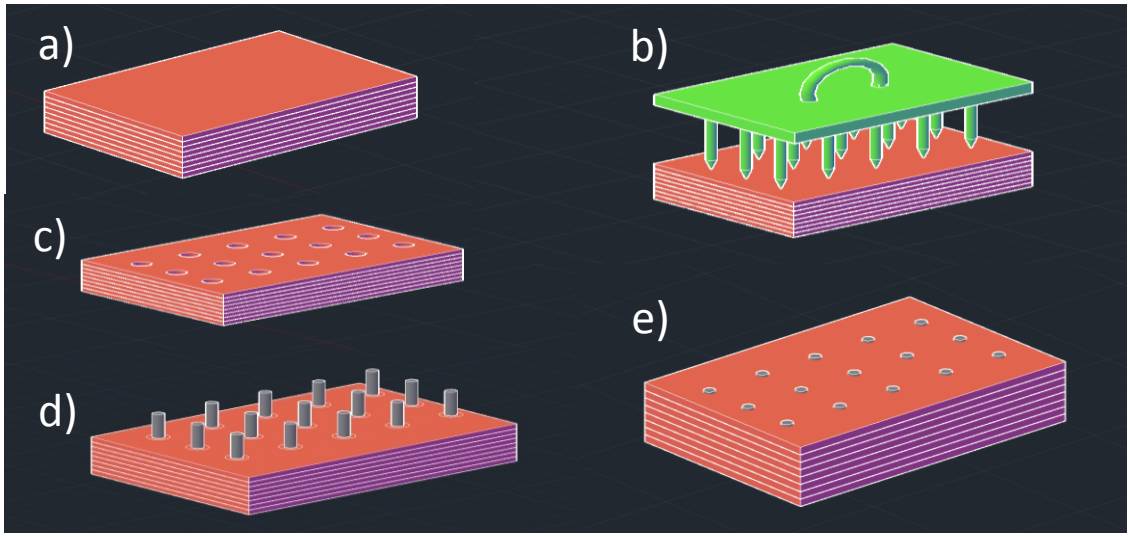

Figure 4.2 Image showing the fabrication process for multifunctional Nano composite for extreme application and performance (a) composite lay-up (b) die tool for creating reinforcement pattern (c) Cylindrical pattern created for CNT reinforcement (d) Patterned CNT arrays inserted through the thickness for interlaminar and delamination resistance (e) Multifunctional composite ready for curing process.

Subsequently, the top and bottom of the layup is finally covered with as-received IM7/977-3 carbon fiber prepreg for final consolidation. After successfully creating the 3-D reinforcement of the laminated composite sample, the mold needed for further processing of the layup is then prepared for final consolidation so as to achieve defect free composite panels for testing and evaluation.

4.3.2 Mold Set-up

Mold preparation is an important step in composite processing since it helps improves the reliability and surface finish of the fabricated composite. It generally reduces the effect of inclusions, weak material properties, poor surface finish etc. The presence of any kind of dust or impurities on the mold before fabrication will ultimately effect the properties of final fabricated sample. Here are some steps taken while preparing the mold for vacuum bagging and final curing:

1. Sanding the mold surface: Prior to vacuum bagging process and final layup of the prepreg, cleaning the surface of the mold is an important step which involves sanding the bottom surface of the mold with a sand paper (emery 400) in order to remove irregularities and contours on the surface of the mold. After sanding of the mold, a paper towel is dipped into acetone solution which is being used to wipe the surface so as to create a smooth and dry surface in no time due to fast evaporation of acetone. The mold is finally allowed to dry up for a while under room temperature.
2. Applying cleaner: After the first step, the mold is subsequently cleaned with XTEND CX-500 Cleaner (AXEL PRODUCTS, Cleaner). XTEND CX-500 Cleaner is a cleaner designed to create an effective surface adhesion of the release agent which is usually applied after this procedure. XTEND semi-permanent cleaner is designed to also remove

styrene build-up. The cleaner was carefully applied on the surface of the bottom of the compression mold and applied by using a natural soft bristle brush. Also health and safety procedures were adhered to while applying the cleaner on the surface of the mold in order to mitigate any lab accidents like spills and skin burns etc. Personal protective equipment like Butyl Rubber Gloves, Goggles with side shields were worn while applying the cleaner on the mold to eliminate these effects. The mold was allowed to dry after the application of the cleaner. The cleaner is supposed to chemically prepare the surface of the mold for release agent.

3. Applying the release agent: After the cleaning and drying process is done based on the above steps, release agent is then applied on the surface of the mold. The release agent when applied on the mold helps in easy removal of the composite sample, stainless steel block and bagging tape from the mold. Also, the release agent was thoroughly allowed to dry up after its application so it does not create spots on the surface of the sample during curing, hence; the release agent has to be carefully chosen. The release agent used is XTEND 19 SAM Release agent (AXEL PRODUCTS, Release) as shown in previous chapter. It's an external mold release agent which can be used for all types of molds. A very thin layer of release agent was applied uniformly on the mold surface and stainless steel block. Two coats had to be applied with an interval of 10 minutes as directed by the manufacturer.

Figure 4.3. Image of vacuum pump used for composite laminate consolidation.

4.3.3 Lay-up and Consolidation Process

Once all the prepreg are laid up in the desired sequence and fiber orientation, vacuum bagging preparations are made as shown in figure 4.4 for curing and consolidation of the part. The steps required for vacuum bagging are as follows;

1. As seen in the previous chapter, the bleeder serves to absorb moisture and excess resin coming from the stack of prepreg composite sample.

2. Apply separator film directly on top and bottom of all the stacked up prepreg composite sample. Peel ply fabrics are applied on the top and bottom of prepreg layers if consolidated parts are to be adhesively bonded at a later stage. The peel ply creates a good bondable surface finish on the fabricated part.

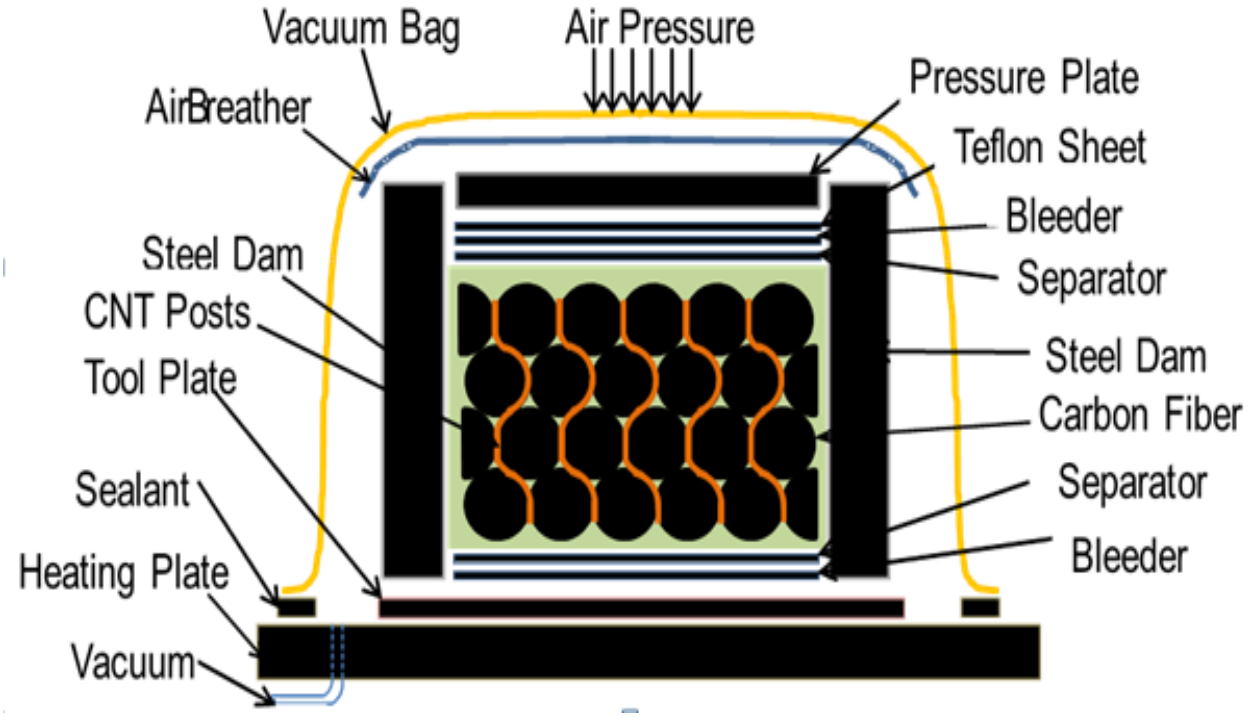

Figure 4.4. Fabrication and Lay-up process for long CNT post reinforced laminated composite [figure by Dr. Yi Song with permission].

3. Apply a breather layer, which is a porous fabric that is quite similar to the bleeder. The breather helps to impart uniform pressure around the consolidated part while allowing entrapped gases to escape.
4. Apply a pressure plate, a stainless steel block of the same cross section with composite sample of interest. Its function is to create direct pressure on the sample when the vacuum bag is compressed. This creates a better interlocking between the transferred VACNT arrays and the carbon fiber prepreg during compression process.
5. Apply the air breather layer, a porous fabric which is similar to the bleeder. It functions as the breather above.

6. Vacuum bag is a reusable elastomeric film which sits at the top. This film is sealed on all sides of the stacked prepreg using bagging tape. Once the vacuum bag is sealed up, the top mold is placed on the bottom mold and then ready for curing process. The bagging tape material helps to create a vacuum area for parts during consolidation.

After lamination and bagging, the mold is placed in between the top and bottom of a composite press machine for curing and consolidation. The composite press can equally maintain the desired pressure and temperature inside the chamber when the top and bottom of the press is fully closed due to application of load at the top and bottom. A typical cure cycle is shown in previous chapter where the assembly is introduced into a composite press in which a vacuum (15 psig) was applied, and the specimens were cured following the manufacturer recommendations (100 psig of total pressure, heat at 5^{o}F/min to 355^{o}F, hold for 6 h, cool at 5^{o}F/min to 140^{o}F and vent pressure and the let it cool to room temperature). The cure cycle depends on the type of resin material and the geometry of the part involved.

The pressure required for composite consolidation is created in two ways: Using the stainless steel pressure plate to apply direct pressure on the sample via compression of the vacuum bag as well as the external pressure inside the enclosed mold via a high pressure line. The vacuum bag creates a vacuum inside the bagging material and thus helps in proper consolidation. The vacuum pump squeezes air out of the bag and in turn compresses the stainless steel plate directly on the sample for efficient consolidation.

External pressure inside the press is created by injecting pressurized air through a high pressure line connected to mold. Thus, the external pressure outside the bagging area and the vacuum inside the bag creates sufficient pressure to compact the laminate against the mold and

create intimate contact between each layer. The heat for curing comes from heated air since the pressurized gas supplied to the chamber comes heated to increase the temperature inside the composite press.

4.4 Preparation of Test-Piece

After curing of the composite samples, both the baseline and Nano reinforced composite panels are brought out of the mold. The edges of both panels (5 in. x 2 in.) are first sectioned in order to create a well-shaped rectangular pattern so that the plates can be cut into the desired dimensions prior to testing. Two sets of test are to be performed on these samples for mechanical characterization;

1. Short Beam Shear Test
2. In-Plane Tension Test

For the short beam shear samples, four samples each from both 12-ply baseline laminated composite panel and 12-ply vertically aligned CNT array reinforced laminated composite panel were cleanly cut from the bulk composite panel using Beuhler ISOMET 1000 diamond abrasive cutting machine. In order not to create notches and delamination on the samples during preparation, the rotation of the circular diamond saw blade was kept at a low speed and dimensions were marked on the panel in order to achieve a better dimensional tolerance of all samples. Based on ASTM specification [110] for short beam shear test, the span-to-thickness ratio is 4 as recommended by ASTM D2344/D2344M.

For the in-plane tension test, the mechanical response of both non-reinforced and long vertically aligned CNT laminated composite under tensile loading is also investigated to

determine the effect of pin holes created in through-the-thickness direction on the tensile property when compared to the baseline sample without pin holes. Since work based on previous research [122-124] have shown an increase in properties in through-the- thickness direction with respect to the number of stitches created per unit area [123], while there is generally a significant drop in in-plane tensile properties which becomes increasingly degraded as stitch density increases due to stitch insertion damage and interaction [125, 126]. Here, after sectioning the specimen to desired dimension, the ends of the specimens are un-tabbed with polymer tab but are rather wrapped with 400-grit sandpaper with the use of an adhesive. The use of un-tabbed geometries is per current recommendations for testing of composite materials [127-129].

The sectioning of the specimen is carefully done so that two rows of vertically aligned CNT posts are retained on each specimen and not directly protruding at the edges of the samples which could create spots for crack initiation if the CNT posts do not fully fit into the pin holes.

4.5 Experimental Set-Up for Mechanical Testing

4.5.1 Interlaminar Shear Test (SBS)

A short beam shear test (essentially a 3-point bending test with a short span) was applied (see Figure. 3.13b) in a similar condition and environment as that conducted in previous chapter. Four samples each of both 12-ply non-reinforced and CNT reinforced laminated composite are subjected to quasi-static load application using an Instron 4465 test machine with a 2KN calibrated load cell. The specimen dimensions were also selected following the standard [110]. A span-to-depth ratio of 4 is used for the 3-point bending test as recommended. The composite laminate is composed of unidirectional 0^o carbon fiber aligned to the test axis of the specimen. The laminate is subjected to a 3-point bending test at a constant crosshead speed of 0.05 in/min.

The samples are loaded to failure and the failure load is imputed in the calculation of the average shear strength of the laminate ply interface. The procedure for setup and testing are well adhered to in order to ensure that failure occurs at the mid-plane of the laminate following guidance in the standard.

4.5.2 Tensile Test Set-up

In-plane tension test is carried out on vertically aligned CNT post reinforced composite to verify the effect of pin-hole creation on tensile properties of the laminated hybrid composite. These coupons were cut into multiple test specimens according to ASTM standards [130] for in-plane tension test.

The in-plane tension test is performed using an Instron 4206 test machine with a calibrated 20KN load cell with a fixed bottom fixture and a movable top tensile test fixture. The already prepared tensile test specimen is loaded unto the top and bottom fixture. Then the tensile specimen is clamped in the test fixture. The sand paper tab on both ends helps increase the frictional force between the grip surface and the sample specimen in order to resist slipping of the sample during load application and also to protect the specimen from possible damage as a result of crushing effect on the specimen while clamping. In addition, one end of each tab is tapered in order to reduce the stress concentrations during the loading process. The experimental setup of the in-plane tension test is shown in Figure 4.5

The laminate is subjected to an in-plane tensile test at a constant crosshead speed of 0.05 in/min. The load is applied until failure occurs and the failure load is imputed in the calculation of the average tensile strength of the laminate ply interface. This procedure was adhered to while

carrying out four tests each for both non-reinforced and vertically aligned CNT post reinforced laminated composite.

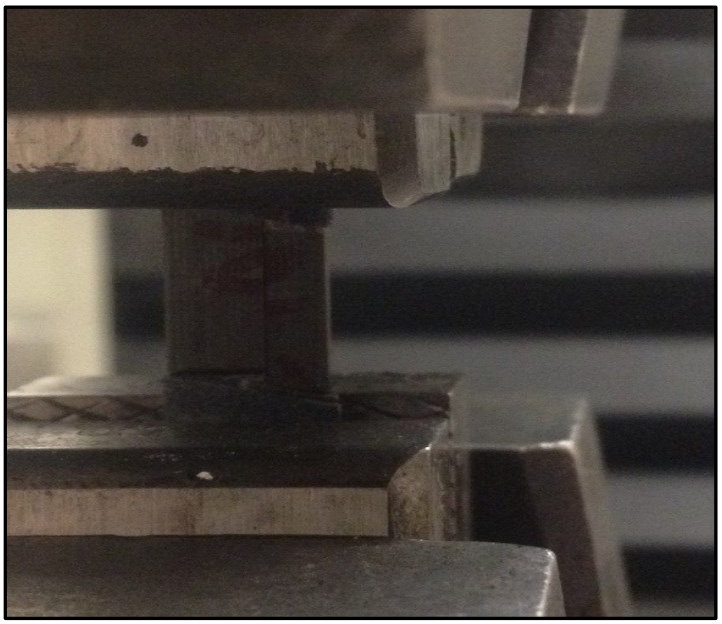

Figure 4.5 CNT Post reinforced laminated composite undergoing in-plane tensile loading.

4.6 Results and Discussion of Test Samples

The mechanical response of both non reinforced and reinforced CNT post laminated composite is both analyzed and discussed in this section. Both test carried out for interlaminar shear and in-plane tension test, are all cut out from a bulk composite panel.

4.6.1 Short Beam Shear Test Data

In the Short Beam Shear test, the determination of interlaminar shear failure is based on the same procedure used in chapter 3 to mechanically characterize the interlaminar shear failure of both baseline and CNT post reinforced laminated composite. For a beam of rectangular cross-section loaded in three-point bending, the maximum interlaminar shear stress occurs at the mid-

plane of the laminate composite beam between the center and end supports and is calculated to be;

$$\mathbf{F^{sbs} = 0.75 \cdot \frac{P_m}{bd}} \tag{4.1}$$

Where the F^{sbs} is the short beam strength, P_m is the maximum load observed during the test, b is the sample width and d is sample thickness.

Four samples each consisting of 12-ply baseline and CNT post reinforced carbon fiber laminated composite were tested and the load-displacement results computed after each test are used to generate interlaminar shear strength and deflection plot. Table 4.1 shows the overall data computed from the short beam shear test and its respective sample dimension. Figure 4.6 and 4.7, show the individual shear strength and displacement plot of both baseline carbon fiber composite and CNT post reinforced laminated composite samples respectively.

Figure 4.8 shows a bar chart comparing the mean shear strength of both samples with their respective error bars on each sample type. It can be seen that the baseline composite has mean shear strength of 81.8MPa with a deviation of 16.1MPa while the CNT post reinforced composite has mean shear strength of 116.4MPa with a deviation of 12.7 MPa. A 42% increase in interlaminar shear strength is recorded while comparing the result between the baseline and CNT post reinforced composite. This increase is attributable to the role of micron size, long CNT post reinforcement used to interlock the plies from the top to bottom which creates a “nail like” effect on the composite panel.

It can also be seen from figure 4.6 and 4.7 that the failure pattern of the baseline composite samples is quite different from that obtained for the CNT post reinforced samples respectively. From the baseline plots, there is a continuous increase in shear strength of the panel

until a point is reached showing an onset of delamination in the mid-plane where shear stress is maximum after which there is a slight drop and increase in shear strength which corresponds to either matrix cracking in the laminates or delamination of the neighboring plies above or below the mid-plane or a combination of both failures. There also exist a slight increase in shear strength after the sudden drop and increase as seen in the plot which is followed by the final failure of the composite panel. This might be due to the samples being able to withstand bending stresses before the load carrying carbon fibers finally failed.

For the CNT post reinforced composite shown in figure 4.7, it can be seen that the composite panel is able to withstand much higher shear stresses and delamination of the plies were insignificant prior to final failure of the composite as compared to the baseline samples. This shows that the effect of vertically aligned CNT post reinforcement architecture can be clearly seen with respect to delamination resistance and in-plane shear effect as a result of the loading condition.

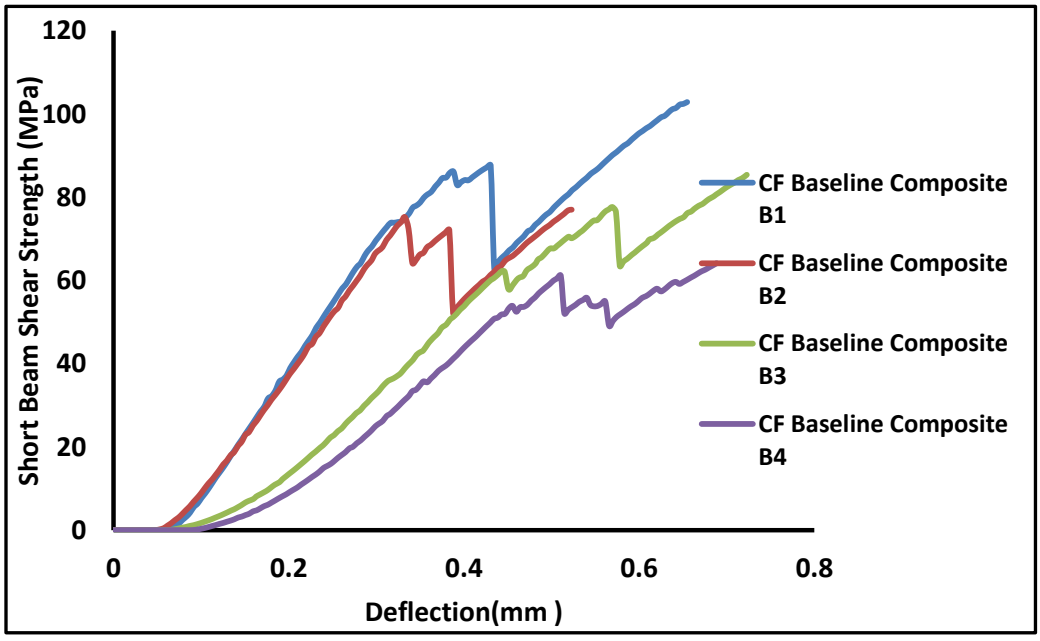

Figure 4.6. Short beam shear test curves for 12-ply baseline laminated composites samples.

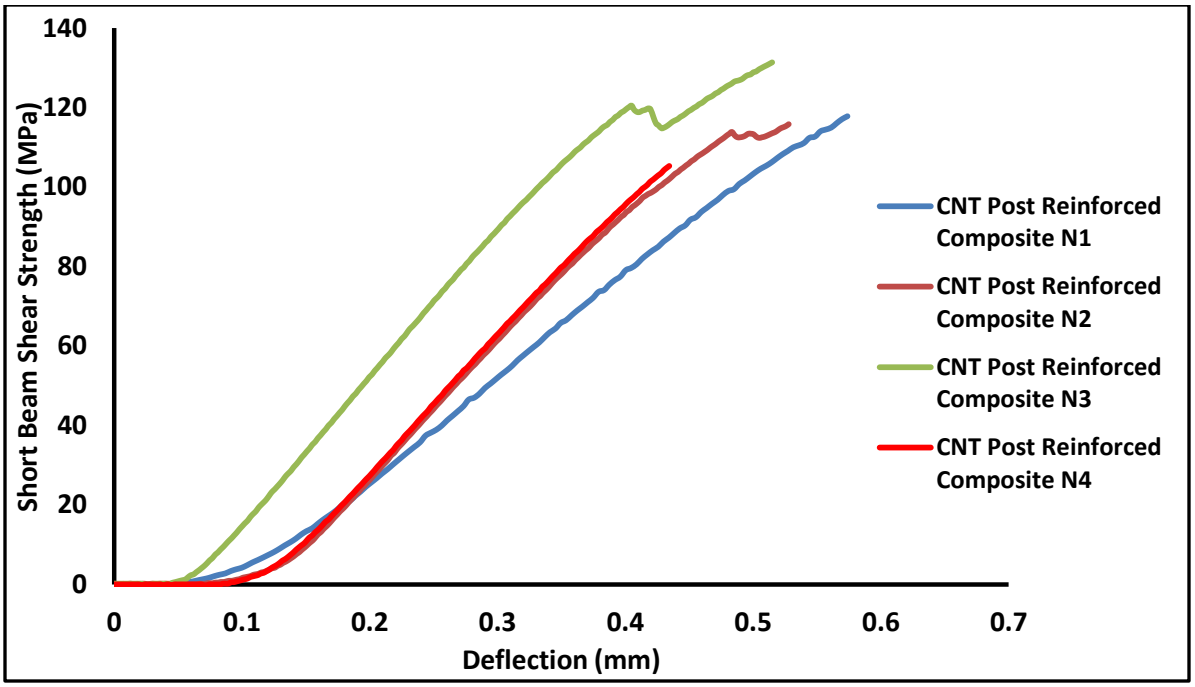

Figure 4.7. Short beam shear test curves for 12-ply CNT post reinforced laminated composite samples.

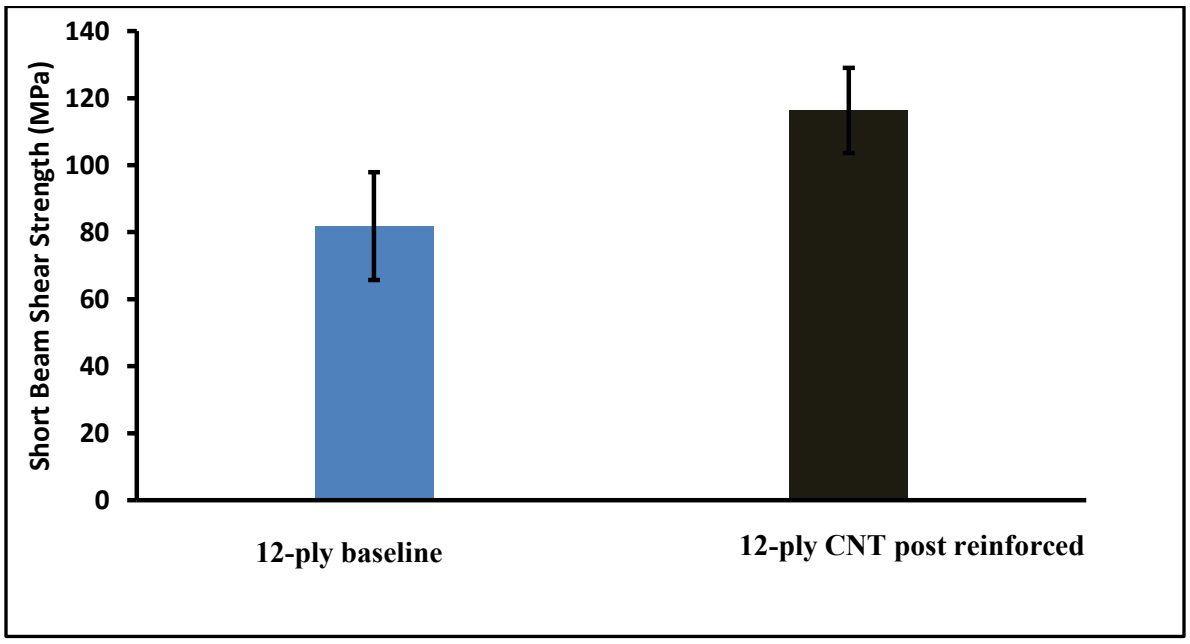

Figure 4.8. Bar chart showing a comparison between the shear strength of 12-Ply baseline composite and long CNT post reinforced laminated composite.

Table 4.1 Short Beam Shear test result for baseline and CNT post reinforced laminated composite.

	Sample Number	Width (mm)	Thickness (mm)	Shear Strength (MPa)	Mean Shear Strength (MPa)	STDEV	Increase of Shear Strength (%)
Baseline 12-ply IM7 Composites	B1	4.29	1.24	102.8	81.83	16.1	0
	B2	4.22	1.35	77			
	B3	8.08	1.27	83.4			
	B4	7.98	1.35	64.1			
12-ply CNT tile reinforced IM7 composites	N1	8.74	1.32	117.8	116.38	12.7	42.2
	N2	8.67	1.32	100.5			
	N3	8.53	1.4	115.8			
	N4	7.32	1.37	131.4			

4.6.2 In-Plane Tensile Test Data

In order to determine the in-plane tensile strength for a beam of rectangular cross-section, both unidirectional 12-ply baseline and CNT post reinforced laminated composite are loaded in tension in which the load applied is parallel to the fiber direction and the maximum load applied is divided by the original cross section of the rectangular beam as shown below;

$$\sigma_{11} = \frac{P_m}{bd} \tag{4.2}$$

Where σ_{11} is the in-plane tensile strength, P_m is maximum load applied during testing while b and b are the width and d sample thickness of the samples respectively.

From the Table 4.2, two different sets of test are conducted for the in-plane tensile strength in order to determine if the CNT post reinforcement has an adverse effect on the in-plane properties due to pin-hole creation and reinforcement. Both long and short samples are tested within the limits of criteria as specified by ASTM [130]. Table 4.2 also shows the overall

data generated with respect to the test conducted for both types of samples which can also be seen in figure 4.9 showing the mean strength and its respective standard deviation.

For the long samples, three samples each for the baseline and CNT post reinforced composite are tested but only data of one sample from the CNT post reinforced composite test is recorded due to damage of the sample while gripping both ends to the top and bottom fixtures. Figure 4.10 and 4.11 show the individual tensile strength and strain plots of both long baseline carbon fiber composite samples and long CNT post reinforced laminated composite samples respectively. From Table 4.2, it can be seen that the long baseline composite has a mean tensile strength of 1985.4MPa with a deviation of 220.3MPa while the long CNT post reinforced composite has mean shear strength of 1891.1MPa with no deviation since only one sample was tested.

This shows a 4.8% decrease in tensile strength as recorded while comparing the result between the baseline and CNT post reinforced composite. While for the shorter sample, three samples each for both baseline and CNT post reinforced laminated composite are tested but only data of two samples from the baseline composite test is recorded due to damage of the sample while gripping both ends to the top and bottom ends of the loading fixture.

Plots from figure 4.12 and 4.13 depict the regular curve usually obtained from composite stress-strain plots in which the sample reaches its maximum load and then undergoes catastrophic brittle failure.

Table 4.2 In-Plane tensile test results for baseline and CNT post reinforced laminated composite.

SHORT COMPOSITE SAMPLE RESULT							
	Sample Number	Width (mm)	Thickness (mm)	Tensile Strength (MPa)	Mean (MPa)	STDEV	Tensile Strength Increase (%)
Baseline 12-ply IM7 Composites	B1	6.93	1.27	1225.1	1186.9	54.1	0.0
	B2	3.3	1.27	1148.6			
12-ply CNT tile reinforced IM7 composites	N1	5.94	1.22	1269.4	1252.6	52.9	5.5
	N2	7.77	1.24	1295			
	N3	8.53	1.27	1193.3			
LONG COMPOSITE SAMPLE RESULT							
	Sample Number	Width (mm)	Thickness (mm)	Tensile Strength (MPa)	Mean (MPa)	STDEV	Tensile Strength Increase (%)
Baseline 12-ply IM7 Composites	B1	5.89	1.24	1732.4	1985.4	220.3	0.0
	B2	5	1.22	2089			
	B3	4.95	1.22	2134.9			
12-ply CNT tile reinforced IM7 composites	N1	7.21	1.3	1891.1	1891.1	_	-4.8

From Table 4.2 above, it can be seen that the short baseline composite has a mean tensile strength of 1186.9MPa with a deviation of 54.1MPa while the short CNT post reinforced composite has a mean tensile strength of 1252.6MPa with a deviation of 52.9 MPa. This shows a 5.5% increase in tensile strength while comparing the result between the baseline and CNT post reinforced composite. Figure 4.14 also highlights this feature which shows a bar chart of the in-plane tensile strength for the short sample configuration and its respective standard deviation.

Based on the above analysis and a look at Table 4.2, it is very likely that a 5.5% increase in strength in the shorter samples is due to a 2% reduction in thickness of the vertically aligned CNT post reinforced composite while a 4.8% decrease in tensile strength properties for the long CNT post reinforced composite sample might have influenced by a 6% increase in thickness of the CNT reinforced composite when compared to the baseline sample. This slight percentage changes might also have been due to error within the limits of the test performed.

This shows that the reinforcement architecture proposed herein; addition of CNT bundles for enhancing through-the-thickness properties will likely not affect its in-plane structural properties and integrity but controlling its thickness is a critical step in this process. With a new growth process of synthesizing CNT array post [131,132] in huge quantities, it is believed that this challenge can be overcome thereby significantly improving the tensile properties of Nano engineered composite with a minimally invasive technique while keeping the thickness of the hybrid structure unchanged.

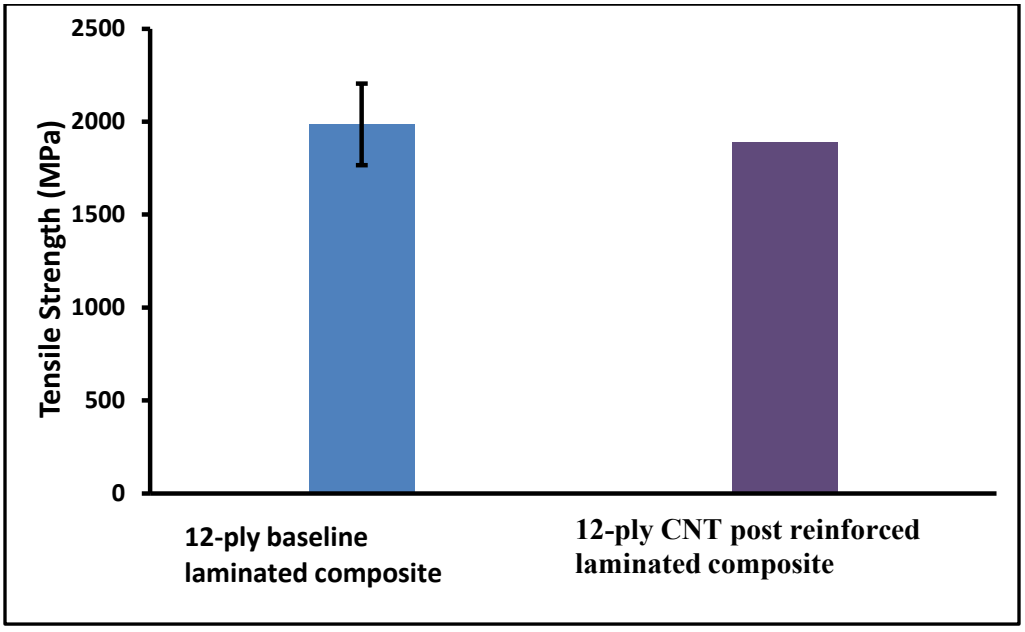

Figure 4.9. Bar chart showing a comparison between the in-plane tensile strength of long 12-Ply baseline composite and long CNT post reinforced laminated composite.

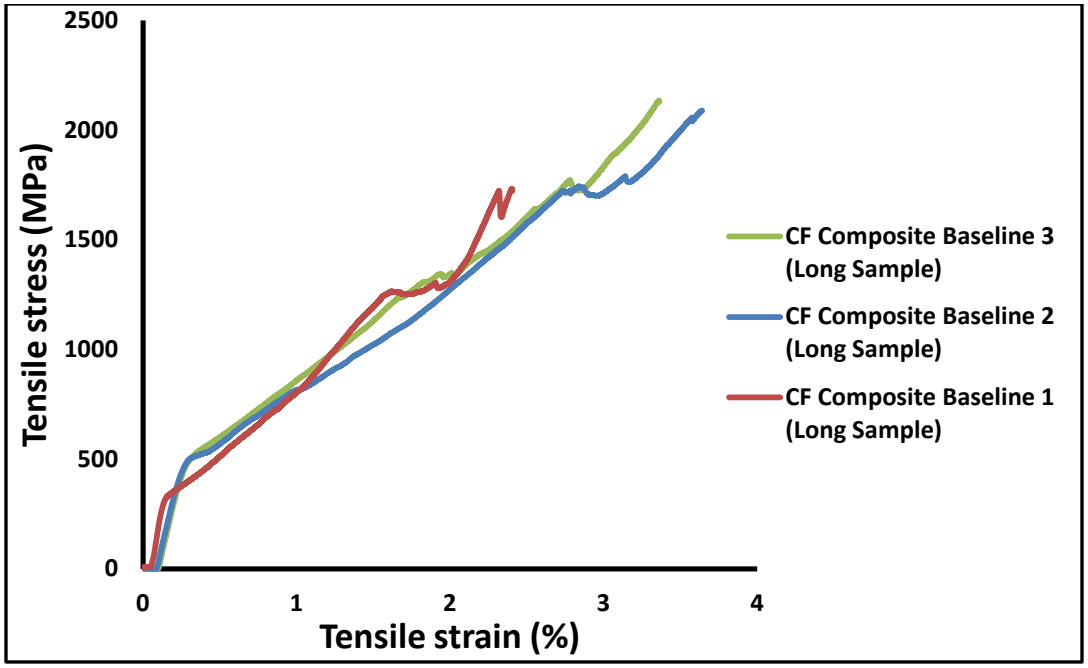

Figure 4.10. In-Plane tensile test curves for long 12-ply baseline laminated composites samples.

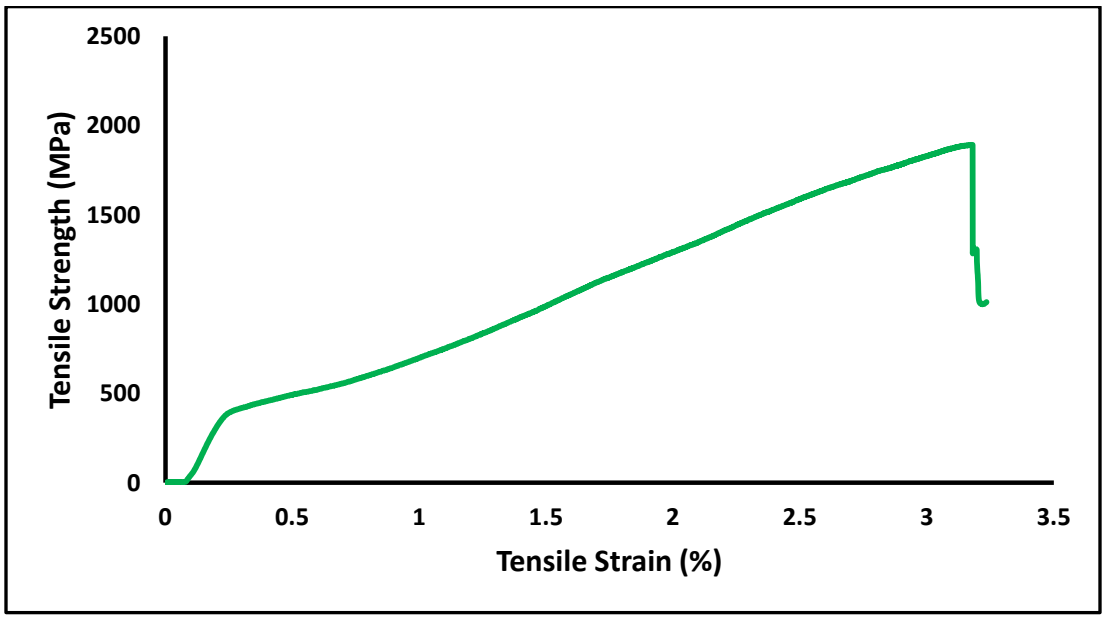

Figure 4.11 In-Plane tensile test curve for long 12-ply CNT post reinforced composites sample.

SHORT IN-PLANE TENSILE TEST PLOT

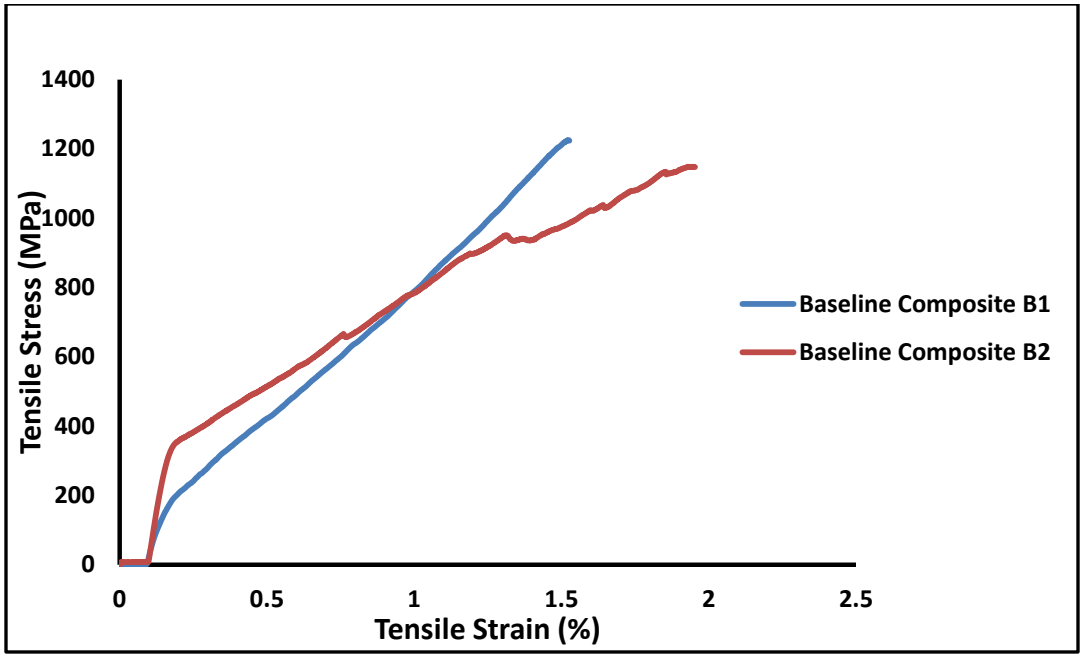

Figure 4.12 In-Plane tensile test curves for short 12-ply baseline laminated composites samples.

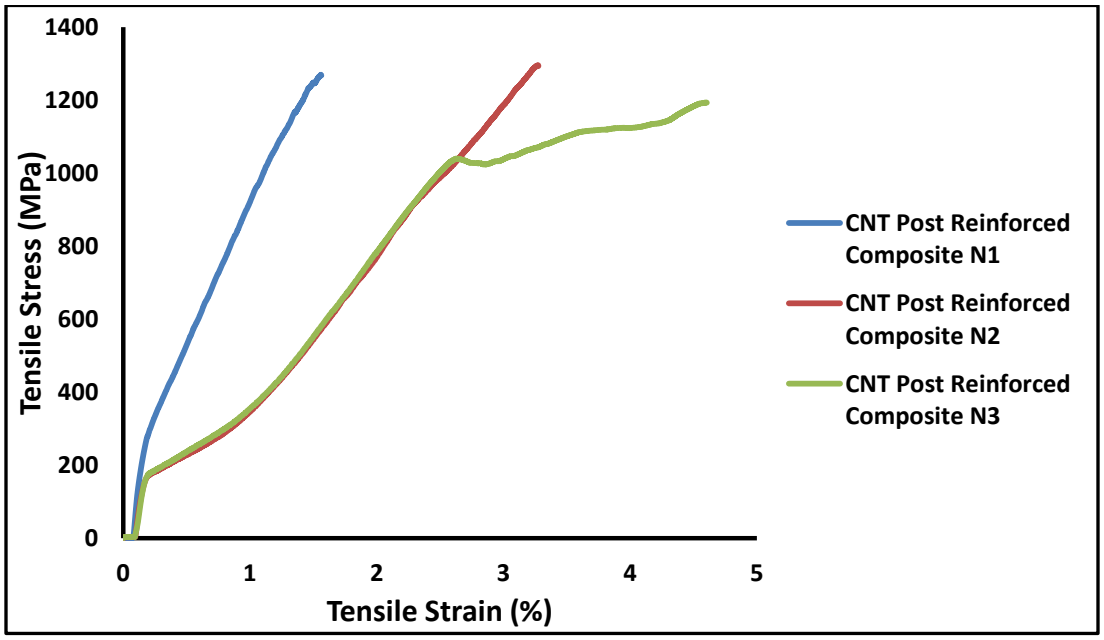

Figure 4.13 In-Plane tensile test curves for short 12-ply CNT post reinforced laminated composites samples.

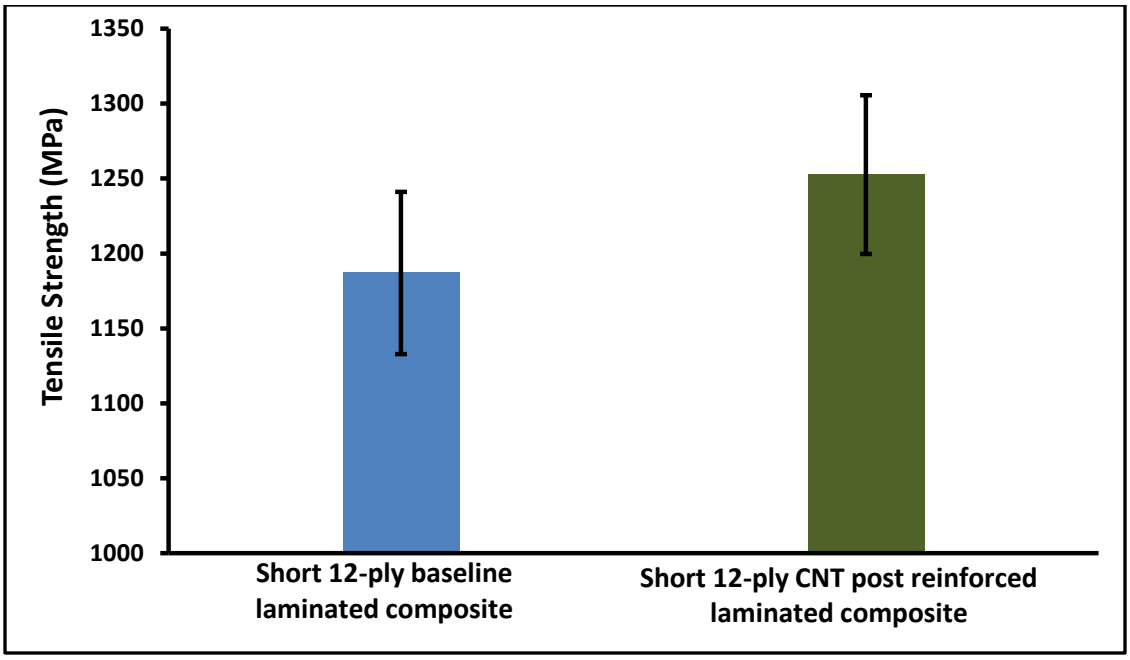

Figure 4.14 Bar chart showing a comparison between the in-plane tensile strength of short 12-Ply baseline composite and CNT post reinforced laminated composite.

4.7 Evaluation of Failure Surface

The interfacial shear strength of vertically aligned CNT reinforced IM7/977-3 hybrid composite and that of baseline composite without vertically aligned CNT (VACNT) array was characterized by SEM in order to understand the reinforcement mechanism provided by the CNT post during shear test. The reinforced hybrid composite showed about 42% increase in interlaminar shear strength as compared to the baseline sample which takes into account three suspected types of reinforcement mechanisms:

1. One is based on crack deflection mechanism where the transversely aligned CNT tiles act as crack arrestors, deflects the crack away from the fiber/matrix interface and creates a load transfer path between the matrix and carbon fiber . Therefore, failure occurring preferentially within the CNT tiles rather than along the matrix dominated fiber/matrix interface which was observed in the failure mode for the baseline composite where the

failure was a matrix dominated process as shown in Figure 4.15a. There are only horizontal cracks present in the baseline composites.

2. The second is based on energy dissipation mechanism in which a huge amount of strain energy is absorbed when the horizontal crack at the fiber/matrix interface tries to propagate through the transversely aligned CNT tile which in turn increases the amount of load that is needed to propagate the crack through the strong and stiff VACNT arrays. That leads to increase of the interfacial shear strength of the hybrid composites. This is shown in Figure 4.15b where the crack in the non-reinforced zone has an angle of 0° while the crack in the VACNT reinforced zone has a zigzag failure surface. Figure 4.15c and Figure 4.15d shows the crack occurred in the CNT/matrix interface.
3. The third involves the transversely aligned CNT arrays mechanical interlocking in between the fibers and the matrix in the composite thereby making it difficult to easily create an in-plane shear affect at low load application thus enhancing the fracture toughness and in-plane shear strength.

This is a preliminary result and further research including high resolution SEM and TEM will be done for further understanding of failure mode of individual CNTs.

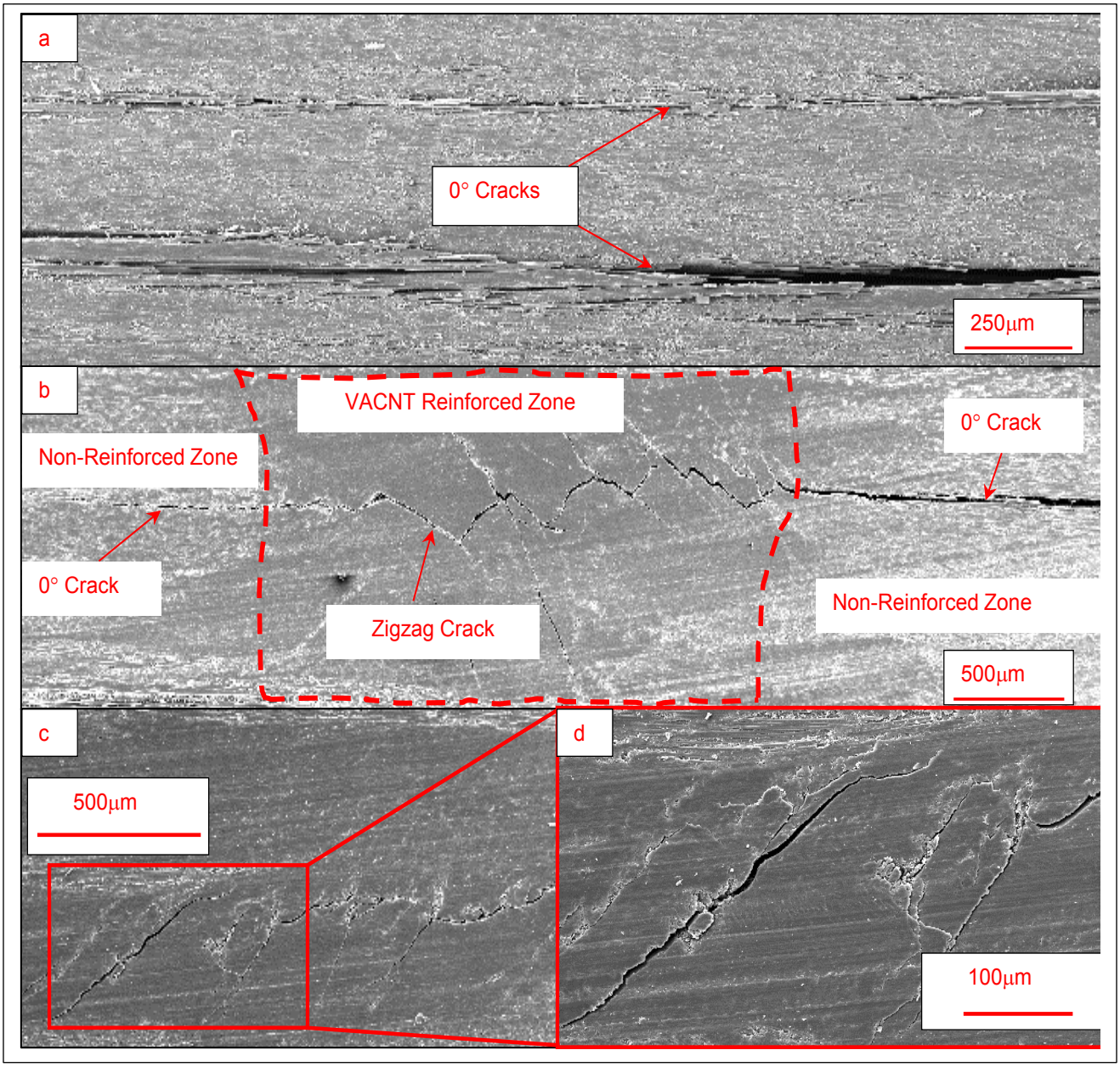

Figure 4.15. Morphological research of failure mode of multi-scale composites: (a) failure surface of baseline composites without CNT tile reinforcement; (b) failure surface of multi-scale composites with vertically aligned CNT tiles; (c) crack in CNT tile/matrix interface (d) close-up view of crack.

The effect of CNT reinforcement on the matrix dominated failure of carbon fiber reinforced composite have also been seen to have a significant effect on the fatigue life of nano reinforced composite. Results have shown that carbon nanotube aspect ratio (length/diameter) and reinforcement architecture has a significant impact on the fatigue behavior of hybrid nanocomposite. Analyses of test data [133] indicate that longer MWNTs with small diameters (i.e. higher aspect ratios) are well suited for the reduction of fatigue crack growth.It is also stated that the fatigue limit for carbon fiber composites falls between two critical threshold levels which corresponds to the onset of transverse cracks and the appearance of local delamination, respectively.

From the tension-tension fatigue life test carried out both in the fiber and other bias directions, Gorbatikh et al [134] also found out that there is no significant change in the number of cycles to failure for the baseline (FRC) and nano-engineered composite (nFRC) fatigue test carried out in the in-plane direction for higher stress levels. He claims that the fatigue properties for low cycle fatigue are mostly fiber dominated failure which are controlled by the properties of the fibers, hence nano modification of the matrix has little or no effect. The number of cycles shows a significant increase at lower stress levels. He believes that the high cycle fatigue behavior is markedly affected by fatigue performance of the resin matrix and the resin rich lamina interface, which enhanced the improvement of the nano-engineered composite due to nano phase reinforcement of transverse and shear crack propagation.

CHAPTER 5

Design and Manufacturing Analysis of Multi-scale Composites for Higher Performance

5.1 Overview of Multi-Scale Composites

The quest for higher performance, reliability and efficiency of composite materials is driving the need for further research in the field of Nano-engineered hybrid composite materials for future application [1-10,]. As highlighted earlier in previous chapters, laminated composites provide high specific strength and high performance but weak failure modes such as delamination, matrix micro cracking, impact damage etc. limit the performance of composite materials which as a result, they fail well below the yield strength of the material while in service. Mitigating the weak failure modes of laminated composites would have a significant effect and also create new areas of structural application in a wide range of industry including increasing the safety and performance of high cost air vehicles [135-136].

CNTs have been widely used by researchers for composite reinforcement due to their small size. Its exceptional mechanical, electrical and thermal properties which it possess, also make them a good candidate for improving the properties of composite material and also for sensor application and damage detection [137-141] if tailored to explore those properties. Prior techniques have been published in literature regarding the use of various forms of CNTs to reinforce composites [45-49, 102-106] which involve the use of dispersion methods, powdered nanotubes, nanotube thread spun from short nanotubes, fuzzy nanotubes grown onto carbon fiber, and Bucky paper sheet formed using short nanotubes.

Results have shown that these techniques provide certain improvements in some particular failure mode when compared to baseline composites but in general; do not provide a multiplying effect on the overall multifunctionality of the composites as expected. Powdered nanotubes, nano fibers, clay and grapheme usage have been investigated extensively in the past and have been shown to reinforce matrix micro-cracking but does not significantly improve the strength of composites since these nanotubes are too short to either form a continuous load path through the composite or are not long enough to mechanical interlock the individual fiber plies in the composite.

Based on analysis and results shown in chapter 4, it can be seen that the optimum process of achieving an all-round multifunctionality of laminated composites is with use of long nanotubes that are patterned into small diameter vertically aligned post which brought about an improved shear performance and will potentially improve the impact, electrical, thermal, OHC and other structural properties of composite. Also, spinning of long CNT arrays into microns size yarns and thread which have not been available in our laboratory until recently [142-145] and are still being developed to optimize their performance, have also not been used to reinforce composites in the way we propose herein. It is envisaged that in-plane reinforcement of composites with long CNT yarns and arrays will help increase the volume fraction of the composite while reinforcing the micro size gaps in between carbon fibers which are points for crack initiation, growth and propagation.

5.2 Motivation for Proposed Technology

Laminated composite materials possess high strength-to-weight ratio and stiffness. However, a limitation of the matrix material (e.g. epoxy) between the fibers and plies is that the

matrix rich regions are sites for failure initiation and propagation in composites [102]. The excess resin matrix in composite reduces its fiber volume fraction, increases crack nucleation sites due to their brittle nature and reinforcing with traditional microscale fibers can be quite difficult. Moreover, fabrication process anomalies, post fabrication damage, and the environment can also reduce the mechanical properties of composites in some cases to 60% of the tensile strength of a baseline material as shown in Figure 5.1.

If the allowable design region of composites could be expanded by 10% or more, this would be a major advance in the composite industry and manufacturers would obviously want to modify their fabrication process techniques to achieve improved properties (per discussion with composites engineers at Boeing St. Louis).

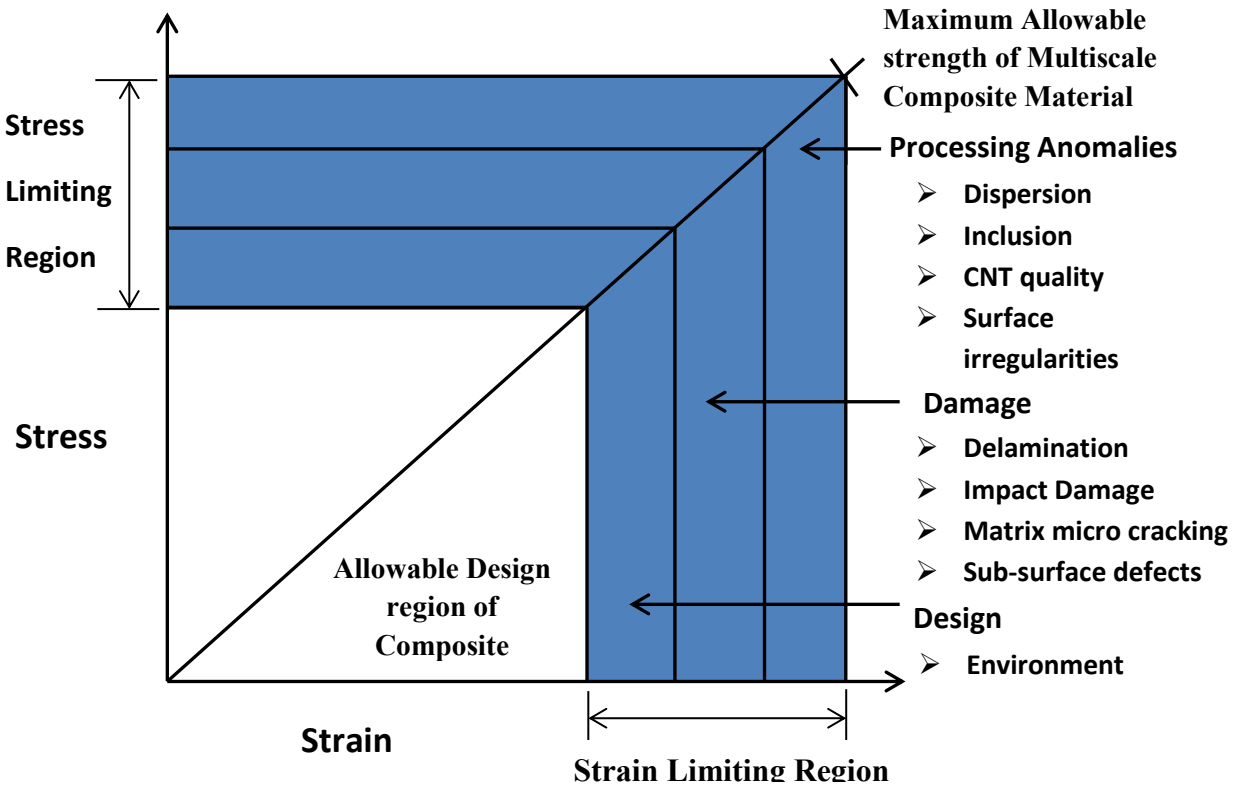

Figure 5.1. Limitations in current composites technology: composites have a large knock-down factor

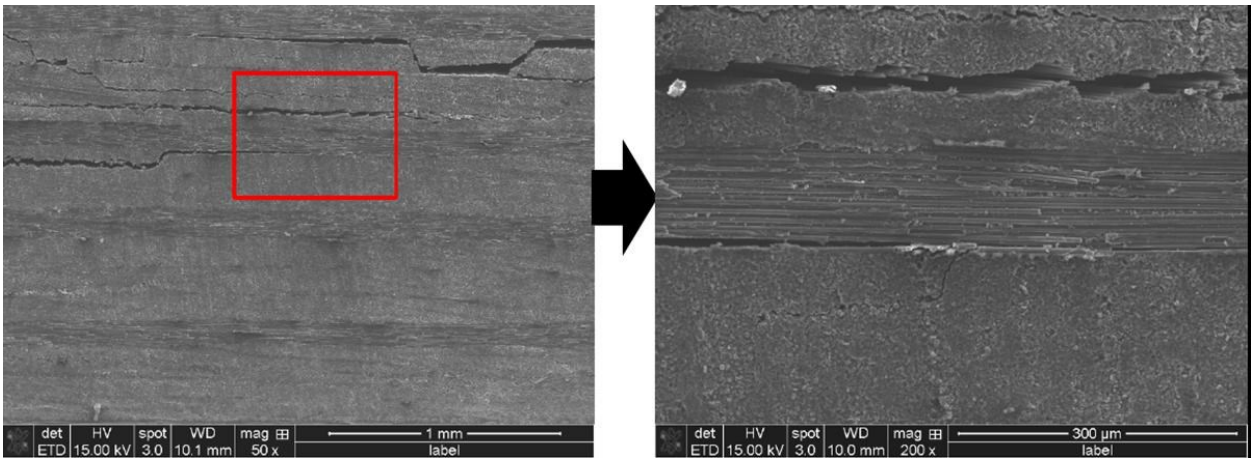

Figure 5.2. (a) Matrix cracking occurs in the 45 and 90^0 plies. Cracking is between fibers and does not fracture the carbon fibers; (b) the 0^0 ply is intact.

UC Nanoworld group has been working in fabricating composites and reinforcing weak failure modes while also collaborating with other researchers for a long time. From work done in chapter 3, an IM7 977-3 composite laminate with quasi-isotropic symmetric layup: [0 90 45 -45 0 90 45 -45 0 90]$_s$ was fabricated and tested in different failure mode. The off-axis plies are susceptible to fail due to matrix cracking between the carbon fiber plies which also gave an insight of how best composites can be reinforced.

The failure modes of composites are quite unique and complex in different load application and at varying stress concentrations. Also, as an example, the open-hole compression (OHC) test depicts a weak failure mode in laminated composite. The stresses involved are usually complex (combination of shear, compression, and buckling) all present at the time. The vertical and axial nano-reinforcement proposed herein is expected to significantly increase the OHC properties of composites which is argue-ably the most significant failure to reinforce and a big problem for composite air vehicles due to the large number of rivets and fasteners (up to

72,000 rivets). Up until now, limited amount of success has been achieved reinforcing composites [101-106] with traditional fillers.

Powder CNTs and CNT arrays have also been used for this process which also has its own limitation with respect to resin viscosity [102-105]. Due to theoretical projections carried out, we believe only long and strong nanotube posts with micron size diameter can efficiently reinforce composites transverse to the in-plane direction, and that is the uniqueness of this approach along with the approach of integrating CNT threads in between carbon fibers for hybrid composite. Work done in chapter 4 is a reference in describing the technology where through-the-thickness pin-holes are created by pushing the carbon fibers apart and inserting long CNT post running continuously from top to bottom. The composite can be reinforced in the all 3-directions (x, y, z direction) with different CNT forms to produce a strong multiscale composite [45-49, 106-107].

5.3 Basic Design and Innovation of the Proposed Method

Our proposed approach [109] in reinforcing the weak failure modes of laminated composites is to integrate CNTs into composites in two different orientations: (i) CNT spun thread of 1-2 micron diameter integrated in between the micro spaces parallel to conventional micro-sized carbon fibers; (ii) long carbon nanotube (CNT) bundles or post integrated transversely to carbon micro-scale fibers.

For CNT reinforcement parallel to the micro-sized carbon fibers, Figure 5.3 and 5.4 show the overview of the process. Note that in composites, reinforcement plies can be aligned in multi direction based on the performance criteria. The CNT threads are inserted into the micro spaces between carbon fibers and plies as seen in Figure 5.3. From Figure 5.4, a prepreg

manufacturing process is fabricated by using 1-2µm diameter CNT thread to integrate in between carbon fibers of 7µm diameter. This manufacturing process help increase the volume fraction of fiber reinforcement in the composite by replacing resin filled areas with CNT threads between the carbon fibers.

This process is known as a high volume fraction composite (HVFC) manufacturing process [132] where by the volume fraction of fiber materials (carbon plus CNT) is increased, thus reducing the volume fraction of matrix material (thermoplastic or thermoset) in composites. HVFC material can be fabricated since the CNT strands and threads produced are pliable, strong and tough and thus can undergo prepreg manufacturing process without breaking apart during drawing and stretching process. The approach is also visible since using all CNT reinforcements would be too expensive and CNTs threads and fibers in large quantities are not available presently.

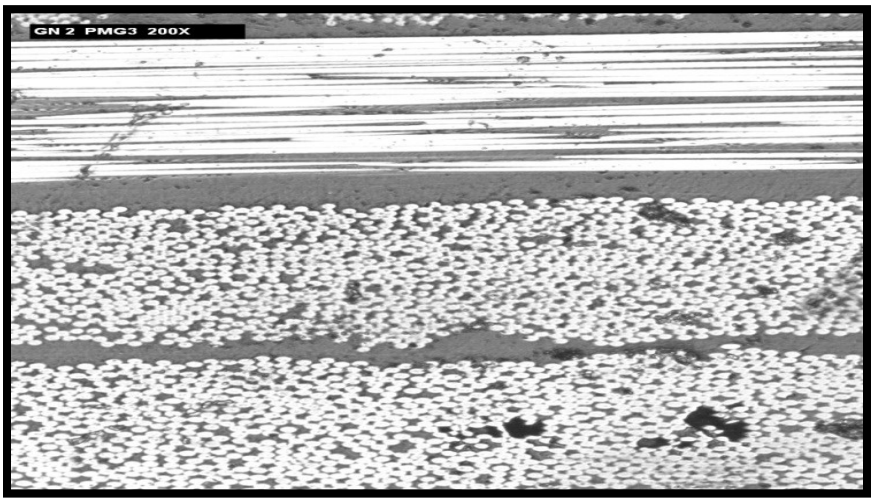

Figure 5.3. Close-up of fibers and matrix rich areas in composites that can be partly filled with long CNT [Figure by Dr. Mark Schulz with permission].

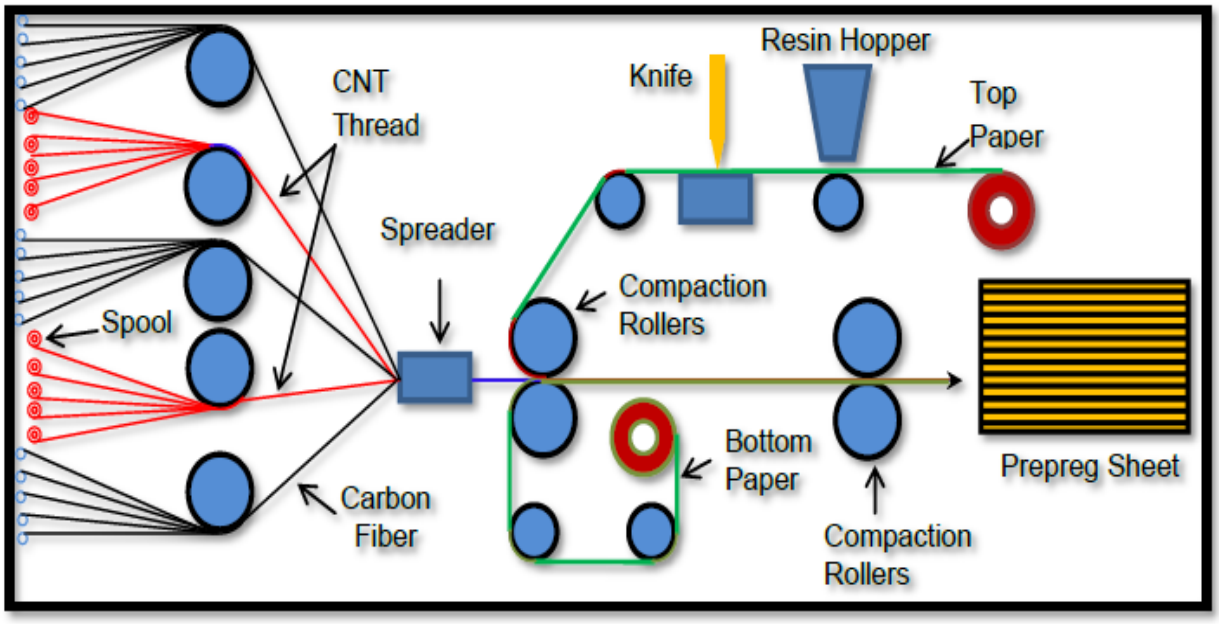

Figure 5.4. CNT thread being integrated within a carbon fiber tow in the carbon fiber manufacturing process. [Figure by Dr. Yi Song with permission].

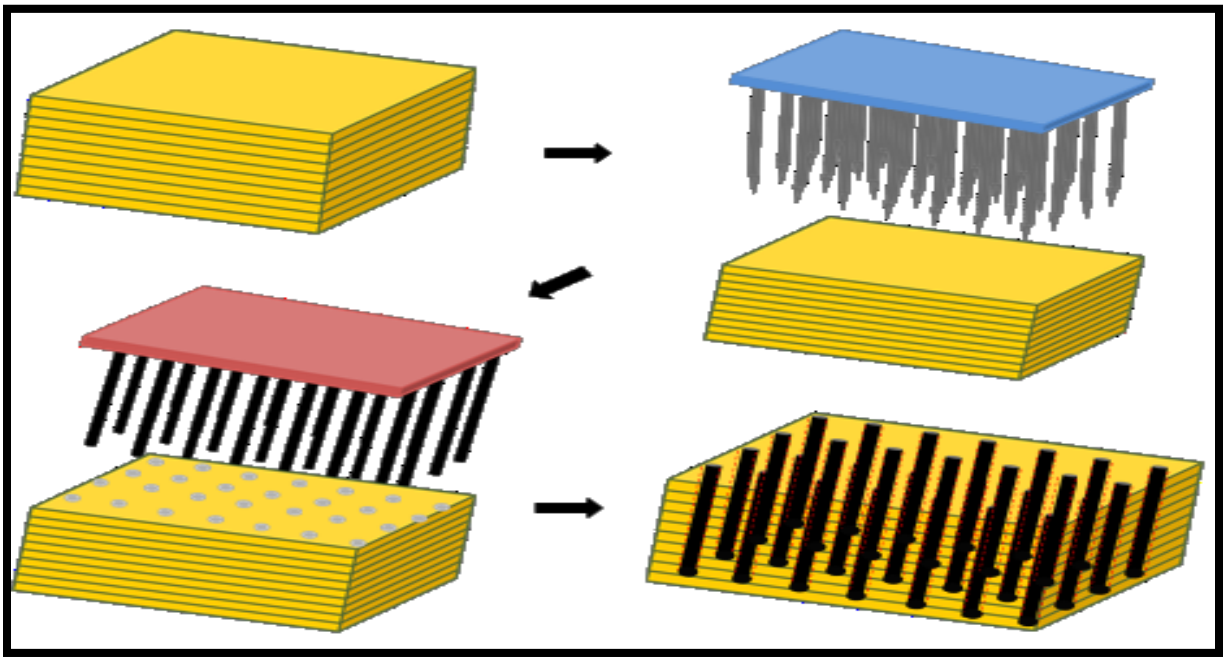

Figure 5.5. Transverse CNT bundles to reinforce laminated composites, first carbon fiber-CNT prepreg plies are stacked in a desired layup, then a pin fixture gently expands the prepreg plies, patterned long carbon nanotube posts are inserted into the holes in the prepreg stack, and face plies are added at the top and bottom, this process can be automated [Figure by Dr. Yi Song with permission].

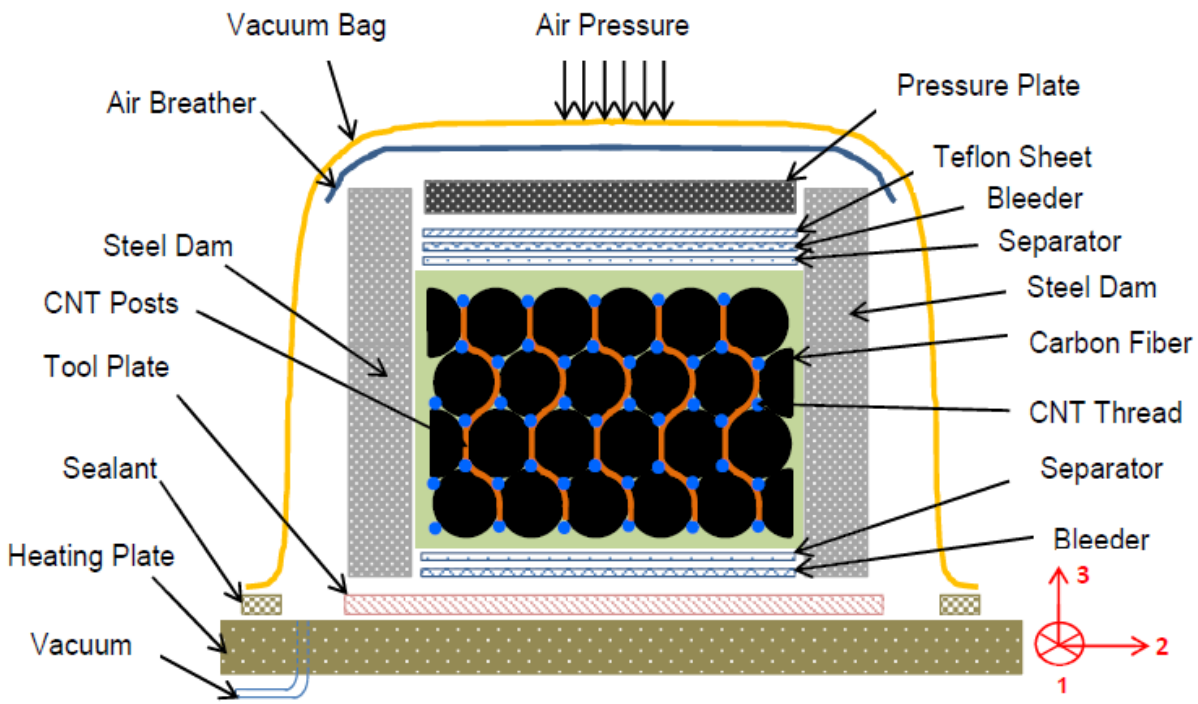

Figure 5.6. Cross-sectional view of the composite with longitudinal (blue dots) and transverse (red lines) reinforcement, a mold compresses the material laterally and transversely and squeezes the nanotubes to be in tight contact with the carbon fibers and the composite is cured. [Figure by Dr. Yi Song with permission]

HVFC technology is predicted to improve strength, toughness, impact resistance, strain sensing and conductivity of polymeric composites which will become a more sophisticated engineering material with high performance and reliability for energy efficient, safe, environmentally friendly, and corrosion resistant air/ground vehicles. The amount (%) of CNT reinforcement is very critical in this process and will be determined experimentally which also depends on the diameter and strength of the CNT thread used. An analysis is performed in the next section [132] to determine the area of the micro space between the compressed carbon fibers to be filled with CNT threads. The strength of laminated composites is limited by weakness in interlaminar shear.

Thus the second reinforcement orientation is transverse to the micro-sized carbon fibers. Figure 5.6 shows the fabrication process for inserting CNT posts of 5-10 mm long with micro-sized diameter as shown in figure 5.7 a, b and c which shows a close up view of the cross section of the patterned array that will be used to produce an automated process of inserting the CNT posts to interlock all the plies in the composite together. This process was demonstrated in chapter 4 where CNT arrays are manually sectioned into CNT posts as seen also in figure 5.7 d, e, and f, in which the post are sliced out from a bunch of CNT array tiles. New method and processes for making CNT posts with a near perfect geometry are recently available as shown and will be incorporated into this research.

The CNT posts are being grown in patterns with desired diameter and spacing based on photolithography process and subsequently annealed to make them stronger and straighter. During the curing process, epoxy from the carbon fiber-CNT thread prepreg will infiltrate and wet the micron diameter CNT posts and compress the laminate composite set-up during consolidation stage. Figure 5.5 shows curing of the multi-scale composite with both parallel and perpendicular reinforcement [132].

In figure 5.6, the CNT posts and threads are shown in a cross-section of the front view but can also be seen in a 3D view of the hybrid laminated composite in figure 5.6 which shows the micro-sized diameter CNT post been inserted in between the carbon fiber-CNT thread prepreg laminate.

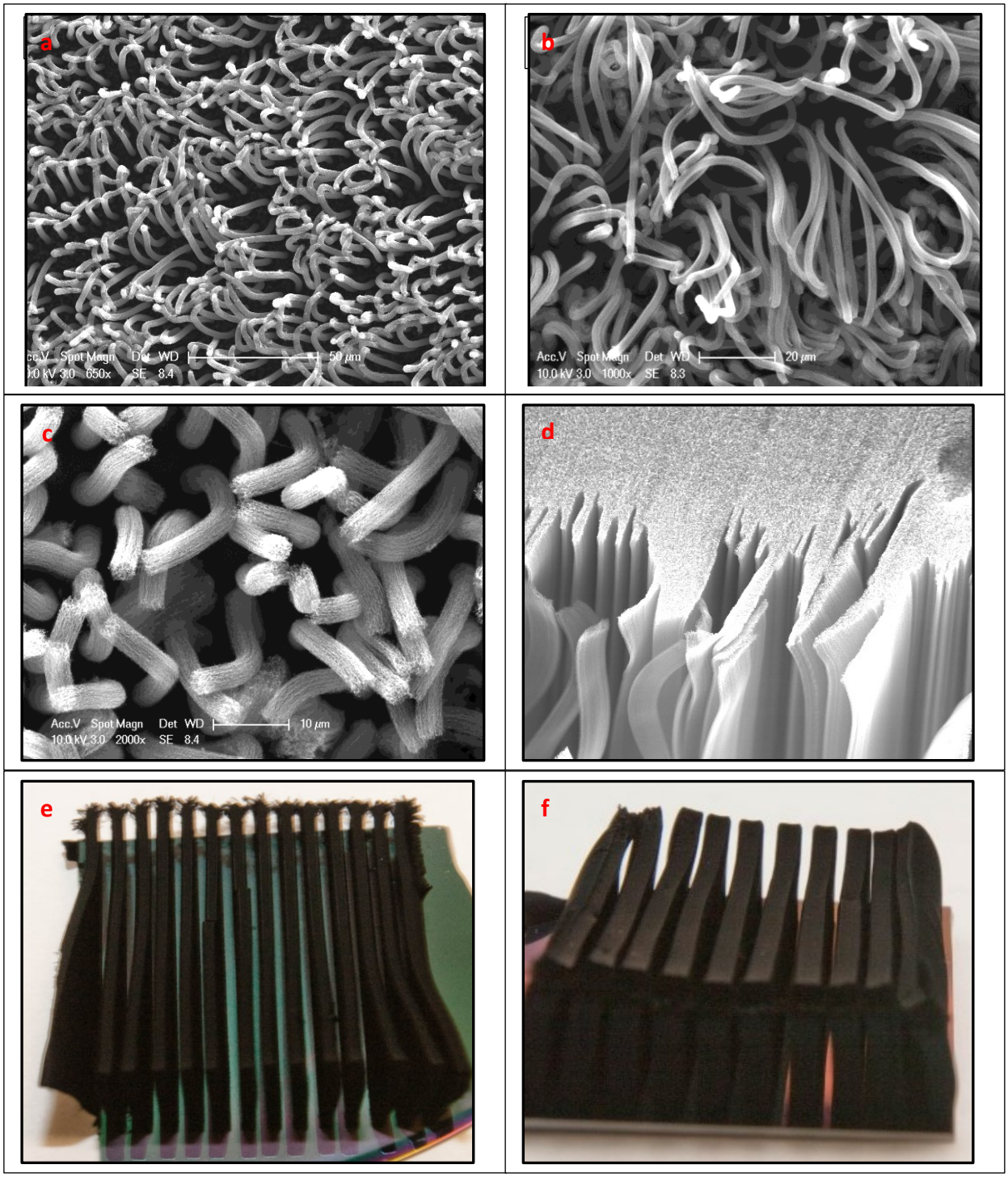

Figure 5.7 Images of CNT post; New CNT patterned posts to be used for transverse reinforcement of composites. Magnification increases from a- c (a) low; b) Medium; c) High. CNT array panel for manual insertion from Nano to millimeter thickness; CNT Panels 1.5 cm height, 5 cm width (d) Nano; e) Micro; f) Millimeter thickness [Figure by Dr. Wongdong Cho with permission]

5.4 Determination of CNT Fiber Diameter for In-Plane Reinforcement

An analysis is performed to determine the area between the carbon fibers that will be available to fill up with CNT thread. Figure 5.8 shows the cross section of closely packed carbon fibers. The region in the middle and around the carbon fibers is to be reinforced with the long CNT or spun CNT thread.

From the diagram in Figure 5.8, the reinforcement area will be the area of the triangle – 3 x the area of the sector, that is;

$$A_c = \frac{1}{2}\mathrm{A}\times\mathrm{B}\times\sin\theta - 3\times\frac{\theta}{360}\times\pi R^2 \ , \qquad (5.1)$$

Where A and B are the radius of the touching circles and θ is the angle of the equilateral triangle.

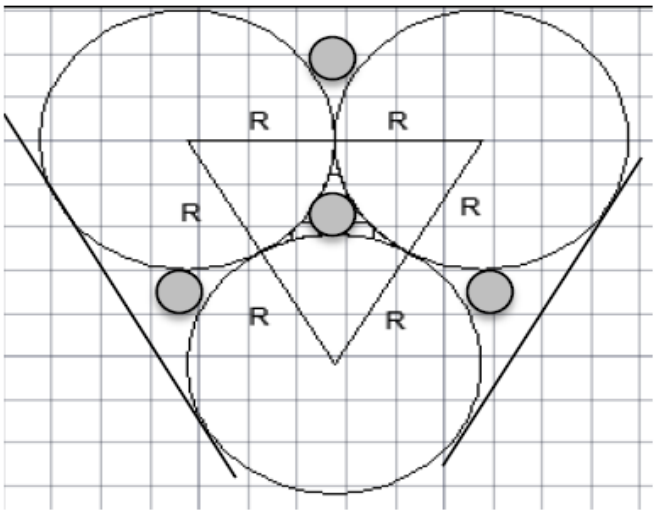

Figure 5.8. Cross section of closely packed carbon fibers. The region in-between the three carbon fibers are to be reinforced with long CNT or CNT thread.

Substituting values into (1) gives;

$$A_c = R^2\sqrt{3} - \frac{1}{2}\pi R^2 = R^2(0.161)\,. \qquad (5.2)$$

The average diameter of the typical carbon fiber is 7μm while its radius of 3.5μm is used to determine the maximum reinforcement area. Thus the area of the shaded region in (5.2) will be;

$$\mathrm{A_c} = 1.97x10^{-12}m^2$$

This will be the approximate area of the CNT thread that will reinforce (fill in) the micron sized gaps. Thus;

$$A_{cnt} = \frac{\pi d_{cnt}^2}{4} = 1.97x10^{-12}m^2\,.$$

The diameter of the CNT thread or long CNT needed to provide this reinforcement will be

$$d_{cnt} = \sqrt{\frac{4\left(1.97x10^{-12}\right)}{\pi}} = 1.6x10^{-6}m\,.$$

Based on theoretical estimation above, it can be seen that about 1.6μm diameter or smaller thread can be used to fill in the gaps between carbon fibers in order to achieve a much desired result proposed herein. From geometry shown in figure 5.8, about one CNT thread will be needed for every carbon fiber in the composite ((6 perimeter regions/3 + the center region)/ 3 carbon fibers) results to 1 CNT per carbon fiber.

The area of the carbon fiber material will increase by the fraction;

$$\frac{A_{cnt}}{A_{cf}} = \left(\frac{d_{cnt}}{d_{cf}}\right)^2 = \left(\frac{1.6}{7}\right)^2 = 0.05(5\%) \tag{5.3}$$

The typical volume fraction of carbon fiber present in a fiber reinforced composite is 62% while that of the matrix volume fraction is about 38%. Therefore, the carbon fibers are not densely packed, as a result, and there is potentially more than 5% room for addition of CNT thread. This also means that CNT thread with a larger diameter than 1.6 microns can be used, but the smaller diameter thread would allow tighter packing.

This analysis suggests that CNT thread might be interlaid in the region between carbon fibers to increase the volume fraction of carbon reinforcement. The matrix must be able to wet the carbon fiber and CNT thread. Detailed analysis is needed to determine how high of volume fraction of carbon fiber/CNT can be achieved.

5.5 Analysis of Improving the Mechanical Properties Using Long CNT Post and Micron Size CNT Thread Reinforcement

5.5.1 Evaluating In-Plane Tensile Properties

A unidirectional IM7/997-3 Carbon fiber/epoxy prepreg with a carbon fiber volume fraction of 62% which is basically the leading high performance material used in the aerospace industry will be reinforced with unidirectional bundles of long CNT or small diameter CNT thread placed in between the interlayers and the carbon fibers of unidirectional carbon fiber material in order to improve the tensile strength. A critical factor to consider while reinforcing

the carbon fiber plies with CNT is the wettability of the CNT by the epoxy during the curing process. A uniform and homogenous structure that provides a very good interface between the respective fibers and interlayers is needed for effective stress transfer and to produce a structurally stable composite.

To estimate the CNT volume fraction needed for this process, an analysis was performed based on the rule of mixtures to determine the change in strength with respect to the addition of CNT material between the carbon fibers. It is envisioned the CNT can be integrated with the carbon fibers in the tow fabrication process. In this design, that the volume fraction of carbon fiber is fixed. The volume fraction of epoxy is reduced by exactly the volume fraction of CNT added to the composite. The rule of mixtures method used for estimating the strength of three component composites is;

$$\sigma_c = \sigma_e v_e + \sigma_{cf} v_{cf} + \sigma_{cnt} v_{cnt}, \tag{5.4}$$

Where σ_c, σ_e, σ_{cf} and σ_{cnt} are the strengths of the composite, 977-3 epoxy, carbon fiber, and carbon nanotubes respectively, and v_e, v_{cf}, v_{cnt} are the volume fractions of 977-3 epoxy, carbon fiber and carbon nanotube, respectively.

In estimating the strength of the composite, strength results of individual phases in the composite are used while varying the volume fractions of epoxy and CNT respectively. Modeling of nano phase reinforcement geometry in nano composite material has been seen to be an effective tool in evaluating the effect of nano particle geometries, critical aspect ratios and the reinforcement type on the prediction of ply properties in composites.

Research has shown that the modified Halpin-Tsai equation is an effective tool in predicting these properties since it takes into account the various characteristics of the reinforcing phase such as the shape and aspect ratio of the nano phase, packing geometry and regularity and also on loading conditions. These assumptions are believed to have a more reliable effect and achieve a closer result with experimental data when compared to the use of the general rule of mixture equation which assumes the reinforcing phase to be long and continuous fibers with no correction factors built into the equation to account for these variations. The modified Halpin-Tsai equation is seen below;

$$p_c = \xi\left(p_f v_f + p_m v_m\right) \tag{5.5}$$

$$P_c = p_m\left(\frac{1+\xi\eta v_f}{1-\eta v_f}\right) \tag{5.6}$$

where,

$$\eta = \left(\frac{p_f - p_m}{p_f + \xi p_m}\right) \tag{5.7}$$

where P_c is the composite elastic property (which may be an elastic modulus, a Poisson ratio, or a shear modulus), P_f and P_m are the corresponding properties for the fiber and matrix material, respectively, v_f and v_m are the volume fractions for the fiber and matrix phase, respectively, and ξ is a user-specified empirical constant which is dependent on various characteristics of the reinforcing phase such as the shape and aspect ratio of the fibers, packing geometry and regularity and also on loading conditions. It is necessary to determine ζ empirically by fitting the curves to experimental results. This modified equation will be used to estimate the material properties of the nano engineered composite while taking the geometry of the nano phase into consideration.

Our goal is to achieve at least a 15% increase in strength with the addition of the long CNT. Based on the percentage increase in CNT addition, the increase in strength of the composite was computed. Figure 5.8 shows the strength of composite with the increase in CNT loading. CNT thread with three different strengths was considered. The highest strength thread was 10 GPa which is presently under development in Nanoworld lab here at UC. This technology proposed is not disruptive since it can be easily incorporated into present manufacturing processes of high strength composite. An improved manufacturing process will be seen later in order to achieve this goal.

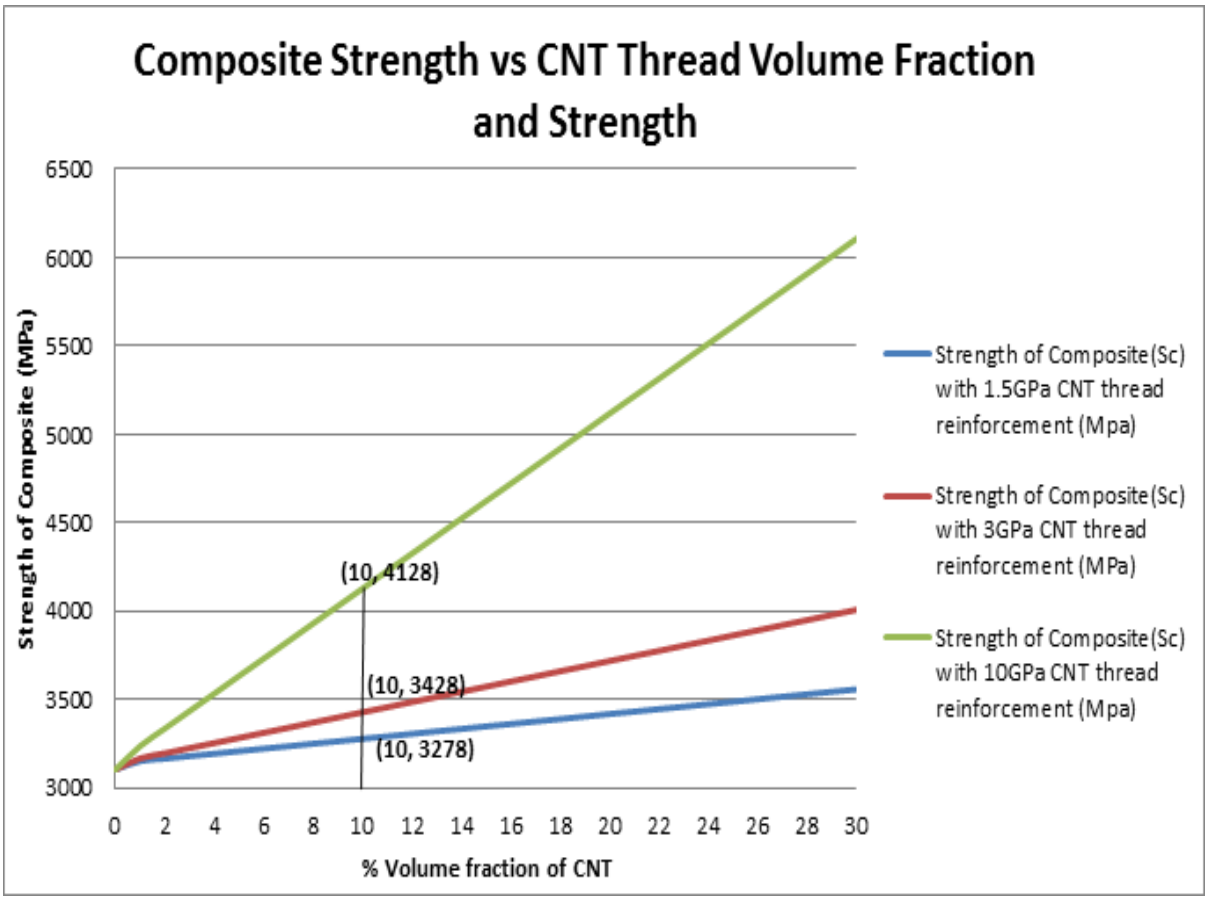

Figure 5.9. Strength of the hybrid composite with increase in CNT loading and strength. Analysis based on equation (5.4).

From Figure 5.9, it can be seen that there is a linear relationship between the strength of the composite and a corresponding increase in the CNT volume fraction between the interlayers and the unidirectional carbon fibers. From the theoretical analysis above, it shows that the strength of CNT fiber plays a large role reinforcing the carbon fiber composite. The percentage increase in strength as a result of the CNT material addition is computed as:

$$\frac{\sigma_{cwcnt} - \sigma_{cwncnt}}{\sigma_{cwncnt}} \times 100\% \text{ ,} \qquad (5.8)$$

Where σ_{cwcnt} and σ_{cwncnt} are the strength of composite with CNT and strength of composite without CNT, respectively. A summary of the analytical results is shown in Table 5.1.

From figure 5.10, it can be seen that in order to improve the strength of the composite by about 10%, a corresponding CNT volume fraction of 3% will be needed for a 10GPa CNT thread in the composite laminate, whereas a 10% CNT volume fraction will be needed for a 3GPa CNT thread to improve the strength of the composite by 10%. This shows that improving the strength of the reinforcing phase will ultimately improve the overall strength of the composite and only a small volume fraction of high strength CNT can provide a significant increase in strength of the composite.

In this analysis, the matrix volume fraction is 38%. Thus the CNT volume fraction must be well lower than this to allow enough matrix material to wet the fibers. The volume fraction of CNT that is practical to achieve must be determined experimentally and will depend on the diameter of the long CNT. To make the strongest composite, 10 GPa CNT thread could be used to replace carbon fiber which will in turn require a smaller amount of CNT volume fraction as

compared to a 3GPa CNT thread which will require a higher CNT volume fraction to achieve the same result.

Table 5.1 Percentage increase of composite strength with different volume fraction and strength of CNT reinforcement.

CNT Loading (V_{cnt})%	Strength of Composite with 1.5GPa CNT thread reinforcement (MPa)	Strength of Composite with 3GPa CNT thread reinforcement (MPa)	Strength of Composite with 10GPa CNT thread reinforcement (MPa)	% Increase with 1.5GPa CNT thread	% Increase with 3GPa CNT thread	% Increase with 10GPa CNT thread
0	3103	3103	3103	0	0	0
1	3152	3167	3237	1.55	2.03	4.28
2	3166	3196	3336	2.00	2.97	7.47
3	3180	3225	3435	2.45	3.90	10.65
4	3194	3254	3534	2.90	4.83	13.84
5	3208	3283	3633	3.35	5.76	17.02
6	3222	3312	3732	3.80	6.70	20.21
7	3236	3341	3831	4.25	7.63	23.39
8	3250	3370	3930	4.70	8.56	26.58
9	3264	3399	4029	5.15	9.50	29.76
10	3278	3428	4128	5.60	10.43	32.95
11	3292	3457	4227	6.05	11.36	36.13
12	3306	3486	4326	6.50	12.29	39.31
13	3320	3515	4425	6.95	13.23	42.50
14	3334	3544	4524	7.40	14.16	45.68
15	3348	3573	4623	7.86	15.09	48.87
16	3362	3602	4722	8.31	16.03	52.05
17	3376	3631	4821	8.76	16.96	55.24
18	3390	3660	4920	9.21	17.89	58.42
19	3404	3689	5019	9.66	18.82	61.61
20	3418	3718	5118	10.11	19.76	64.79

The prediction says that a very significant (50%) increase in strength can be achieved using 16% volume fraction loading of 10 GPa CNT materials. This approach of adding super strong CNT thread to reinforce composites is not disruptive and provides a good increase in properties with a small amount of material. However, the larger fiber diameter leaves tiny gaps in the film. Thus a certain percentage of smaller fiber diameters are mixed with the large ones and then compacted to create a highly dense product which is similar to processes used in

powder metallurgy. The same with composites, the large carbon fibers are the bulk of the composite, and the CNT thread fill in the gaps to give a dense composite.

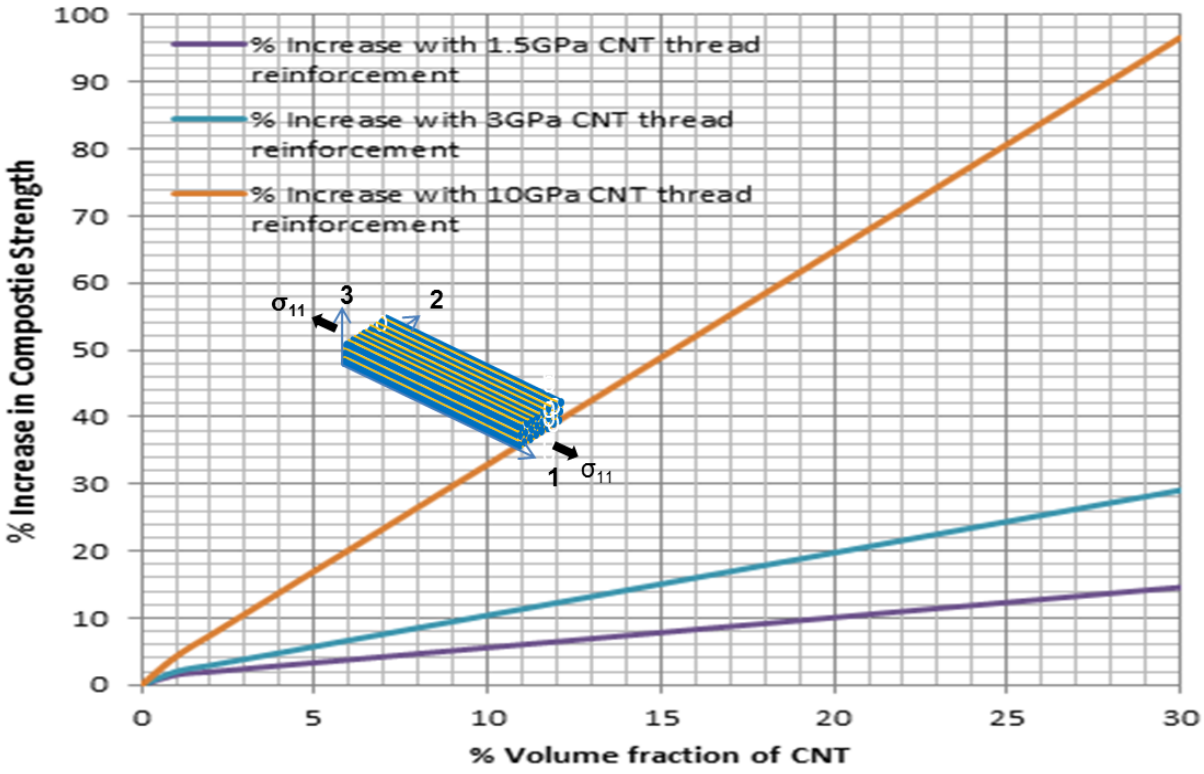

Figure 5.10 Shows a graph of the percentage increase in strength of the composite with respect to the strength of reinforcing phase and its corresponding volume fraction.

5.5.2 Estimation of Interlaminar Shear Properties

Based on interlaminar shear test conducted in previous chapter, in as much as short VACNT arrays improved the interlaminar shear strength of the laminated composite, the SEM images showed that the arrays resisted crack growth at the ply interfaces but did not successfully drive the away from the interface. Also, the short VACNT arrays reinforcement could not effectively interlock all the plies together which brought about matrix shearing at the mid-plane where shear stress is at maximum.

The transverse reinforcement using CNT posts proposed will allow the CNT to penetrate into the plies and tie them together to increase shear strength. There will also be an increase in shear modulus which will create a stiffer composite. A theoretical analysis was done to estimate the effect of CNT post reinforcement on polymer composite using an epoxy matrix system (Epon 862) as shown in Table 5.2.

Table 5.2 Showing theoretical prediction of percentage increase in interlaminar shear strength using CNT post reinforcement.

ν_{CNT} (%)	0	2	5	10	15	20	25	30
τ_{epoxy} (MPa)	75	75	75	75	75	75	75	75
τ_{CNT} (MPa)	1000	1000	1000	1000	1000	1000	1000	1000
τ_{13} (MPa)	75	93.5	121.25	167.5	213.75	260	306.25	352.5
Increase (%)	0	24.7	61.7	123.3	185.0	246.7	308.3	370.0

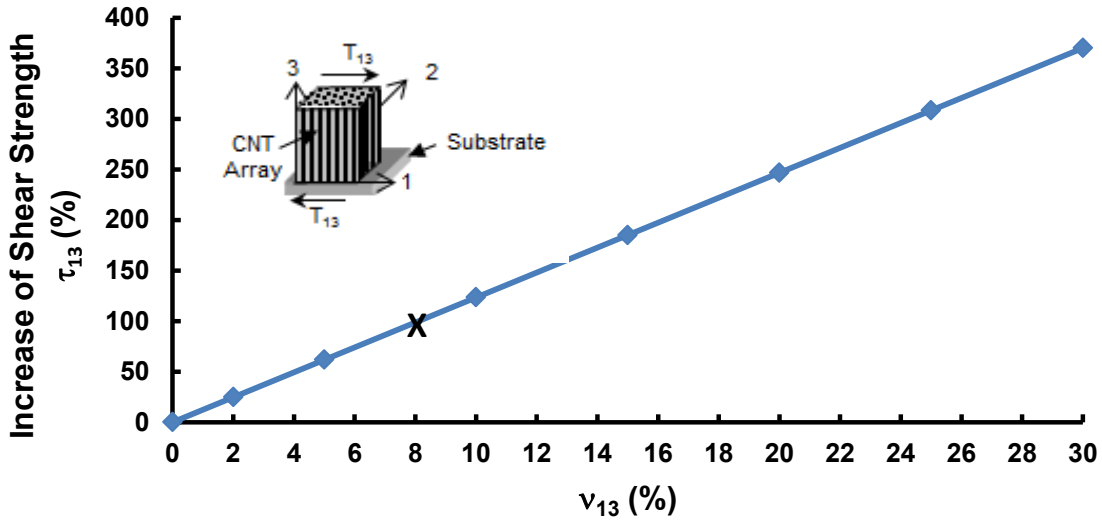

Figure 5.11. Theoretical prediction of shear strength of CNT Post reinforced composites (CNTs and epoxy only) [Figure by Dr. Yi Song with permission].

From figure 5.11 above, a plot of increase in volume fraction of CNT post as against percent increase in interlaminar shear strength with respect to CNT addition. From the plot above, about 8% volume fraction of CNT post reinforcement will yield a 100% in interlaminar shear strength of the laminated composite which will obviously increase the use of composite materials in extreme application.

Also from figure 5.11 above, it can be estimated that about 3% volume fraction of CNT post is presently used in achieving about 42% increase in interlaminar shear strength as seen in the previous chapter. This also shows that the higher the strength of the CNT post reinforcement, the higher the interlaminar shear strength of the composite and as a result, the lower the volume fraction of the CNT post that will required to impart such improvement in shear properties.

5.6 Post-Processing of Long and Strong CNT Array Post and CNT Thread

Post processing of various CNT forms after synthesis of the arrays, yarns etc. have shown to improve the mechanical performance of composite materials since it creates a functional interface between the fibers and the matrix in order to improve the load transfer mechanism between the fiber and the matrix. As seen in previous chapters, this is a limiting factor in composite fabrication which requires adequate attention when processing these composites.

As regards mechanical properties, for example, interfacial adhesion and interlaminar properties could be enhanced through covalent or non-covalent interaction between a functional group created on the nanotube surface and ends and the polymer matrix. This work will utilize the use of plasma functionalization and thermal annealing processes.

5.6.1 Plasma Functionalization

It has been recently reported [146] that carbon nanotubes can be grafted with hydroxyl (~C-OH) and carboxyl (~C-OOH) groups by using oxygen plasma at atmospheric pressure. Compatibility between the CNT surface and the polymer matrix will help improve load transfer. This process is quite similar to the sizing process [147] used on carbon fiber in order to create a better interaction with the matrix. In this proposed work, CNT will be functionalized using the Atmospheric Plasma Deposition System Atmoflow 400D from Surfx Technologies

This portable equipment is capable of generating high-density plasma of reactive species at atmospheric pressure and temperature. Application of plasma deposition on the substrate is a simple process by moving the torch on the surface of the substrate for a specified time as seen in Figure 5.12. It produces low temperature plasma (below 75°C) and will not damage CNT materials.

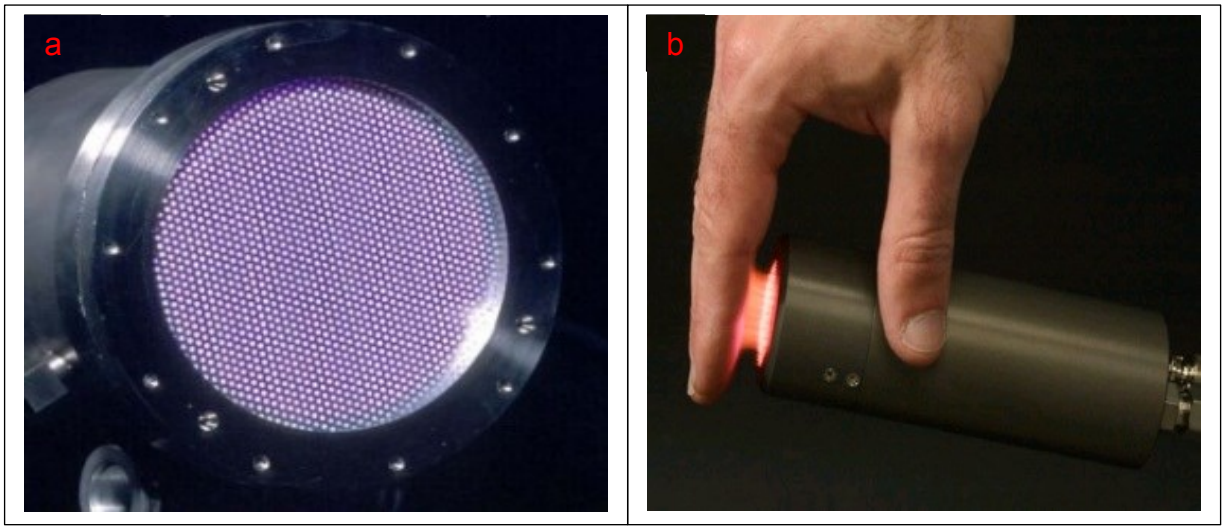

Figure 5.12. RF Plasma functionalization: (a) O¬2 plasma source in action; (b) mild nature of the plasma [Figure by Dr. Vesselin Shanov with permission]

5.6.2 Thermal Annealing

The synthesized CNT arrays, posts and threads will be thermally annealed since graphitization (heat treatment at 2800^{o}C) have shown to anneal defects out of CNTs and removes residual iron catalyst particles remaining in the CNT [20]. This system is now available and a new thermal annealing furnace that can operate to 2,800^{o}C is just being installed at UC. Although long nanotubes have defects as grown, they can be annealed to almost pristine condition with much improved properties.

5.7 Evaluating Material Performance of HVFC

Material performance will be characterized by comparing results of reinforced composites and non-reinforced composite with respect to different failure modes, optimize performance, and also compare experimental results to analytical predictions.

5.7.1 Characterizing the failure modes of HVFC composite material

An overview of testing to be performed is shown for different types of tests. Background results are based on non-reinforced samples and samples with short (20 micron long) CNT arrays placed between plies in the composite for reinforcement and also result for manual integration of CNT post in the through-the-thickness direction as seen in chapter 4. The background test does not include testing of the new in-plane and transverse reinforcement approaches proposed. Different figures in the previous chapters illustrate several tests and failure modes that would be used to investigate the structural properties of this new approach and process.

5.7.1.1 Open Hole Compression (OHC) Testing with Background

Testing was carried out and results were compared between carbon fiber composites

with no reinforcement and that with short VACNT arrays placed between plies in the composite for interface reinforcement [99-104]. The CNT arrays were fully transplanted to cover the complete surface of every individual ply interface in the composite and the arrays possess a CNT spatial density of about 5%. The testing was carried out at UC with the collaboration of General Nano who supplied materials for the test and results showed that for OHC strength, there exist no significant improvement by using short CNT arrays in-between each ply as reinforcement.

The failure mode in this process was analyzed to be buckling and compression. Also, the type of fiber reinforcement used does not really affect the value of the OHC because despite the fact that IM7 carbon fiber is stronger than AS4 carbon fiber, they still both showed about the same properties when tested for OHC strength. SEM imaging carried out on some of the failed samples indicated a buckling failure process which was attributed to the stiffness of the short CNT arrays since stiffness is a driving factor for this failure mode.

The VACNT arrays used for reinforcement between the individual plies in laminate composite help increased OHC strength by only 1% and could not efficiently reinforce against buckling possibly because the nanotubes could not mechanically interlock the individual plies which tend to de-bond from the matrix-carbon fiber interface and are also very thin to resist buckle. The performance of composite systems when used as fasteners or in rivets is highly limited due to its low strength in OHC (350MPa) and results achieved during the test also agree with that in literature. Previous test conducted in chapter 3 using short CNT arrays between individual plies indicates that through-the-thickness reinforcement is needed which led to reinforcement modification in chapter 4 and the OHC results also helped lead us to the development of the transverse reinforcement approach proposed in this chapter. Both parallel and transverse reinforcement have shown promise to increase the OHC strength and will be

tested.

Transverse CNT bundles that span through the complete thickness of the composite and interlock the plies together to resist buckling and improve the in-plane and interlaminar shear properties will also be evaluated in the research. Adding fine CNT thread parallel to the carbon fiber in the composite may also increase the stiffness; limit matrix micro cracking, bucking load and OHC strength.

5.7.1.2 In-plane Shear Testing

Testing will be performed and results will be compared using carbon fiber composites with no reinforcement and the same material with vertically aligned long CNT post and axially aligned CNT threads placed entirely through the plies in the composite. The test performed in chapter 3 was done at UC in collaboration with General Nano. The result showed an increase in shear strength of about 50% using CNT array reinforcement between the plies. The failure mode showed signs of delamination at the neutral axis as expected per SEM images.

Functionalized CNT and a thin laminated beam with 4:1 span-to-depth ratio were used. The short VACNT arrays used actually reinforce interlaminar shear, but the load transfer between the matrix and carbon fiber plies may still be poor. The transverse reinforcement using CNT posts proposed will allow the CNT to penetrate into the plies and interlock them together to increase shear strength. Also the shear modulus should improve which will make the composite stiffer.

5.7.1.3 Flexural Test

Testing will be performed using a 3-point bend test set-up and results will be compared between a carbon fiber composite with no reinforcement and a carbon fiber composite with CNT post and thread reinforcement. The testing will be performed at UC in collaboration with General

Nano. Previous result in 3-Pt bending showed an increase in strength of 11%. The failure mode was a combination of bending and shear but compression at the loading nose and support is sometimes expected as failure mode. The beam span-to-depth ratio is 10:1 which showed a mixed failure mode since a 16:1 span-to depth ratio could not be achieved due to limited amount of specimens during the test and the shear strength was low for the thin samples.

The CNT perpendicular array between plies does not directly reinforce bending due to the reinforcement orientation. But the composite with CNT array reinforcement was slightly thicker than the composite without reinforcement which increased the 3-Pt bending strength. This problem can be solved by keeping the thickness for the samples with transverse reinforcement unchanged. This proposed work will be to add CNT thread longitudinally in the composite to increase the flexural strength while the transverse reinforcement will increase the shear strength.

5.7.1.4 Transverse Shear Testing

In this test method the specimen is notched at both ends as shown in figure 5.13. With the CNT reinforcement between plies the transverse shear testing showed 45% increase in transverse shear strength. The longitudinal reinforcement proposed may provide a greater improvement in transverse shear strength. The transverse reinforcement may also improve the strength by mechanically interlocking the whole laminate thus reducing shear in the complex failure mode produced by the notching effect. The proposed work is will be test the effect of CNT thread in-plane which may help reinforce (toughen and increase strength) in tension and in transverse shear.

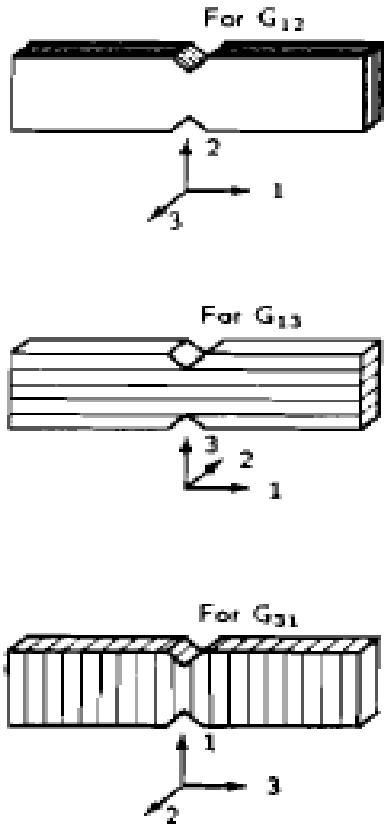

Figure 5.13 Orientation of material planes with unidirectional laminate [ASTM D5379/D5379M-05 [112].

5.8 Advantages of Multiscale Composites with High Volume Fraction

Composites are well known to exhibit high strength to weight ratio because they combine different orientation of high strength micron-size fiber reinforcement phase with a polymer matrix phase. However, this high strength material is susceptible to delamination, matrix micro cracking and other premature failure modes due to weak intralaminar, interlaminar, in-plane and poor thermal and charge transport properties in the transverse direction to the laminate. Hybrid composites with nanoscale reinforcement in the in-plane and through the thickness direction are

an advanced multifunctional material that will enhance the usage of composites in several different applications. Advantages of Multiscale Laminated Composites are:

1. **High Strength**- The strength of composite material will increase due to increased volume fraction with the addition of CNT thread, as well as improved interlaminar shear strength with the addition of micron sized CNT post reinforcement in the z- direction.

2. **Damage Limiting**- This innovation can also limit damage in composite materials since carbon fibers break at a lower failure strain than its nano reinforced CNT thread which has a higher failure strain and improved toughness since higher stresses will be transferred onto it thus holding the composite together and making it resilient. This reinforcing effects and crack turning/bridging can also be studied using stress-strain curves and microscopic examination of the failure pattern to further understand it effect.

3. **High Transport properties**- Composite will possess improved transport properties both in the longitudinal and transverse direction. With these improved properties, composites can also serve as heat sinks and damage sensing material.

4. **No Significant Added Mass/Size**- Based on the proposed innovation, there will be slight addition to the weight of the composite with no relative change in size since excess matrix phase will be replaced by micron size diameter CNT fibers. There exist a tradeoff between slight weight gain and multifunctionality of next generation composite but the advantages of the latter will far more outweigh that of the former.

5. **Modest Additional Cost-** Cost for the CNT materials and composites processing is modest because the volume fraction of nanotube materials used is small, about 9%.

6. **Multifunctional-** Interwoven integration allows the CNT/thread to be built into ply layers; Stiffness, Toughness, Thermal Stability, EMI Shielding, and added damping are advantages.

7. **Future composites-** will have "Nano Inside" for ultimate performance.

The main effort in this future research work will be to manufacture composite materials reinforced with nanotubes and thread and evaluate test coupons with different architectures of reinforcement. Analytical predictions of the improved properties of the composite structure will be compared to experimental results. An objective is to demonstrate substantially improved properties of the multiscale composite for several failure modes. Mechanical testing and micrographic analysis will help verify the performance and validate the analytical predictions. Finally the ultimate goal is to quickly commercialize the new composite material technology.

5.9 Concluding Remarks

The HVFC architecture proposed will reinforce the weaker failure modes in composites such as interlaminar shear, delamination, and open-hole compression, and allow breakthrough design limits in composites. Since the use of composites is pervasive in society, modest improvements in performance will have a widespread geographic impact in many product areas. Manufacturing multiscale composites will involve a chain of industries starting from the makers of nanofurnaces to nanotube synthesis companies to composites fabricators all of whom will have a beneficial economic impact in America and in the world.

CHAPTER 6

Summary and Conclusions With Suggestions for Future Research

6.1 Summary and Conclusions

Composite materials have high strength in-plane and are lightweight which has motivated their use in advanced applications. Howerver, weak failure modes such as delamination and matrix-dominated regions at ply interfaces have reduced the performance and limited the widespread use of composites. Low interlaminar shear strength and increased susceptibility to damage, lack of toughness (brittle failure), and poor through-the-thickness properties (strength and conductivity) reduce the multifunctionality of composites when compared to traditional engineering metals. Aluminum, for example, is heavier than composites. But Al has higher thermal and electrical conduction and can better absorb energy (by bending and locally deforming) under implact and there is no delamination failure mode to weaken the material.

The high specific strength and specific stiffness of composites cannot be achieved using any other material system. Thus composites would offer unique advantages for many applications if their toughness and weak failure modes could be improved. The need to improve the weaknesses of composite materials has prompted researchers to investigate reinforcing composites using carbon nanotubes in different forms and reinforcement architecture were utilized in this work to create a functional interface which as result, improved the interlaminar shear properties, flexural properties based on mechanical characterization and also improved the toughness of the material based on microstructural evaluation of the failure pattern when compared between the reinforced and unreinforced composite materials. The combination of

unique fabrication processes and post processing of the carbon nanotube arrays by thermal annealing of CNT arrays, have also shown to have added some improved properties to the nano reinforced composite by mechanically interlocking the plies together, created a defect-free array for improving the stiffness and also improving the load transfer mechanism between the fibers and the matrix.

Based on the studies and test conducted thus far, progresses were made and are highlighted below:

1. An effective fabrication process which creates a through-the-thickness reinforcement of 20μm high CNT array reinforced laminated composite that were efficiently transferred unto the IM7/977-3 carbon fiber prepreg using a ply-to-ply reinforcement pattern, thus creating an interface with higher interlaminar shear strength of 51.9% when compared with the baseline laminated composite using short beam shear test (SBS). A flexural test was also conducted to evaluate the stiffness of the nano composite and result showed an 11% increase in flexural strength of the CNT array reinforced composite when compared to the baseline IM7/977-3 carbon fiber composite. Also, the interlaminar shear strength was also evaluated using Iosipescu interlaminar shear test method and a 42% increase in interlaminar shear strength was recorded when compared to the baseline material.
2. Based on SEM evaluation of the first reinforcement architecture of the short CNT array reinforced laminated composite, a new reinforcement pattern was introduced to create a better and efficient load transfer mechanism since this is a vital mechanism for improving the interlaminar shear properties.

   In this approach, we introduced micron-sized, long and continuous CNT post to reinforce a 12-ply laminated IM7/977-3 carbon fiber prepreg in the thickness direction (z-

direction) from top to bottom of the ply layup by inserting long CNT posts into pinholes created on the laminate by pushing apart the carbon fibers and subsequently compacted during consolidation and curing process to produce a multiscale composite with increased design limit. Short beam shear (SBS) result showed about 42% increase in interlaminar shear properties when compared with baseline material while In-plane tensile test showed no adverse effect of the pin-hole insertion on the tensile properties. The SEM image showed a better load transfer mechanism and an enhanced crack deflection pattern when compared to the baseline material.

3. We also developed a new concept based on theoretical analysis and experimental data obtained from this work. This new approach is called "High Volume Fraction Composite". This concept is built on increasing the volume fraction of fiber reinforcing phase in the composite by longitudinally inserting long 2μm diameter CNT threads in between closely packed 7μm diameter carbon fiber due to micro voids created as a result of low packing density of the carbon fiber. Also, a patterned long CNT post grown with desired diameter, period and spacing will be used to transversely reinforce the stacked up laminate in the z-direction. This concept is designed to improve the overall performance of composite and if successful, HVFC technology will significantly improve in-plane tensile strength by 15%, interlaminar shear strength by 100%, Open Hole Compression (OHC) by 10%, toughness, impact resistance, thermal and electrical conductivity of polymeric composites which will become a new high performance material for energy efficient, safe, multifunctional, and corrosion resistant air/ground vehicles.

If the use of CNT can improve the weaknesses of composites as predicted, the use of composite materials could be expanded to many other applications such as lightweight automotive and

transportation systems. Details of future work needed to achieving the goal of multiscale composites is described next.

6.2 Future Work

The goal of this research was to improve the interlaminar shear strength properties of IM7/977-3 laminated composite by studying and characterizing the impact of introducing carbon nanotubes arrays and post in small volume fractions using different reinforcement architecture to reinforce traditional laminated composite materials.

To further improve the interlaminar shear properties, it is necessary to investigate how the transfer and alignment processes of introducing carbon nanotube arrays and posts into the hybrid material affect the shear properties. This analysis will further help in improving the manufacturing process of fabricating these hybrid composite materials.

The specimen size and thickness plays a significant role in improving the mechanical properties of composite materials. Generally, the mechanical properties increase as the size and thickness of the composite specimen decreases since a potential increase in dimension of the specimen could result to addition of more flaws and defects in the material, a concept known as "size effect". Since a new interface is created with the addition of micron sized CNT array, it is necessary to investigate this process to evaluate the optimum amount of pressure needed during consolidation to create an interface that will not likely have an adverse effect on both in-plane tensile and interlaminar shear properties.

The optimum height of the CNT reinforcing phase needed for improved mechanical properties could also be investigated by introducing CNT arrays and post of slightly different

heights and array densities during the fabrication stage and then mechanically characterized in various failure modes under the same loading conditions so as to compare the hybrid material with the most improved properties. The interface failure surface could also be characterized using ESEM and TEM to better understand the load transfer mechanism and interaction between the CNT array/resin matrix/carbon fiber interfaces.

Improving the multifunctionality of new generation hybrid composite materials is of great importance since this could open a new sphere of structural materials that would serve high-end engineering application. To this effect, the hybrid composite material could be subjected to a number of tests such as electrical conductivity, thermo-mechanical conductivity, open-hole compression, open-hole tension, in-plane tension, fracture toughness and impact tests. All these tests if conducted would validate the hybrid composite material to be suitable for robust engineering application.

From theoretical analysis done in this work, improving the in-plane tensile properties would require increasing the volume fraction of fiber reinforcing phase and mitigating the effect of matrix micro cracking which results due to excess resin matrix which fills up the micro spaces created as a result of low packing density of large diameter carbon fiber during consolidation. This approach, as highlighted in previous chapter, would be investigated in future work and will require spinning long and strong CNT threads of 2μm diameter for insertion into these micro spaces created which would eventually increase the volume fraction and also reduce the effect of matrix cracking since failure initiates from these sites.

Finally, based on the experimental analysis and data collected, a model could also be developed based on CNT/matrix interfacial properties, mechanical and thermal properties of

matrix to determine or predict the interlaminar shear and other mechanical properties of hybrid composite material. Also, the choice of fabrication process, the CNT quality and reinforcement architecture based on alignment and distribution of nanotubes would also be a better tool to enhance this model. The understanding of this model can also be transferred in improving other mechanical properties of composite materials which will eventually translate into better composite design for advanced engineering applications.

References

1. *Abot, J. L., Song, Y., Sri Vatsavaya, M., Medikonda, S., Kier, Z., Jayasinghe, C., Rooy, N., Shanov, V. N. and Schulz, M. J., Delamination detection with carbon nanotube thread in self-sensing composite materials. Compos. Sci. Technol. 70 (7): 1113-1119 (2010).*

2. *Song, Y. and Abot, J. L. On the mechanical response of carbon nanotube array laminated composite materials. J. Reinf. Plast. Comp. 29(22): 3401-3410 (2010).*

3. *Veedu V.P., et al, Multifunctional Composites Using Reinforced Laminae with Carbon-Nanotube Forests. Nature Materials. 2006 June; 5: 457-462.*

4. *Thostensen E.T., et al, Aligned Multi-Walled Carbon Nanotube-Reinforced Composites: Processing and Mechnical Characterization. Journal of Physics. D, Applied Physics. 2002; 35(16): 77-80.*

5. *Thostensen E.T., et al, On the Elastic Properties of Carbon Nanotube-Based Composites: Modeling and Characterization. Journal of Physics. D, Applied Physics. 2003; 36(5): 573-82.*

6. *Frogley M.D., et al, Mechanical Properties of Carbon Nanoparticle- Reinforced Elastomers. Composite Science and Technology. 2003; 63(11): 1647-54.*

7. *Iijima S. Helical microtubules of graphitic carbon. Nature 354; pg. 56-58 (1991).*

8. *Gonnet, P., Liang, Z., Choi, E.S., Kadambala, R.S., Zhang, C., Brooks, J.S., Wang, B., Kramer, L. "Thermal Conductivity of Magnetically Aligned Carbon Nanotube Buckypaper and Nanocomposites." Current Applied Physics. 6(2006):119-122.*

9. *Park, Jin Gyu, Louis, Jefferey, Cheng, Qunfeng, Bao, Jianwen, Smithyman, Jesse, Liang, Richard, Wang, Ben, Zhang, Chuck, Brooks, James S., Kramer, Leslie, Fanchasis, Percy, Dorough, David. "Electromagnetic Interference Shielding Properties of Carbon Nanotube Buckypaper Composites." NanoTechnology. 20(2009): 415702.*

10. *Poe C., Reeder J. R., and Yuan F. G. "Fracture Behavior of a Stitched Warp-Knit Carbon Fabric Composite," NASA/TM-2001-210868, 2001.*

11. *Glaessgen E. H., Raju I. S., and Poe C. C. "Modeling the influence of stitching on delamination growth in stitched warp-knit composite lap joints," Proceedings of ICCM-12, Paris, France, Paper No. 449, 1999.*

12. *Glaessgen E. H. and Raju I. S. "Three-dimensional effects in the plate element analysis of stitched textile composites," Proceedings of the 40th AIAA/ASME/ASCE/AHS/ASC Structures, Structural Dynamics, and Materials Conference and Exhibit St. Louis, Missouri, AIAA-99-1416, 1999.*

13. *Stickler P. B., Ramulu M. "Investigation of mechanical behaviour of transverse stitched T-joints with PR520 resin in flexure and tension," Composite Structures 52, 307-314, 2001.*

14. *Stickler P. B. and Ramulu M. "Parametric analyses of stitched composite T-joints by the finite element method," Materials and Design 23, 751–758, 2002.*

15. *Stanley L. E. and Adams D. O. "Development and Evaluation of Stitched Sandwich Panels,"NASA/ CR-2001-211025, 2001.*

16. *Krueger R. and O'Brien T. K. "A shell/3d modeling technique for the analysis of delaminated composite laminates," NASA-2000-TM210287, 2000.*

17. *Davila,C. G. "Solid-To-Shell Transition Elements for the Computation of Interlaminar Stresses, Computing Systems in Engineering 5 2, 193-202, 1994.*

18. *Ma, P. C. and Kim, J. K. (2011). Carbon Nanotubes for Polymer Reinforcement. Boca Raton, FL: Taylor & Francis.*

19. *Ma, P. C., Siddiqui, N. A., Marom, G., and Kim, J. K. (2010). Dispersion and functionalization of carbon nanotubes for polymer-based nanocomposites: a review. Composites Part A: Applied Science and Manufacturing, 41, 1345-1367.*

20. *Andrews, R., Jacques, D., Qian, D., and Dickey, E.C. Carbon, 39, 1681 (2001).*

21. *Dalton, A.B., Collins, S., Munoz, E., Razal, J.M., Ebron, V.H., Ferraris, J.P., Coleman, J.N., Kim, B.G., Baughman, R.H. Nature 2003, 423, 703.*

22. *Daniel, IM., Ishai O. Engineering Mechanics of Composite Materials. New York: Oxford; 2006.*

23. *Fan, Z. Flow and rheology of multiwalled carbon nanotubes thermoset resin suspensions in processing of glass fiber composites, 2007.*

24. *Wang, S., Liang, R., Wang, B., Zhang, C. High-strength and multifunctional fabric of single-walled carbon nanotubes. Adv Mater 2007; 19: 1257–61.*

25. *Wang, S. Optimal functionalization degree of carbon nanotubes. Curr Appl Phys 2009:1146-50.*

26. *Wang, S. Role of structure and morphology in the elastic modulus of carbon nanotube composites. J Mater Sci 2008; 43: 5837–44.*

27. *Kim, J-K., Mai, Y-W., Engineered Interfaces in Fiber Reinforced Composites. Elsevier, Oxford (1998).*

28. *Agarwal, B D., Broutman, L J., Chandrashekhara, K.., Analysis and Performance of Fiber Composites. John Wiley, Hoboken, N.J. (2006).*

29. *Thostenson, Erik T., Chunyu Li, and Tsu-Wei Chou. "Nanocomposites in context." Composites Science and Technology 65.3 (2005): 491-516.*

30. *Thostenson ET, Ren Z, Chou TW. Advances in the Science and Technology of Carbon Nanotubes and Their Composites. Composites Science and Technology. 2001; 61(13): 1899-1912.*

31. *Messersmith P, Giannelis EP. Synthesis and Characterization of Layered Silicate-Epoxy Nanocomposites. Chemistry of Materials. 1994; 6(10): 1719-1725.*

32. *Gao, J., Itkis, M.E., Yu, A., Bekyarova, E., Zhao, B., Haddon, R.C. Continuous spinning of a single-walled carbon nanotube-nylon composite fiber., Journal Of the American Chemical Society. 127 (2005) 3847-54.*

33. *Liu, L., Barber, A.H., Nuriel, S., Wagner, H.D. Mechanical Properties of Functionalized Single-Walled Carbon-Nanotube/Poly(vinyl alcohol) Nanocomposites, Advanced Functional Materials. 15 (2005) 975-980.*

34. *Park, J.U., Cho, S., Cho, K.S., Ahn, K.H., Lee, S.J. Effective in-situ preparation and characteristics of polystyrene-grafted carbon nanotube composites, Korea-Australia Rheology Journal. 17 (2005) 41–45.*

35. *Ramanathan, T., Liu, H., Brinson, L.C. Functionalized SWNT/polymer nanocomposites for dramatic property improvement, Journal Of Polymer Science Part B: Polymer Physics. 43 (2005) 2269-2279.*

36. *Thostenson ET, Li WZ, Wang DZ, Ren ZF, Chou TW. Carbon nanotube/carbon fiber hybrid multiscale composites. J Appl Phys 2002; 91(9):6034–7.*

37. *Veedu VP, Cao A, Li X, Ma K, Soldano C, Kar S, et al. Multifunctional composites using reinforced laminae with carbon-nanotube forests. Nat Mater 2006; 5:457–62.*

38. *Yang, Z., Pu, Y., Zhou, L., Chen, C., Li, W., Xu, L., Yi, B., and Wang, Y., 2007, "Facile Approach to Obtain Individual-Nanotube Dispersion at High Loading in Carbon Nanotubes/Polyimide Composites," Polym. Adv. Technol., 18, pp. 458–462.*

39. *Fagan, J. A., Landi, B. J., Mandelbaum, I., Simpson, J. R., Bajpai, V., Bauer, B. J., Migler, K., Walker, A. R. H., Reffaelle, R., and Hobbie, E. K., 2006, "Comparative Measures of Single-Wall Carbon Nanotube Dispersion," J. Phys. Chem. B, 110, pp. 23801–23805.*

40. *Narh, K. A., Jallo, L., and Rhee, K. Y., 2008, "The Effect of Carbon Nanotube Agglomeration on the Thermal and Mechanical Properties of Polyethylene Oxide," Polym. Compos., 29_7_, pp. 809- 817.*

41. *Xie, X.-L., Mai, Y.-W., and Zhou, X.-P., 2005, "Dispersion and Alignment of Carbon Nanotubes in Polymer Matrix: A Review," Mater. Sci. Eng. R., 49, pp. 89–112.*

42. *Fan Z, Hsiao KT, Advani SG. Experimental investigation of dispersion during flow of multi-walled carbon nanotube/polymer suspension in fibrous porous media. Carbon 2004; 42:871-6.*

43. *Yun YH, Shanov VN, Tu Y, Subramanian S, Schulz MJ. Growth Mechanism of Long Aligned*

Multiwall Carbon Nanotube Arrays by Water-Assisted Chemical Vapor Deposition. Journal of Physical Chemistry B. 2006; 110: 23920-23925.

44. Shafi Ullah Khan and Jang-Kyo Kim, Impact and Delamination Failure of Multiscale Carbon Nanotube-Fiber Reinforced Polymer Composites: A Review, Int'l J. of Aeronautical & Space Sci. 12(2), 115–133 (2011).

45. Bekyarova, E., Thostenson, E. T., Yu, A., Kim, H., Gao, J., Tang, J., Hahn, H. T., Chou, T. W., Itkis, M. E., and Haddon, R. C. (2007). Multiscale carbon nanotube-carbon fiber reinforcement for advanced epoxy composites. Langmuir, 23, 3970-3974.

46. Li, Y., Hori, N., Arai, M., Hu, N., Liu, Y., and Fukunaga, H. (2009). Improvement of interlaminar mechanical properties of CFRP laminates using VGCF. Composites Part A: Applied Science and Manufacturing, 40, 2004-2012.

47. Arai, M., Noro, Y., Sugimoto, K.I., and Endo, M. (2008). Mode I and mode II interlaminar fracture toughness of CFRP laminates toughened by carbon nanofiber interlayer. Composites Science and Technology, 68, 516-525.

48. Zhu, J., Imam, A., Crane, R., Lozano, K., Khabashesku, V. N., and Barrera, E. V. (2007). Processing a glass fiber reinforced vinyl ester composite with nanotube enhancement of interlaminar shear strength. Composites Science and Technology, 67, 1509-1517.

49. Khan, S. U. and Kim, J. K. (2011). Interlaminar shear properties of CFRP composites with CNF-bucky paper interleaves. The 18th International Conference on Composite Materials, Jeju, Korea.

50. Fan, Z., Santare, M. H., and Advani, S. G. (2008). Interlaminar shear strength of glass fiber reinforced epoxy composites enhanced with multi-walled carbon nanotubes. Composites Part A: Applied Science and Manufacturing, 39, 540-554.

51. Endo, M., Takeuchi, K., Igarashi, S., Kobori, K., Shiraishi, M., Kroto H.W."The production and structure of pyrolytic carbon nanotubes (PCNTs)", J. Phys. Chem. Solids 54(12) (1993), 1841–1848.

52. *Kang I, et al, A Carbon Nanotube Strain Sensor for Structural Health Monitoring. Smart Materials and Structures. 2006; 15(3): 737-748.*

53. *Haibo Zhao, Fuh-Gwo Yuan. Carbon nanotube yarn sensors for structural health monitoring of composites, Nondestructive Characterization for Composite Materials, Aerospace Engineering, Civil Infrastructure, and Homeland Security 2011, edited by H. Felix Wu, SPIE Vol. 7983, 79830P, 2011.*

54. *Kang, Inpil, et al. "Introduction to carbon nanotube and nanofiber smart materials." Composites Part B: Engineering 37.6 (2006): 382-394.*

55. *http://phys.org/news151938445.html; http://www.spaceelevatorblog.com/?cat=9.*

56. *Liu, K.; Sun, Y. H.; Lin, X. Y.; Zhou, R. F.; Wang, J. P.; Fan, S. S.; Jiang, K. L. Scratch-Resistant, Highly Conductive, and High- Strength Carbon Nanotube-Based Composite Yarns. ACS Nano 2010, 4, 5827–5834.*

57. *Shi, Donglu, et al. "Magnetic alignment of Ni/Co-coated carbon nanotubes in polystyrene composites." Composites Part B: Engineering 42.6 (2011): 1532-1538.*

58. *Swanson, S.R., Smith, L.V. Comparison of the biaxial strength properties of braided and laminated carbon fiber composites, Composites Part B: Engineering. 27 (1996) 71-77.*

59. *Partridge, I.K. , Rezai, A., Marasco, A.I., Cartie, D.D.R. Mechanical properties balance in novel Z-pinned sandwich panels : Out-of-plane properties, 37 (2006) 295-302.*

60. *Byrd, L.W., Birman, V. Effectiveness of z-pins in preventing delamination of co-cured composite joints on the example of a double cantilever test, Composites Part B-Engineering. 37 (2006) 365-378.*

61. *Green, K. J., Dean, D. R., Vaidya, U. K., and Nyairo, E. (2009). Multiscale fiber reinforced composites based on a carbon nanofiber/epoxy nanophased polymer matrix: Synthesis, mechanical, and thermomechanical behavior. Composites Part A: Applied Science and Manufacturing, 40, 1470-1475.*

62. *Garg A.C. Delamination - A Damage Mode in Composite Structures. Engineering Fracture Mechanics. 1988; 29: 557-584.*

63. *Kinloch A.J, Wang Y, Williams J.G, Yayla P. The Mixed-Mode Delamination of Fiber Composite-Materials. Composites Science and Technology. 1993; 47: 225-237.*

64. *Wang S.S. Edge Delamination in Angle-Ply Composite Laminates. AIAA Journal. 1984; 22: 256-264.*

65. *Thouless M.D, Cao H.C, Mataga P.A. Delamination from Surface Cracks in Composite Materials. Journal of Materials Science. 1989; 24: 1406-1412.*

66. *Shu D.W, Mai Y.W. Effect of Stitching on Interlaminar Delamination Extension in Composite Laminates. Composites Science and Technology. 1993; 49: 165-171.*

67. *Gao, L.M., Chou, T-W., Thostenson, E.T., Zhang, Z.G. and Coulaud, M. "In situ sensing of impact damage in epoxy/glass fiber composites using percolating carbon nanotube networks," Carbon, 49(10): 3382-3385 (2011).*

68. *Tong, T., Zhao, Y., Delzeit, L., et al. Dense, vertically aligned multiwalled carbon nanotubes arrays as thermal interface materials. IEEE Trans Components Packag Technol 2007; 30:92–100.*

69. *Xu, J., Fisher, T.S. Enhancement of thermal interface materials with carbon nanotubes arrays. Int J Heat Mass Transfer 2006; 49:1658–66.*

70. *Wang, S., Tambraparni, M., Qiu, J., Tipton, J., Dean, D. Thermal expansion of graphene composites. Macromolecules 2009; 42:5251–5.*

71. *Stone, B.R., Tessmer, G.J., Dreifus, D.L. (1993). Bias assisted etching of diamond in a conventional chemical vapor deposition reactor, Appl Phys Lett 62:1803*

72. *Jing, X., Klages, C-P (1993). Epitaxial diamond thin films on (001) silicon substrates,Appl Phys Lett 62:3438.*

73. *Ganesan, Y., Peng, C., Lu Y., Loya, P.E., Mooney, P., Barrera, E., Jacobson, B.I., Tour, J.M., Ballarini, R. and Lou, J. 2011 ACS Appl. Mater. Interfaces 3 129*

74. *Aymerich, F., Priolo, P. and Sun, C.T. 2003 Int. J. Fract. 63 907.*

75. *Qiu J, Zhang C, Wang B, Liang R. Carbon nanotubes integrated multifunctional and multiscale composite. Nanotechnology 2007; 17: 275708 1–275708 11.*

76. *Jeong B-W, Kim J-K, Sinnott SB. Tensile mechanical behavior of hollow and filled carbon nanotubes under tension or combined tension–torsion. Appl Phys Lett 2007; 90:023102 123.*

77. *Kim M, Park Y-B, Okoli O, Zhang C. Processing, characterization, and modeling of carbon nanotubes–reinforced multiscale composites. Compos Sci Technol 2009; 69:335–42.*

78. *Song Y.S. Multiscale fiber–reinforced composites prepared by vacuum-assisted resin transfer molding. Polym Compos 2007:458–61.*

79. *JIA, Z., WANG, Z., XU, C., LIANG, J., WEI, B., WU, D., et al., Study on poly(methyl methacrylate)/carbon nanotube composites, Materials Science and Engineering A. 271 (1999) 395-400.*

80. *Zhu, J., Kim, J., Peng, H., Margrave, J.L., Khabashesku, V.N., Barrera, E.V. Improving the Dispersion and Integration of Single-Walled Carbon Nanotubes in Epoxy Composites through Functionalization, Nano. 3 (2003) 1107-1113.*

81. *Zhu, J., Peng, H., Rodriguez-Macias, F., Margrave, J.L., Khabashesku,V.N., Imam, A.M. et al., Reinforcing epoxy polymer composites through covalent integration of functionalized nanotubes, Advanced Functional Materials. 14 (2004) 643–648.*

82. *Barrera, E.V., Zhu, J., Khabashesku, V., Imam, M.A., Crane, R., Lozano Karen, Processing and Properties of Polymer Composites Reinforced by Functionalized SWNTs, Materials Science Forum. 475-479 (2005) 1059-1062.*

83. *Chen, J., Ramasubramaniam, R., Xue, C., Liu, H. A Versatile, Molecular Engineering Approach to Simultaneously Enhanced, Multifunctional Carbon-Nanotube- Polymer Composites, Advanced Functional Materials. 16 (2006) 114-119.*

84. *Bao, J. W., et al. "Mechanical Properties of Functionalized Nanotube Buckypaper Composites." 17th International Conference on Composite Materials. 2009.*

85. *Coleman J.N, Khan U, Blau W.J, Gun'ko Y.K. Small but strong: a review of the mechanical properties of carbon nanotube–polymer composites. Carbon 2006; 44:1624–52.*

86. *Mazumder, S.K. (ed.). (2002). Composites Manufacturing, Materials, Product and Process Engineering, CRC Taylor & Francis, ISBN 0-8493-0585-3.*

87. *Sun, L., Warren, G. L., and Sue, H. J. (2010). Partially cured epoxy/SWCNT thin films for the reinforcement of vacuum assisted resin-transfer-molded composites. Carbon, 48, 2364-2367.*

88. *Sahoo, Nanda Gopal, et al. "Polymer nanocomposites based on functionalized carbon nanotubes." Progress in polymer science 35.7 (2010): 837-867.*

89. *Hu N., Zhou H., Dang G., Rao X., Chen C., Zhang W. Efficient dispersion of multi-walled carbon nanotubes by in situ polymerization. Polym Int 2007; 56:655–9.*

90. *Vigolo B., Penicaud A., Coulon C., Sauder C., Pailler R., Journet C., et al. Macroscopic fibers and ribbons of oriented carbon nanotubes. Science 2000; 290(5495):1331–4.*

91. *Coleman J.N., Blau W.J., Dalton A.B., Munoz E., Collins S., Kim B.G. et al. Improving the mechanical properties of single-walled carbon nanotube sheets by intercalation of polymeric adhesives. Appl Phys Lett 2003; 82(11):1682–4.*

92. *Mamedov A.A., Kotov N.A., Prato M., Guldi D.M., Wicksted J.P., Hirsch A. Molecular design of strong single-wall carbon nanotube/ polyelectrolyte multilayer composites. Nat Mater 2002; 1(3):190–4.*

93. *Olek M., Ostrander J., Jurga S., Mohwald H., Kotov N., Kempa K., et al. Layer-by-layer assembled composites from multiwall carbon nanotubes with different morphologies. Nano Letters 2004; 4(10): 1889–95.*

94. *Qin S., Qin D., Ford W.T., Zhang Y., Kotov N.A. Covalent crosslinked polymer/single-wall carbon nanotube multilayer films. Chem Mater 2005; 17(8):2131–5.*

95. *Bockrath M., Cobden D.H., McEuen P.L., Chopra N.G., Zettle A., Thess A., Smalley R.E., "Single-electron Transport in Ropes of Carbon Nanotubes", Science 1997, 275, 1922.*

96. *Piyush R., Thakre, Yordanos B., Dimitris C. L., "Electrical and Mechanical Properties of Carbon Nanotube-Epoxy Nanocomposites", Journal of Applied Polymer Science, Vol. 116, 191–202 (2010).*

97. *Yu M., Lourie O., Dyer M.J., Moloni K., Kelly T.F., Ruoff R.S., "Strength and breaking mechanism of multiwalled carbon nanotubes under tensile load". Science 2000; 287:637–40.*

98. *Di, Jiangtao, Dongmei Hu, Hongyuan Chen, Zhenzhong Yong, Minghai Chen, Zhihai Feng, Yuntian Zhu, and Qingwen Li. "Ultrastrong, Foldable, and Highly Conductive Carbon Nanotube Film." ACS nano 6, no. 6 (2012): 5457-5464.*

99. *Jia, J., Zhao, J., Xu, G., Di, J., Yong, Z., Tao, Y., ... & Li, Q. (2011). A comparison of the mechanical properties of fibers spun from different carbon nanotubes. Carbon, 49(4), 1333-1339.*

100. *Lau, K.T., Hui, D. (2002). "The Revolutionary Creation of New Advanced Materials carbon Nanotube Composites". Composites Part B, 33: 263.*

101. *Abot, J.L., Song, Y., Schulz M.J. and Shanov, V.N. "Novel Carbon Nanotube Array Reinforced Laminated Composite Materials with Higher Interlaminar Elastic Properties ,"Composites Science and Technology, doi:10.1016/j.compscitech.2008.05.023.*

102. *Shafi Ullah Khan and Jang-Kyo Kim, Impact and Delamination Failure of Multiscale Carbon Nanotube-Fiber Reinforced Polymer Composites: A Review, Int'l J. of Aeronautical & Space Sci. 12(2), 115–133 (2011).*

103. *Ghasemi-Nejhad M.N., Veedu P.V., Cao A., Ajayan P and Askari D. 2012 US Pub. No.: 20070128960, Int. Pub. No.: WO/2008/054409, Issued No.: 8,148,276*

104. *Zhang, Fu-Hua, et al. "Interfacial shearing strength and reinforcing mechanisms of an epoxy composite reinforced using a carbon nanotube/carbon fiber hybrid." Journal of materials science 44.13 (2009): 3574-3577.*

105. Garcia, E. J., Wardle, B. L., John Hart, A., and Yamamoto, N. (2008b). Fabrication and multifunctional properties of a hybrid laminate with aligned carbon nanotubes grown In Situ. Composites Science and Technology, 68, 2034-2041.

106. Garcia, E. J., Wardle, B. L., and John Hart, A. (2008a). Joining prepreg composite interfaces with aligned carbon nanotubes. Composites Part A: Applied Science and Manufacturing, 39, 1065-1070.

107. Hsiao, K.T., Alms, J., Advani, S.G., Use of epoxy/multiwalled carbon nanotubes as adhesives to join graphite fibre reinforced polymer composites. Nanotechnology 14 (2003) 791-793.

108. PhD Thesis; Multifunctional Composites Using Carbon Nanotube Fiber Materials, Yi Song, University of Cincinnati, 2011.

109. Bradford P.D., Wang X., Zhao H., Maria J., Jia Q., Zhu Y.T. A novel approach to fabricate high volume fraction nanocomposites with long aligned carbon nanotubes. Compos Sci Technol 2010; 70(13):1980.

110. ASTM D2344/D2344M. Standard Test Method for Short-Beam Strength of Polymer Matrix Composite Materials and Their Laminates.

111. ASTM D790. Standard Test Methods for Flexural Properties of Unreinforced and Reinforced Plastics and Electrical Insulating Materials.

112. ASTM D5379/D5379M -05. Standard Test Method for Shear Properties of Composite Materials by the V-Notched Beam Method.

113. Schneider, K., Lauke, B., Beckert, W. Compression Shear Test (CST) – A Convenient Apparatus for the Estimation of Apparent Shear Strength of Composite Materials, Applied Composite Materials. 8 (2001) 43-62.

114. Lauke, K., Beckert, B., Schneider, W. Interlaminar shear strength evaluation of curved composite samples, Applied Composite Materials. 1 (1994) 267-271.

115. Abali, F., Poro, A., Shivakumar, K. Modified Short Beam Shear Test for Measurement of Interlaminar Shear Strength of Composites, Journal of Composite Materials. 37 (2003) 453-464.

116. Rosselli, F., Santare, M.H. Comparison of the short beam shear (SBS) and interlaminar shear device (ISD) tests, Composites Part A-Applied Science and Manufacturing. 28 (1997)

587-594.

117. *Zhu J, Imam A, Crane R, Lozano K, Khabasheku V.N., Barrera E.V, et al. Processing a glass fiber reinforced vinyl ester composite with nanotube enhancement of interlaminar shear strength. Compos Sci Technol 2007; 67:1509–17.*
118. *Garcia E. J. "Characterization of Composites with Aligned Carbon Nanotubes as Reinforcement". Doctoral Thesis, Dept. of Mechanical Eng., U. Zaragoza, Spain, Nov. 2006.*
119. *Riddick J.C., Frankland S. J.V., and Gates T. S. "Multiscale Analysis of Delamination of Carbon Fiber–Epoxy Laminates with Carbon Nanotubes," Proc. 47th AIAA/ASME/ASCE/AH/ Conference, Newport, R.I., AIAA-2006-1676, 2006.*
120. *Wardle B.L. and Kim S.G. "Nano-engineered material architectures: Ultra-tough hybrid nanocomposite system," MIT TLO Case 11260, 2005.*
121. *Garcia E.J., Hart A.J., Wardle B.L., and Slocum A.H. "Production of Reinforced Composite Materials and Aligned Carbon Nanotubes," MIT TLO Case 12029, 2005.*
122. *Dransfield K.A., Jain L.K., Mai Y.W. On the effects of stitching in CFRPs—I. Mode I delamination toughness. Comp Sci Tech 1998; 58:815–27.*
123. *Jain LK, Dransfield KA, Mai YW. On the effects of stitching in CFRPs—II. Mode II delamination toughness. Comp Sci Tech 1998; 58:829–37.*
124. *Partridge I.K., Cartié D.D.R. Delamination resistant laminates by Z-fiber_ pinning: part I manufacture and fracture performance. Compos Part A 2005; 36(1):55–64.*
125. *Mouritz A.P., Leong K.H., Herszberg I. A review of effect of stitching on the inplane mechanical properties of fibre-reinforced polymer composites. Compos Part A 1999; 28:979–91.*
126. *Steeves C.A., Fleck N.A. In-plane properties of composite laminates with through-thickness pin reinforcement. Int J Solid Struct 2006; 43:3197-212.*
127. *Rawlinson, R.A. (1991). In: Proceedings of the 36th International SAMPE Symposium, pp. 1058–1068.*
128. *Hart-Smith, L.J. (1991). In: Proceedings of the 36th International SAMPE Symposium, pp. 1029–1044.*
129. *ASTM D3039/D3039M-00. (2000). American Society for Testing and Materials. West Conshohocken, PA.*

130. *ASTM D3039/D3039M-08. Standard Test Method for Tensile Properties for Polymer Matrix Composite Materials.*
131. *UC 111-007, Carbon Nanotube Thread for Distributed Sensing, Weifeng Li, Surya Sundaramurthy, Vesselin Shanov, Mark Schulz, July 15, 2010.*
132. *UC Invention Disclosure, 112-088, High Volume Fraction Composites (HVFC); Bolaji Suberu, Yi Song, Vesselin N. Shanov, Mark J. Schulz, et al, March 28, 2012.*
133. *Lomov, S.V., Carvelli, V., Verpoest, I. Correlations between damage initiation thresholds in textile composites and fatigue life limits. The Proceedings of the 10th international conference on textile composites: Recent advances in textile composites, edited by Binetruy C. and Boussu F. p. 475-481, 2010.*
134. *Gorbatikh, L., T. Li, N. De Greef, S. V. Lomov, and I. Verpoest. "EFFECT OF CARBON NANOTUBES ON FATIGUE LIFE OF CARBON FIBER/EPOXY COMPOSITES."*
135. *Zhang, Fu-Hua, et al. "Interfacial shearing strength and reinforcing mechanisms of an epoxy composite reinforced using a carbon nanotube/carbon fiber hybrid." Journal of materials science 44.13 (2009): 3574-3577.*
136. *Garcia, E.J., Wardle, B.L., John Hart, A., and Yamamoto, N. (2008b). Fabrication and multifunctional properties of a hybrid laminate with aligned carbon nanotubes grown In Situ. Composites Science and Technology, 68, 2034-2041.*
137. *Adams D, et al, Chaps. 2, 3 and 5. In: Boller C, Chang FK, Fujino Y. Encyclopedia of Structural Health Monitoring. Chichester: Wiley; 2009.*
138. *Giurgiutiu V, et al, Active Sensors for Health Monitoring of Aging Aerospace Structures. International Journal of Condition Monitoring and Diagnostics Engineering. 2003; 6(1): 3-12.*
139. *Roach, D, et al, Health Monitoring of Aircraft Structures Using Distributed Sensor Systems. 9th Joint DoD/NASA/FAA Aging Aircraft Conference, Atlanta, GA, 2006.*
140. *Kim H.S., et al, Development of Embedded Sensor Models in Composite Laminates in Structural Health Monitoring. Journal of Reinforced Plastics and Composites. 2004; 23(11): 1207-1240.*
141. *Schulz M.J, et al, Nanoengineering of Structural, Functional, and Smart Materials. Boca Raton: CRC Press; 2006. Kang I, et al, A Carbon Nanotube Strain Sensor for Structural*

Health Monitoring. Smart Materials and Structures. 2006; 15(3): 737-748.

142. *Schulz, M. J., Kelkar, A. & Sundaresan, M. Nanoengineering of structural, functional, and smart materials (CRC Press, Boca Raton, 2006).*
143. *Abot, J. L. et al. Self-sensing composite materials. Provisional Patent UC 109-064, (2009).*
144. *Yi Song, et al, Basics of Carbon Nanotube Materials for Structural Applications, Nanotechnologies and smart materials for SHM, Ed. A. Catalano, G. Fabbrocino and C. Rainieri, ISBN 978-88-88102-47-4 , Campobasso, Italy, April 2012.*
145. *Yi Song, et al, SHM Applications of Nanotechnologies for Sensor Development and Communication, Nanotechnologies and smart materials for SHM, Ed. A. Catalano, G. Fabbrocino and C. Rainieri, ISBN 978-88-88102-47-4 , Campobasso, Italy, April 2012.*
146. *Kolacyak, Daniel, Jörg Ihde, Christian Merten, Andreas Hartwig, and Uwe Lommatzsch. "Fast Functionalization of Multi-walled Carbon Nanotubes by an Atmospheric Pressure Plasma Jet." Journal of Colloid and Interface Science 359.1 (2011): 311-17.*
147. *PhD thesis; Carbon nanotubes on carbon fibers: synthesis, structures and properties, Qiuhong Zhang, University of Dayton, 2010.*

APPENDIX

SEM IMAGES OF IOSIPESCU INTERLARMINAR SHEAR TEST BASELINE LAMINATED COMPOSITE SAMPLES (CHAPTER 3)

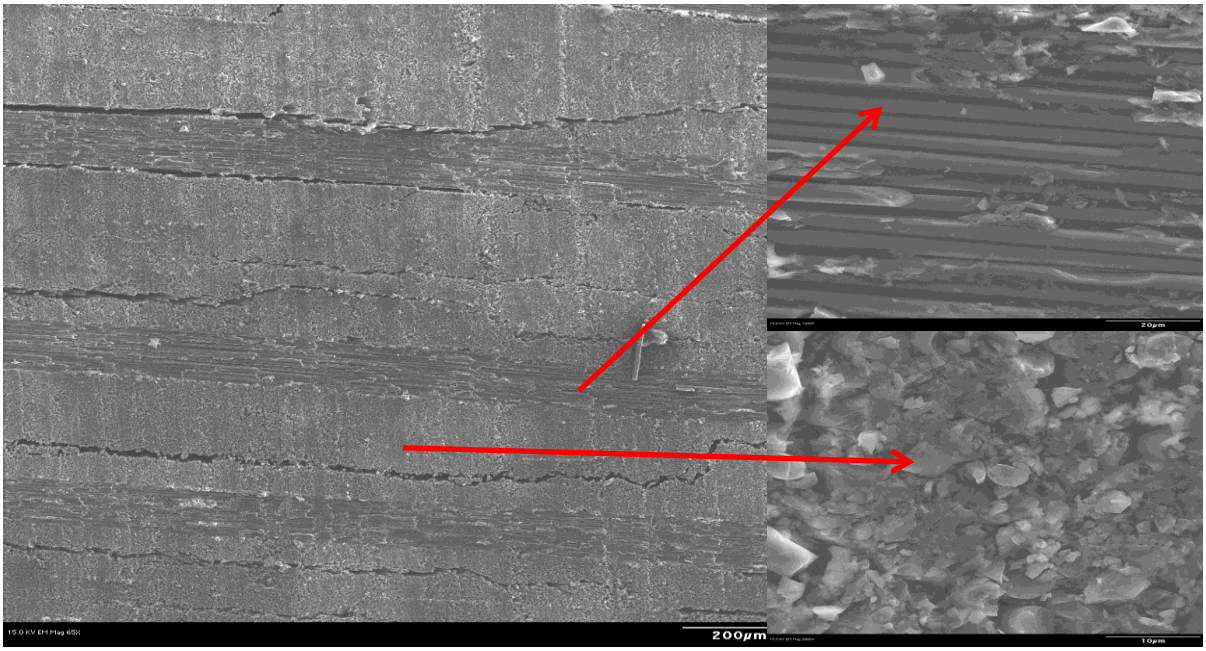

Figure 1.1. Iosipescu Interlaminar Shear Baseline sample 1.

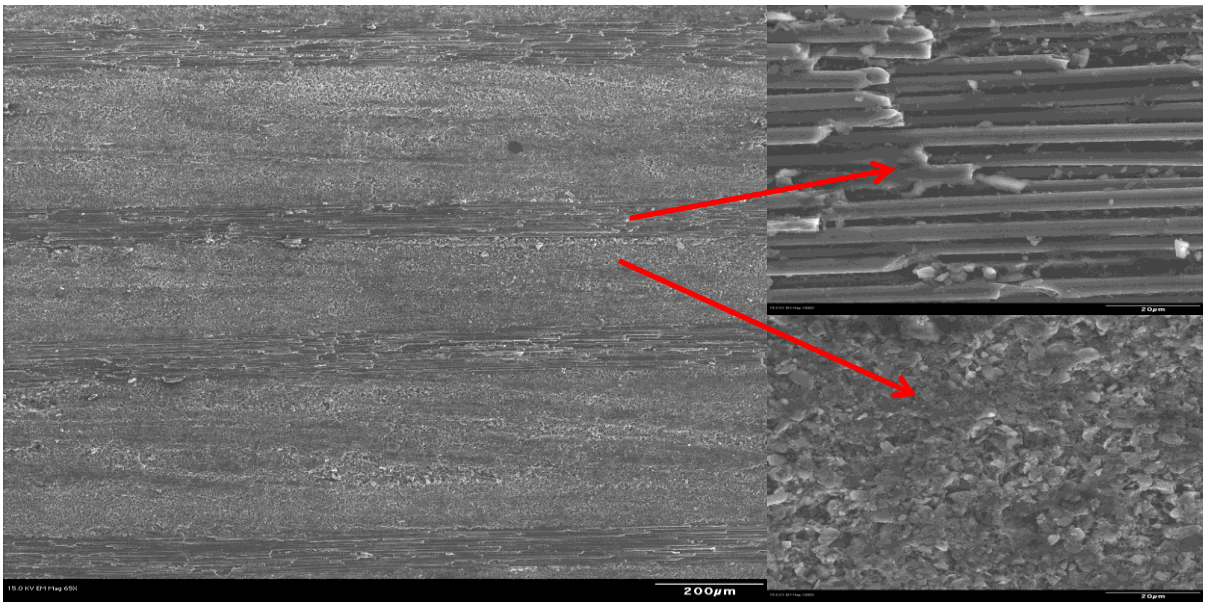

Figure 1.2. Iosipescu Interlaminar Shear Baseline sample 2.

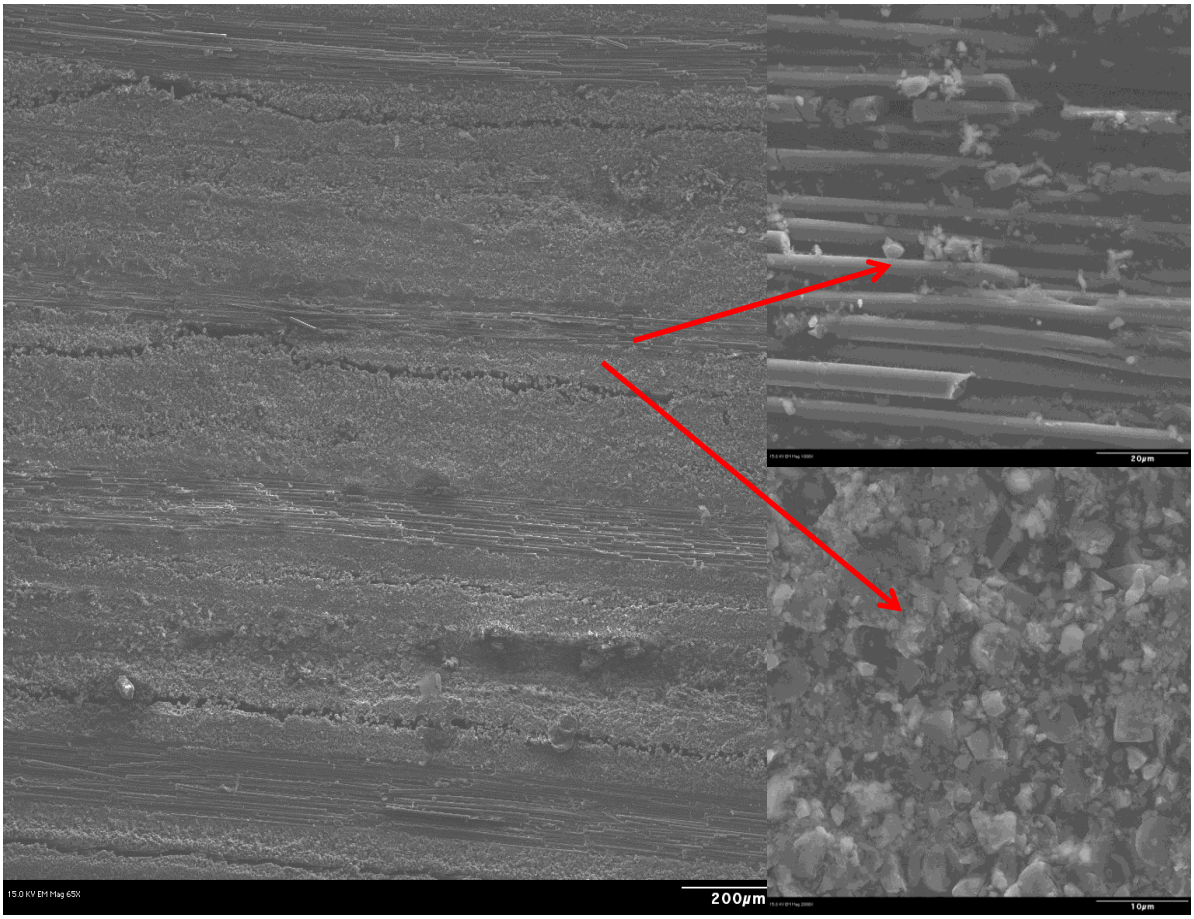

Figure 1.3. Iosipescu Interlaminar Shear Baseline sample 3.

SEM IMAGES OF 3-POINT BENDING TEST BASELINE LAMINATED COMPOSITE SAMPLES (CHAPTER 3)

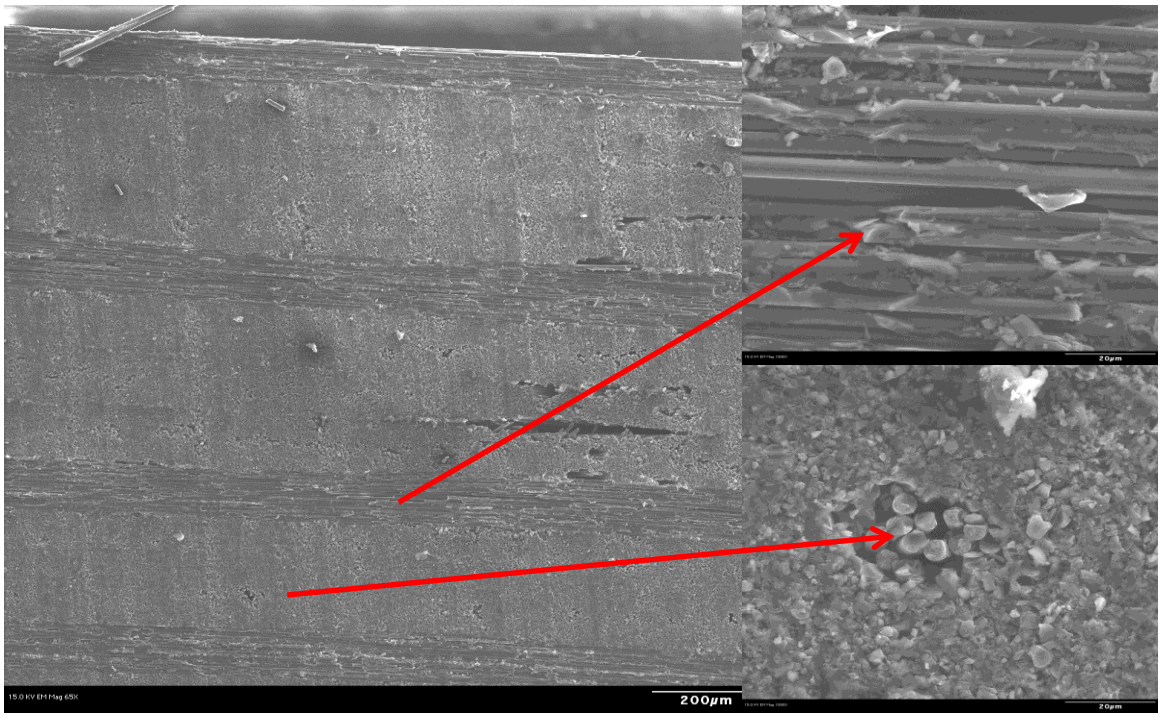

Figure 1.4. 3- Point Bend Baseline Sample 1

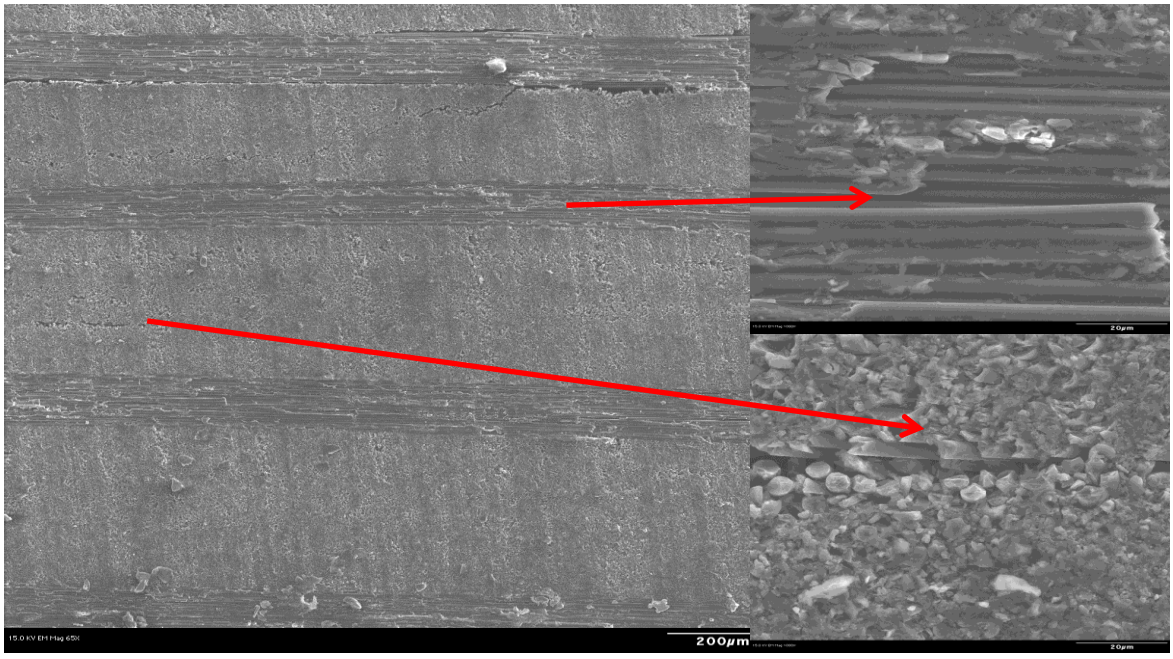

Figure 1.5. 3- Point Bend Baseline Sample 2

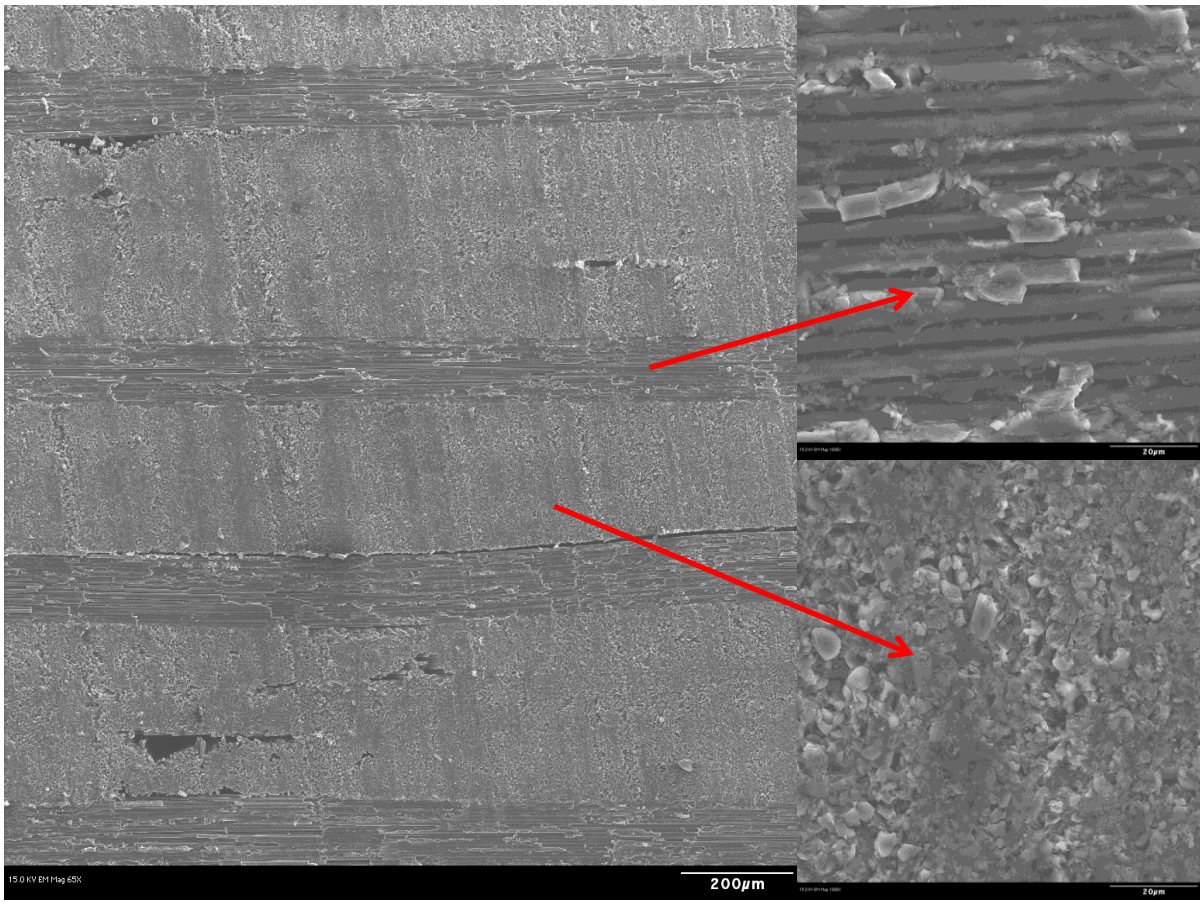

Figure 1.6. 3- Point Bend Baseline Sample 3

SEM IMAGES OF SHORT BEAM SHEAR TEST BASELINE LAMINATED COMPOSITE SAMPLES (CHAPTER 3)

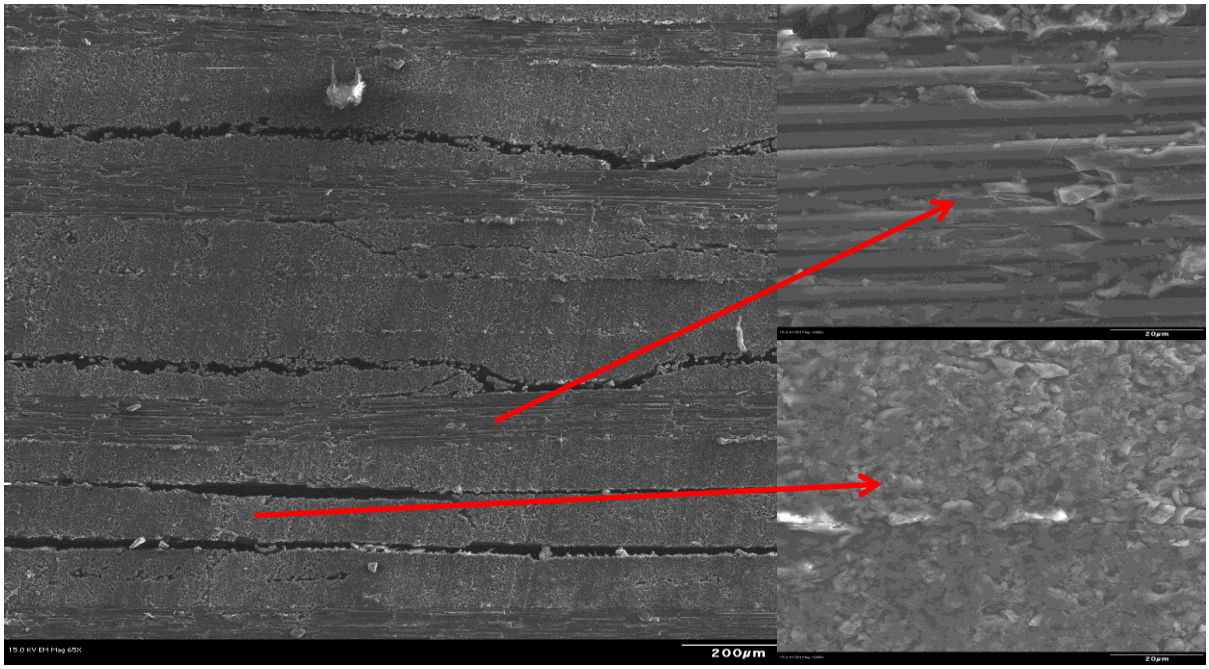

Figure 1.7. Short Beam Shear Baseline sample 1

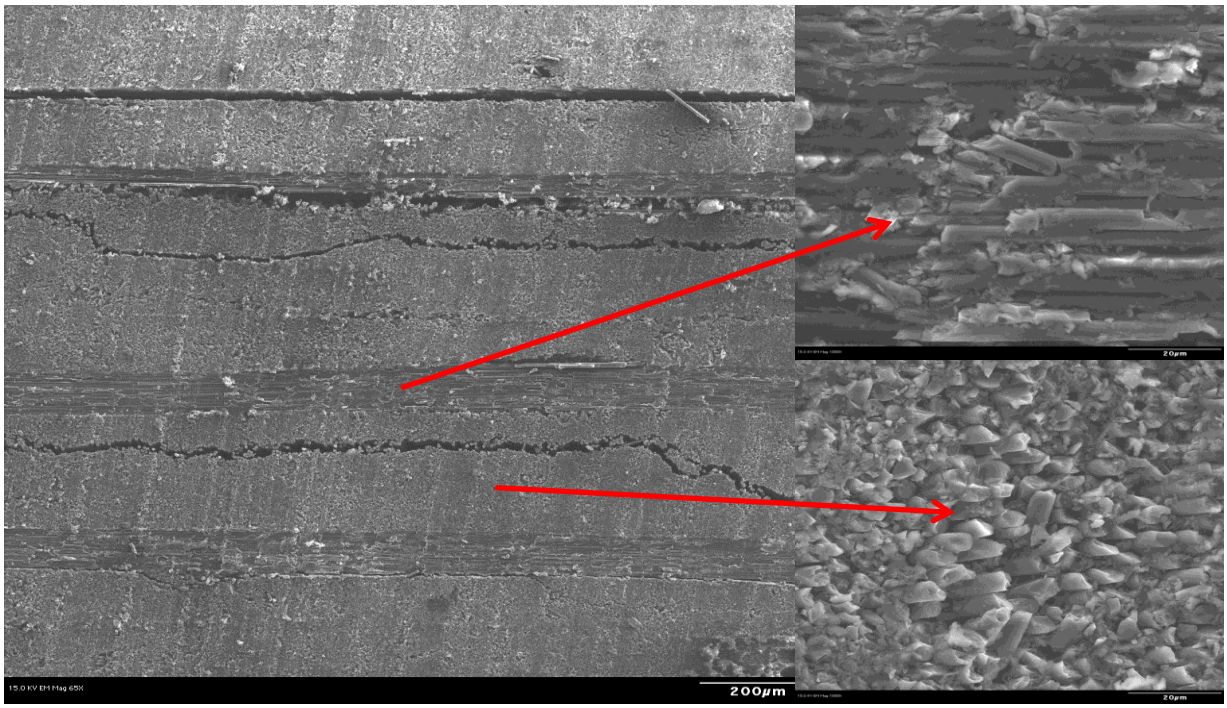

Figure 1.8. Short Beam Shear Baseline sample 2

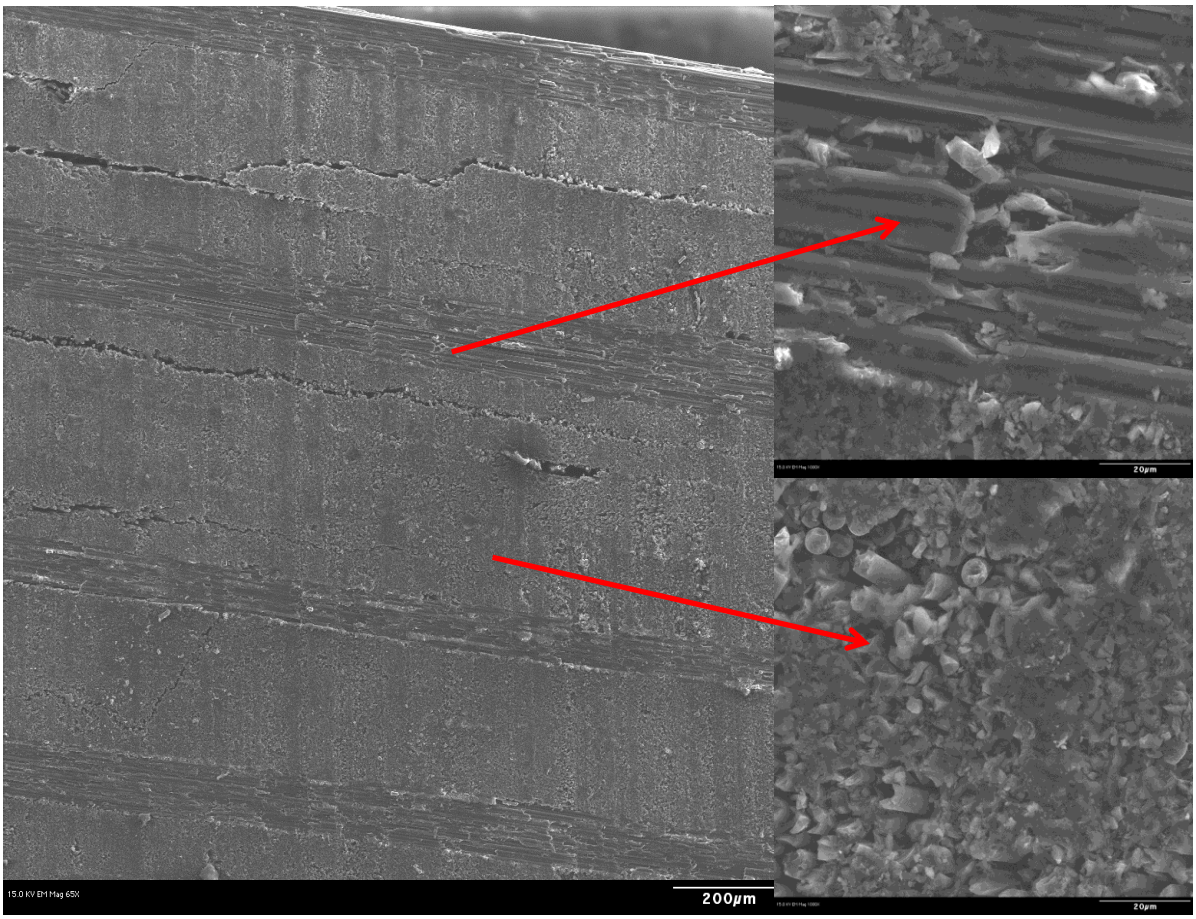

Figure 1.9. Short Beam Shear Baseline sample 3